POLITÉCNICO DE LEIRIA | ESCOLA SUPERIOR DE TECNOLOGIA E GESTÃO

Production of Injection Moulding Plastic Parts with Specific Technical Characteristics

Master's degree in Product Design Engineering

André Antão Costa

Leiria, March of 2023

POLITÉCNICO DE LEIRIA | ESCOLA SUPERIOR DE TECNOLOGIA E GESTÃO

Production of Injection Moulding Plastic Parts with Specific Technical Characteristics

Master's degree in Product Design Engineering

André Antão Costa

Project Report under the supervision of Professor Doctor Pedro Miguel Gonçalves Martinho, and Professor Doctor Artur Jorge dos Santos Mateus

Leiria, March of 2023

Originality and Copyright

This project report is original, made only for this purpose, and all authors whose studies and publications were used to complete it are duly acknowledged.

Acknowledgements

To my supervisor Pedro G. Martinho for the mentorship, guidance, counselling, overall availability, and friendship since the beginning of this process. Even at less convenient hours showed his full availability, which showed to be of utmost importance to successfully finish this project. To him, I dearly show my gratitude.

To my co-supervisor and director of CDRSP-IPL Artur Mateus for allowing me to grow as a professional and an individual while providing me with the tools necessary for this work.

To professor Fátima Barreiros for always helping me with maintaining focus, as well as showing complete support and availability throughout the whole process.

To Engineers Fernanda Carvalho and Jorge Domingues from ESTG for their complete availability on guiding me with the several pieces of equipment at the laboratories.

To my colleagues and friends Artur Potêncio, Ana Costa, Melinda Ramani, and João Meneses for showing me no mercy when I needed it and for helping me continue to work even when times were darker.

To my colleague Anabela Massano for the numerous conversations when all I needed was to talk and interchange ideas.

To all my CDRSP colleagues for listening to my frustrations, but above all for helping me to keep working and learning something new every day.

To professor Pedro Custódio from ESTG and Engineer Teresa Neves from Simulflow for the support in getting the software for simulation and for guiding me through it.

To the S4PLAST consortium, namely António Baptista from CENTIMFE, Mihail Fontul from Iber-Oleff, and Tiago Ruivo from EROFIO for guiding me through the project and for helping me understand what the needs in the industry are and how it works.

To Tiago Marques and workers from Moldetipo for their complete availability whenever I needed them and for the help in getting the mould manufactured and tested.

To professor Fernando Simões from ISEC and Professor Dulce Rodrigues from the University of Coimbra for the support and for allowing me to use the Charpy equipment in a short time which was very important for getting these results.

To my friends and classmates from the master's namely Marina Silva and Madalena Palmeira for always being there and helping through the writing of this work.

To Inês Costa for always showing compassion and friendship, even when we did not see eye-to-eye or when I had major outbursts. For the patience when possible and for always caring for my well-being.

Finally, to my parents and closest family, which, even when I doubted myself, showed complete support, sometimes harsher when needed. For all the conversation hours throughout the years and for giving me the tools to continuously succeed. But, most of all for the patience showed in my darkest moments.

Resumo

Ao longo dos últimos anos os produtos de consumo dispuseram um enorme crescimento. Resultado da melhoria dos materiais, produtos, e processos para alcançar a qualidade do produto, a redução de custos, e ainda a satisfação do cliente. O processo de moldação aparenta ser simples, porém, prever a qualidade da peça final é muito complexo. O que é mais evidente através dos elevados requisitos dimensionais, de forma e de superfície. Paralelamente, o aparecimento de conceitos como a economia circular, resultou na investigação de novas possibilidades na reciclagem de plásticos após o seu fim de vida útil. Para atingir este objetivo, é fundamental compreender como as propriedades dos materiais variam após a reciclagem. Assim sendo, o presente trabalho consiste no desenvolvimento de três casos de estudo, para responder aos problemas apresentados.

Primeiramente, foi elaborado um caso de estudo laboratorial com o objetivo de avaliar a forma como a variação de espessura na peça e o aparecimento de linhas de soldadura terão impacto na qualidade da peça. Para o efeito, inicialmente recorreu-se ao software CAE Moldex3D e, posteriormente procurou-se reduzir defeitos com a introdução de agentes expansores, estudando o seu impacto através de ensaios experimentais. Os resultados obtidos mostram que a utilização de um agente de expansor químico resultou na redução da massa, qualidade de acabamento superficial, e tempo de ciclo. Com estes resultados formou-se um caso de estudo industrial com objetivos similares ao anterior. Neste caso a variação de espessura e aparecimento de linhas de soldadura foram mitigadas por recurso de tecnologias RHCM (Rapid Heat and Cooling Moulding) e canais conformais. Novamente, numa primeira instância, foram realizados estudos numéricos e, depois foram realizados ensaios experimentais. Os resultados alcançados mostram que o uso de RHCM tem impacto positivo tanto nos parâmetros do processo como na qualidade final da peça.

Foi ainda realizado um estudo de reciclagem que avalia as propriedades térmicas e mecânicas de quatro termoplásticos, dois amorfos e dois semi-cristalinos, ao longo de três ciclos de processamento. Os resultados mostram que os materiais amorfos utilizados não sofrem modificações significativas nas suas propriedades, mas exibem alterações nas suas características óticas. Os materiais semi-cristalinos apresentam algumas modificações, nomeadamente o polietileno tereftalato (PET) é o material com maiores alterações, tanto na sua fluidez como nas suas propriedades mecânicas.

Palavras-chave: moldação por injeção, projeto de moldes, agente expansor, variotherm, reciclagem, qualidade de peça.

Abstract

Consumer products have undergone a great deal of improvement over the past few years. This is an effect of improving materials, products, and processes to achieve product quality, cost reduction, and customer satisfaction. At first glance, injection moulding appears to be a simple process, but predicting the quality of the final part is very complex. This is most evident through the high dimensional, shape, and surface requirements. In parallel, the emergence of concepts such as the circular economy has resulted in the investigation of new possibilities in recycling plastics after their end-of-life. To achieve this goal, it is essential to understand how material properties vary after recycling. Therefore, the present work consists in the development of three case studies, to answer the problems presented.First, a laboratory case study was developed with the objective of evaluating how the thickness variation in the part and the appearance of weld lines will impact the quality of the part. For this purpose, the CAE software Moldex3D was initially used, and then the defects were reduced with the introduction of blowing agents, studying their impact through experimental tests. The results obtained show that the use of a chemical blowing agent resulted in a reduction of mass, surface finish quality, and cycle time. With these results an industrial case study was formed with similar objectives as the previous one. In this case the thickness variation and appearance of weld lines were mitigated by using RHCM (Rapid Heat and Cooling Moulding) technologies and conformal channels. Again, numerical studies were performed in the first instance, and then experimental tests were performed. The results achieved show that the use of RHCM has a positive impact on both process parameters and final part quality.

A recycling study was also conducted that evaluates the thermal and mechanical properties of four thermoplastics, two amorphous and two semi-crystalline, over three processing cycles. The results show that the amorphous materials used do not undergo significant modifications in their properties but exhibit changes in their optical characteristics. The semi-crystalline materials show some modifications, namely polyethylene terephthalate (PET) is the material with the greatest changes, both in its fluidity and in its mechanical properties.

Keywords: injection moulding, mould design, blowing agent, variotherm, recycling, part quality.

Contents

List of Figures

List of Tables

List of Abbreviations and Acronyms

ASTM	American Society for Testing and Materials
BLM	Boundary Layer Mesh
CAD	Computer-Aided Design
CAE	Computer-Assisted Engineering
CEAP	Circular Economy Action Plan
CIM	Conventional Injection Moulding
DSC	Differential Scanning Calorimetry
E-mould	Electricity Heating Mould
EC	European Commission
EU	European Union
FIM	Foam Injection Moulding
FTIR	Fourier-Transform Infrared Spectroscopy
G/WAIM	Gas-/Water-Assisted Injection Moulding
GF30	30% Glass Fibre Reinforced
H&C	Heat And Cool Process
HMI	Human-Machine Interface
HTC	Heat Transfer Coefficient
IGES	Initial Graphics Exchange Specification
IMH	Induction Heating Moulding
IML	In-Mould Label
ISO	International Organization for Standardization
MFR	Melt-Mass Flow Rate
MPP	Microcellular Process Pressure
PA6	Polyamide 6
PC	Polycarbonate
PET	Polyethylene Terephthalate
PP	Polypropylene
PS	Polystyrene
PSW	Plastic Solid Waste
RHCM	Rapid Heat and Cooling Moulding

RTC	Rapid Temperature Cycling
S4Plast	Sustainable Plastics Advanced Solutions
SAN	Styrene Acrylonitrile
SCF	Supercritical Fluid
SLM	Selective Laser Melting
STEP	Standard for the Exchange of Product Data

1. Introduction

Throughout the years the plastic industry has become increasingly important. The continuous technological development brought by demands for better product quality, and the adoption of concepts such as sustainability and circular economy have led to research ways to achieve these subjects. For instance, plastic defects create material waste because they lead to parts' rejection which must mitigate the defects and/or understand if there are ways to recycle the material used. All plastics can be recycled, while this is a fact, the reduction of waste must be mitigated. Thus, the improvement of processes is of main essence, one of the possible solutions for this improvement is to design products with intent to reuse it at the end of life, hence, reducing the amount of raw material used in the manufacturing of new products [1–3].

Currently, businesses are controlled by the customer who is the one that defines quality, because it is customer satisfaction that defines the quality of a product. Hence, defects reduce process quality due to the rejection of parts driven by the client's demands. Competition and globalization are among the other reasons that justify the reduction of rejected parts and motivate the improvement of the processes. All these statements create the need for every company to supply their products with good quality, concurrent costs, in time and quickly to be able to retain its market quote, meaning that they need to be competitive at a global level. In the case of the plastic industry, this is possible via improvement and/or innovation of processes, which leads to a reduction of rejects.

In the cases where recycling is feasible, continuous research has led to new possibilities of achieving it at the end-of-life of a product. Nonetheless, it is important to state that there is a major factor to achieve this, which lies in the understanding of the materials' property changes after recycling. Now more than ever, to comply with the 2050's climate neutrality plan implemented by the EU, companies must work on reducing the plastic waste generated by their manufacturing processes [2]. However, manufacturers must adjust in their processes, since a strategy based on a linear economy model is still widely used. Through committing to a circular economy model, by designing out waste and pollution, and through the improvement of waste management infrastructure, companies manage to meet the plan's objectives, such as the innovation of the recycling processes and improvement of waste management.

One of the most used ways to recycle, and the least expensive, is mechanical recycling. However, this type of recycling still has many challenges that must be understood to solve and improve its implementation. The problems to be solved in recycling are:

- Composition, which leads to promoting rejection of parts due to deterioration of the materials' properties;
- Sorting ability, if not controlled results in different material properties;
- Contamination, if present in the material affects the acceptance of a part, this is the main reason for the car industry to not allow recycled plastics in their parts;
- Degradation, is one of the main issues that appear, since both at reprocessing and at service-life oxidation and illumination for the latter, implies instability of the material and later rejection.

1.1. Motivation

This work was developed in cooperation with the S4PLAST – Sustainable Plastics Advanced Solutions project consortium, which intends to contribute to companies on the Engineering & Tooling cluster by adding to the value chain of moulded products with new products with added value, characterised by a high level of recyclability, lighter and with better mechanical resistance, while reducing the number of materials used, and reuse of materials and revalue of waste for the sustainability of the used resources, to answer some of the biggest industrial challenges.

The motivation of this work is the study of plastic parts obtained through injection moulding. Hence, the objectives established were the optimization of parameters for cycle reduction, improvement of the quality of the parts and understanding of materials' behaviour of recycled plastics. This is achieved through the development of the two case studies (laboratorial and industrial) which have the objective of using injection moulding technologies to improve part quality, such as the use of blowing agents to create structural foams and technologies such as Rapid Heat and Cooling Moulding (RHCM).

Moreover, to better understand recycled plastic's behaviour after the recycling process, a mechanical recycling study was made in this work. The latter accomplished by studying successive processing cycles of four materials through the analysis of their thermal behaviour using differential scanning calorimetry (DSC), flowability analysing of its melt flow rate (MFR), and mechanical properties by studying hardness and tensile properties.

1.2. Structure

This project thesis starts with this introductory chapter where the framework is presented as well as its objectives, after this, it is comprised of 6 more which are described below. The report is referenced according to the MDPI style.

Chapter two describes the state of the art in six themes related to the work carried out, namely injection moulding, structural foam, welding lines, rapid heating and cooling, numerical simulation in injection moulding, and recycling. Through this chapter, the objective is to give an understanding of the background in these themes that supports the decision-making and analysis throughout this project.

Chapter three presents the experimental work carried out for the two mould case studies, laboratorial and industrial, and the recycling study. The case studies' sections start by explaining the main objectives of each one. After, the part concept is presented along with an explanation of its geometry and how it answers the objectives. This is followed by a presentation of the mould tool developed for each of the case studies. Each of these sections also makes a context on the CAE (Computer Aided Engineering) simulations made for these studies. The third section of this chapter presents the recycling study which shows its contextualization and the multiple tests and analysis carried out.

Chapter four presents the discussion and results of the experimental work including the simulations performed and the results of the tests and analysis of the injected parts.

The work ends with the main conclusions and future work to be developed in chapters 5 and 6, respectively.

1.3. Scientific papers published

The present project report has resulted in the following published papers in an open-access format:

- Costa, A.A.; Martinho, P.G.; Barreiros, F.M. Comparison between the Mechanical Recycling Behaviour of Amorphous and Semicrystalline Polymers: A Case Study. *Recycling* **2023**, 8, 12. https://doi.org/10.3390/recycling8010012.
- Costa, A.A.; Potêncio, A.; Martinho, P.G.; Barreiros, F.M. Thermal and Mechanical Properties of Recycled Polystyrene. *Mater. Proc.* **2022**, 8, 8088. https://doi.org/10.3390/materproc2022008088

2. Literature Review

2.1. Injection moulding

The evolution of the injection moulding process dates to the early 19th century. The technology was slow to develop until the end of the 1930s when it expanded due to the appearance of new materials at competitive prices. This technology was boosted again in the 1950s, with the appearance of reciprocating screw machines, thus becoming one of the most important processes in the transformation of plastics [4].

According to Crawford, R. *et al* [4], the words polymer and plastic are often synonymous, however, there is some distinction between them. The word polymer is used for material in its pure form, which results from the polymerisation process and is used to describe families of materials with long-chain molecules. The term plastic is applied when additives are added to pure polymers to modify the original properties, such as pigments and blowing agents, for instance.

Polymeric materials can be divided into synthetic and natural. Examples of the latter are collagen, cellulose, keratin, and rubber, which are highly used nowadays. Due to its highly elastic mechanical behaviour, rubber is classified as an elastomer [4].

Currently, injection moulding remains one of the most important processes in the plastics processing industry. As presented by Dzulkipli, A *et al.* [5], , more than 30% of all plastic components are manufactured through this process. This high usage derives from the fact that it enables the production of components with intricate shapes, high dimensional accuracy, and excellent control over the type of surface finish while ensuring high reproducibility [5,6].

One of the factors that continue to motivate both designers and engineers to use plastic materials as feedstock in the creation of new products, is the offer of combinations of properties that cannot be found in any other material. Plastic materials offer advantages such as low density, resilience, corrosion resistance, transparency, and ease of processing, among others. When it comes to their limitations, the ingenuity of designers and engineers is the only limit to their exploitation [4].

2.1.1. Process

As previously mentioned, the high use of the injection moulding process in the transformation of plastics comes from its main advantages, such as the possibility of obtaining identical components with high dimensional accuracy; large-scale production; and above all, extremely fast processing cycles depending on the component(s) to be produced. In addition to these advantages, it is known that at the end of the process, the components extracted have a final shape that needs little to no post-processing, being called a 'net shape[1]' manufacturing process [7].

The injection moulding process is based on a basic principle, which consists of forcing molten plastic material through an injection machine (detailed in section 2.1.2), into a moulding tool, the mould (detailed in section 2.1.3 in which there is a cavity/core corresponding to the desired item.

Typically, the mould is inserted and clamped between two platens on the injection machine, the movable platen, and the fixed platen. By attaching the clamping plate on the extraction side to the movable platen, and the clamping plate on the injection side of the mould to the fixed platen, the mould will move with the machine so that the component is produced inside it when closed and extracted after it is opened [7]. Although there are substantial differences from mould to mould, in general, the moulding process consists of the same moulding cycle (detailed in section 2.1.5), regarding its operation and constitution [7].

For all these mechanisms to work most efficiently, it is necessary for the materials the ability to be forced into the mould during the injection phase, and at the end of the cooling phase, maintain the desired shape. These are the conditions that make a high-productivity process possible. Thus, the material that allows the feasibility of these requirements will be a type of polymer [8].

First, it is necessary to understand what a polymer is. This is a material made up of a long chain of molecular bonds, or macromolecules, which have a central chain of atoms joined by covalent bonds. These are produced through a process called polymerisation, in

[1] Net-shape or near-net shape manufacturing is the word used to define processes with the purpose of obtaining components close to their final shape, or even with their final shape. They aim to reduce the need for finishing processes, reducing the waste of raw material and energy [66].

which chemical reactions take place between simple molecules, and monomers, which through these reactions may form linear or three-dimensional chains. The way these bonds are formed will lead to the formation of one of three types of synthetic polymers. The one of interest for this manufacturing process is formed from a linear or branched chain, called thermoplastics. Given their properties, thermoplastics can be processed by successive heating and cooling without significant loss of their properties, as their molecules are not chemically bonded during processing. Continuous reprocessing and low loss of properties between cycles are the main conditions that make thermoplastics ideal for the injection moulding process [8,9].

Knowing that the process is characterised by the existence of an injection machine, a mould, and a certain material to be processed, it is of utmost importance to explain how this manufacturing process takes place.

The process begins with the insertion of the selected material, in the form of granules or pellets, into the hopper of the machine. These pellets are heated by heating bands placed along the drum. Consequently, the material is melted by the temperature increase through the heat generated by the heating bands and friction created between the material and the cylinder walls. With the material melted, it is then forced through the injection machine's nozzle into the mould. This is when the plastic takes the shape of the cavity and solidifies. After the cooling phase of the process, the mould opens, and the part is ejected [4]. This cycle, detailed in section 2.1.5, is repeated consecutively until the desired quantity of parts is obtained.

2.1.2. The machine

The evolution of the injection moulding machine has undergone multiple iterations since its appearance; however, it is with the appearance of the reciprocating screw injection machine in the 1950s, schematised in figure 2-1, that the injection moulding process becomes one of the most important in the transformation of plastics [10].

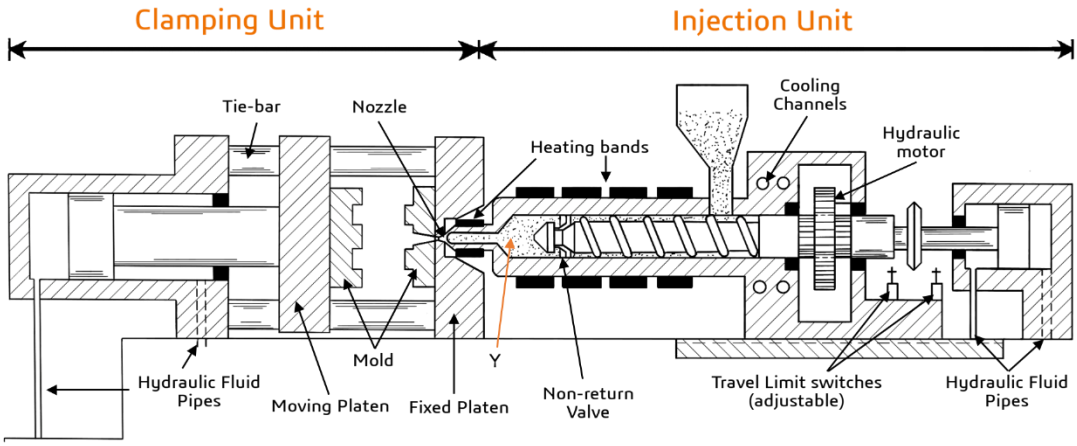

Figure 2-1 – Components of an alternating-screw injection machine [9].

The innovation of the reciprocating screw machine is associated with its mechanism. In this type of machine for injection moulding, the screw plasticises the polymer, initially in a solid state, liquefying the material homogeneously. After the material is melted, the screw works as a plunger to inject the material into the mould. This process is possible due to the shape of the screw, as shown in figure 2-2, which has three working zones: the feeding zone, the compression zone, and the metering zone that has a diameter larger than the feeding zone's and has a non-return valve at its end, which has the function of dosing the quantity of material to be used in the injection process, as well as preparing the next injection when the screw returns to the initial position.

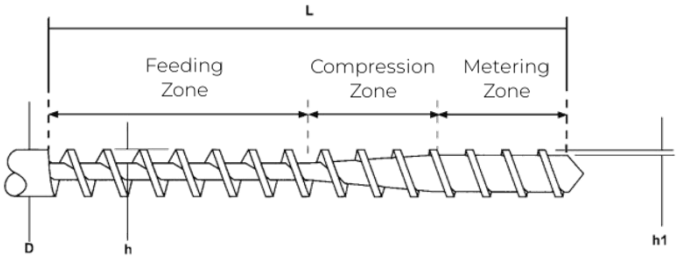

Figure 2-2 – Constituent zones of an injection moulding alternating [11]

The injection moulding machine, shown in figure 2-1, can be divided into two units [12]:

- The injection unit is where the component responsible for plasticizing, transporting, and injecting the material into the mould is located. This system can be divided into three main subsystems: the hopper, where the plastic pellets of the material to be used are placed; the cylinder, where the reciprocating screw and the heating elements for heating the material are located; and the injection nozzle, whose function is to convey the liquefied material into the mould cavity.

- The clamping unit, where the oil-hydraulic (or electromechanical) circuit, the closing system, typically a mechanical clamping toggle mechanism, and the mould are located. The oil-hydraulic circuit is used to drive the cavity clamping plate (or movable side), for closing and opening the mould, as well as for moving the fixed side, *i.e.*, this is also the system that makes the reciprocating screw turn to advance the material inside the cylinder. The closing system ensures the opening and closing, alignment and tightening of the mould throughout the injection process, which may be hydraulic (pneumatic), mechanical or hydromechanical. Finally, the mould, whose function is to guarantee the shape of the part to be produced.

Besides the two units presented above, there is also the command (or control) unit, responsible for ensuring that all the components and respective mechanisms are in sync. This unit is the one that enables the human-machine interface (HMI). The interface not only enables interaction between the operator and machine but also communication with peripheral and data management systems [10]. To support the injection and clamping units there is also the base or power unit that is dimensionally stable, precise, and resistant. It incorporates a hydraulic (or electromechanical) oil system, driven by an electric motor/pump set, which provides the necessary pressure for the various movements of the system.

2.1.3. The tool (the mould)

In the injection moulding process, the tool (mould) is the sub-assembly that essentially allows obtaining the desired shape, surface roughness and dimensions in the moulded part. The mould consists of two sub-assemblies: the core and the cavity. Typically, but not always the case, due to the components present in the mould, the core is responsible for forming the non-visible surfaces, and the cavity for the visible surfaces. To enable extraction and the start of a new injection cycle, the core and cavity are separated with the opening of the mould by the parting line. This line separates the movable part from the fixed part and is visible on some moulded component [13].

To support the moulding elements as well as the functional systems of the mould, the mould system consists of plates, blocks, guides, and various accessories. The plates allow the assembly of the mould in the injection machine and serve to support the moulding element and the injection system. The accessories and the guides, standardized or not, ensure the movement, guidance, and transportation of the plates.

Depending on the part(s) to be produced, the moulds can be of various types, the most used type being the two-plate mould, as shown in figure 2-3 This consists of two halves that open through a partition line. In this case, the material enters the cavity directly through the sprue, or indirectly through the runners in the partition line.

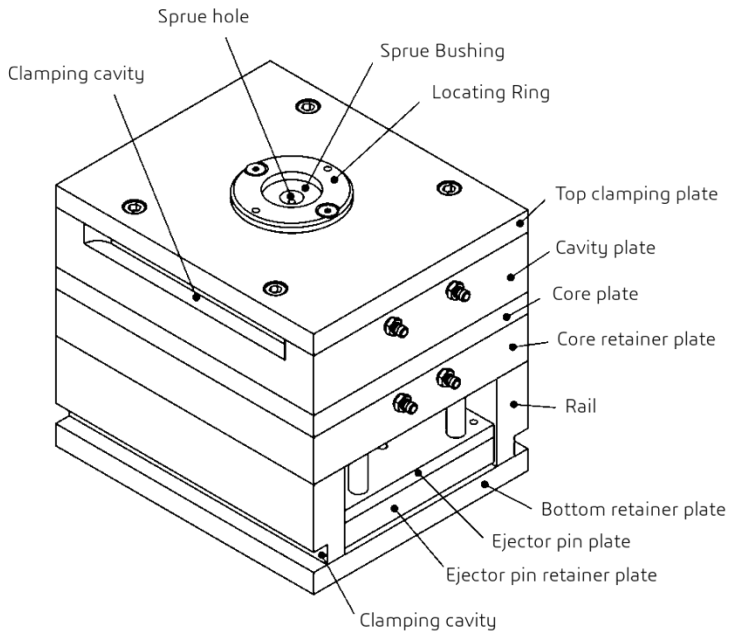

Figure 2-3 – Example of a closed two-plate [7].

As previously mentioned, the mould possesses functional systems, that enables the product specifications, such as dimensions and mechanical properties, and smooth the operation of the mould. The main functional systems of a mould are the mould impression, the guiding and centring system, the feeding system, the venting system, the cooling system, and the ejection system.

Depending on the mould, the quantity and type of components that make the functional systems vary [12]. The guiding and centring system is responsible for guaranteeing the alignment and guidance of the plates for keeping the mould secure while opening and closing. The feeding system is responsible to lead the molten material from the injection moulding machine to the impression. It comprises a maximum of three components which, in some cases, can be replaced by a hot runner system. The main injector, which is where the molten material enters the mould, the runner(s), to convey the molten material to the impression, and the gate(s), which is the transition channel between the runner and the impression and the zone responsible for delivering the material to the impression. The impression is the cavity in the mould responsible for producing the part.

The ejection system is mainly comprised of the ejectors which are responsible for extracting the part(s) after the cooling phase of the injection cycle.

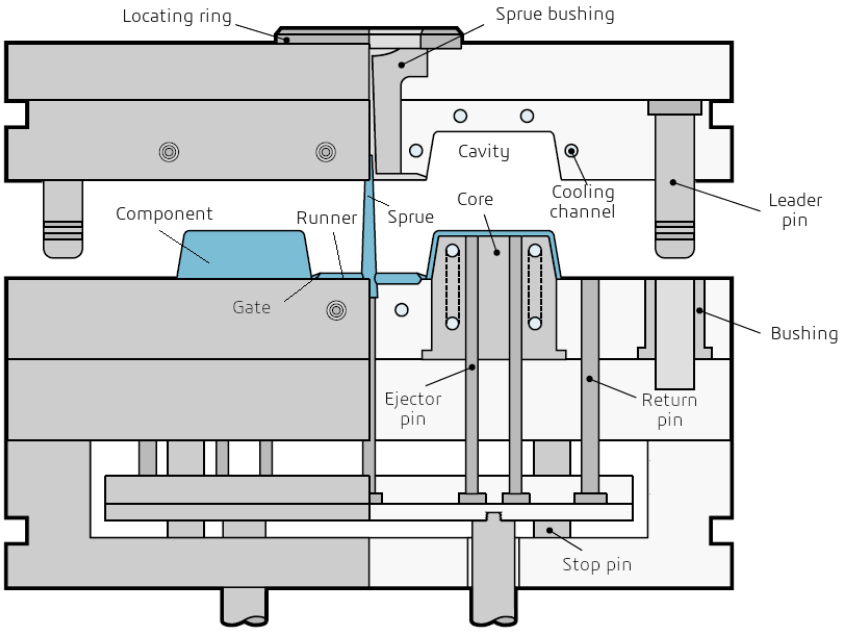

Figure 2-4 – Example of a two-mould plate with identification of some functional systems' components [13].

The venting system is implemented to avoid trapped air in the impression, and finally, the cooling system consists of cooling channels machined into the moulding blocks. These allow for a uniform distribution temperature on the moulding surfaces, as well as a higher mould efficiency. It is through these channels that water passes at a sufficiently low temperature to cool and solidify the material inside the mould. The next section describes these systems in more detail.

2.1.4. Cooling systems

The cost and operation in mould design have a high dependence on some of the systems that are part of the mould, among them, the cooling system is one of the most important systems. However, according to some literature [14,15], this is still one of the most underdeveloped systems in moulds for injection moulding, justifying that the most likely reason for this is the ease of identifying defects related to filling flow compared to those related to temperature distribution.

Incorrect design of cooling channels may lead to undesired results, namely, excessively high cycle time, or multiple temperature gradients along the mould resulting in residual stresses in the moulded components, demonstrated in the form of warping and/or non-uniform shrinkage of the part [13,14].

For the system operation to be efficient, it is necessary during the design phase to focus on the thermal management of the mould without incurring unnecessary complexities, while keeping the cost of its execution to a minimum.

The objectives to be met by cooling systems in moulds are the following: maximise heat transfer rates; maintain the temperature of the moulding zones (impression) at a uniform temperature, while assuring the mould durability; minimise the cost of the mould; minimise the volume occupied by the channels as well as their complexity; maximise the reliability of the system; and facilitate the operation of the mould by identifying the inlets and outlets, as well as placing the connection zones on accessible locations. The number of objectives mentioned is synonymous with the fact that not all of them are optimized simultaneously, so the designer should reach a conclusion in which the accepted compromises achieve a 'fast and uniform cooling', guaranteeing a low cost [14].

As mentioned above, the cooling system has great importance in injection moulding, not only for the reasons already presented, such as the variation of shrinkage during cooling that can lead to warping, distortion, and dimensional problems but also because of the effects of cooling rates in crystallization and shrinkage in semi-crystalline materials [13]. Thus, it is important to define a design approach for the execution of the cooling system, as such. Kazmer, D. [14] defines a seven-step decision support process, where it should be noted: the calculation of the cooling time required; the evaluation of the required heat transmission rate; the estimation of the coolant flow rate; the evaluation of the diameter of the cooling channels; the selection of the distance between the moulding surfaces and the cooling channels (cooling line depth); the selection of the distance between the channels; and finally the routing of the cooling system.

Although in certain situations this process is sufficient to set the circuit, there are cases where it is not enough. The reason for this is supported by the following example, consider a mould with a cavity as shown in figure 2-5. In this case, due to the size of the cavity, the cooling of the part is not optimal. Due to the distance between the cavity and the cooling channel being variable along the part, the cooling gradients are distinct along the part, which will lead to the appearance of defects in the moulded part, to solve this situation, there are some typologies of a cooling system, namely: cooling channel networks; cooling inserts; conformal cooling; high conductivity inserts; and slender inserts cooling.

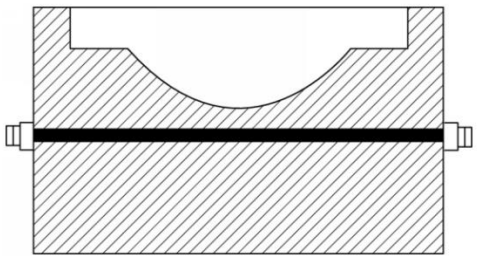

Figure 2-5 – Example of conventional cooling channels of variable moulding surface distance [16].

To allow correct cooling of the injected material, the mould is provided with a network of channels for cooling. This network has several sub-types. The most common and cheapest solution consists in connecting various conventional channels through different types of connections. In this type of mould each typology has its advantages and disadvantages, one of the main problems that arise, is the assembly between the mould and the temperature control machine. Thus, some of the most common types of assembly, and each one has its disadvantages in terms of assembly and/or production costs, for example, the layout depicted in figure 2-6 (a) possesses a circuit that can cause a reduction in the flow of the cooling fluid and a significant increase in its temperature generating an excessive temperature differential, between the input and output, already in the example figure 2-6 (b), the complexity of assembly due to the number of hoses that have to be connected/disconnected may incur in the probabilistic increase of incorrect assembly of the scheme. A solution that solves the problems from figure 2-6 (b) is the one from figure 2-6 (c), which has internal channels in the mould to reduce potential failure modes and has only one inlet and one outlet, however, it has an increase in production cost. Due to some mould typologies, the previous version (figure 2-6 (c)) would pose problems in the introduction of mould accessories. In some cases, the only way to obtain a similar cost while guaranteeing a reduction in failure mode is the solution presented in figure 2-6 (d), which brings the disadvantage of being less efficient.

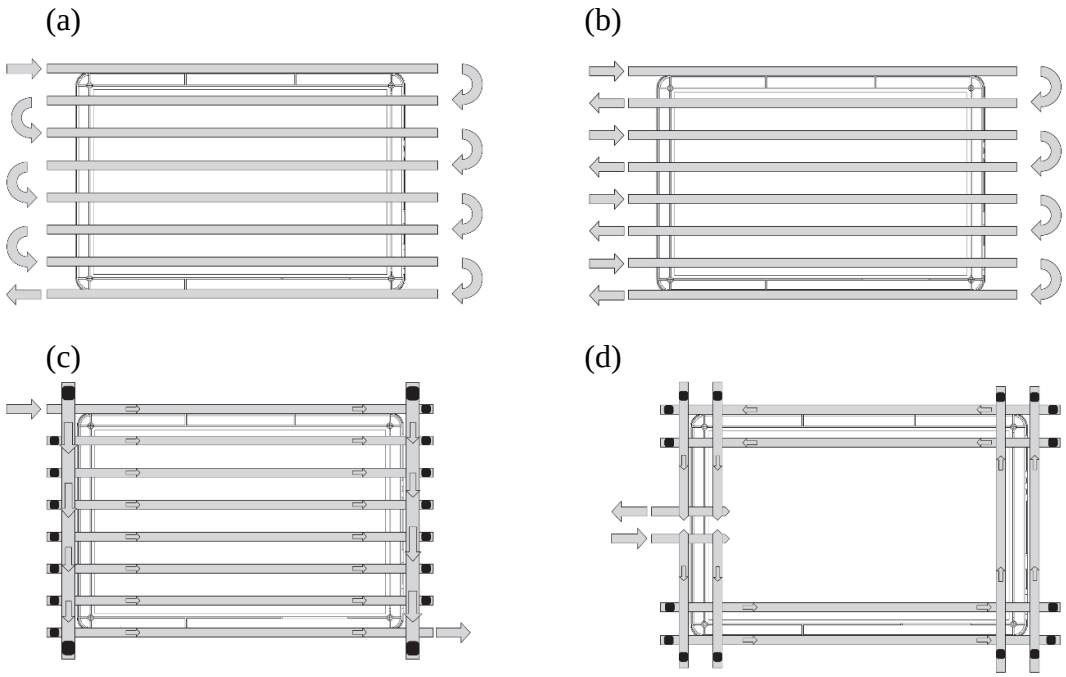

Figure 2-6 – Examples of cooling channel layouts (a) connected in series; (b) four circuits in parallel; (c) internal circuits connected in parallel; (d) peripheral perforated circuit [14].

Another way of cooling can be found in the type of cooling inserts (figure 2-7), in this case, the holes in the mould are replaced by channels machined on the opposite side of the insert(s) of the cavity/core. In this case, it is necessary to introduce sealing elements, such as seals, to avoid leakage. For this type of cooling, there are mentions that leakage may occur in areas near the extractors where there are seals.

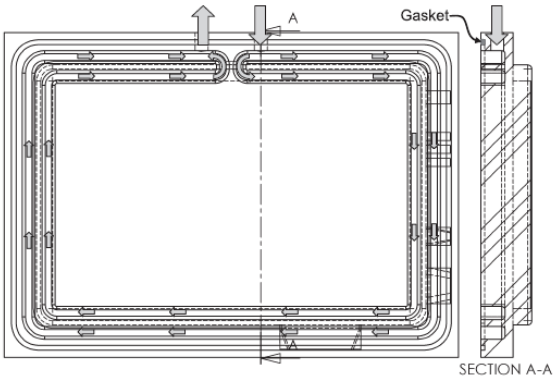

Figure 2-7 – Core insert with machined cooling channels [14].

The previous solution allows better control of heat flow in the mould, nevertheless, in some cases, greater control over this parameter is needed. In recent decades, technological advances in new manufacturing processes have been evident. One, that is worth mentioning, is the evolution of additive manufacturing technologies. Among the additive manufacturing technologies, the SLM (Selective Laser Melting) manufacturing process should be highlighted. This process allows the development of metal components, for example, inserts

and plates, with channels of high geometric complexity, which otherwise could not be produced.

The possibility of using these technologies in moulds grants the opportunity of manufacturing channels conformal to the part geometry, figure 2-8, leading to an improvement on the heat extraction rate and uniformity in temperature distribution. However, the cost associated with this type of component is extremely high and its use must be assessed on a case-by-case basis.

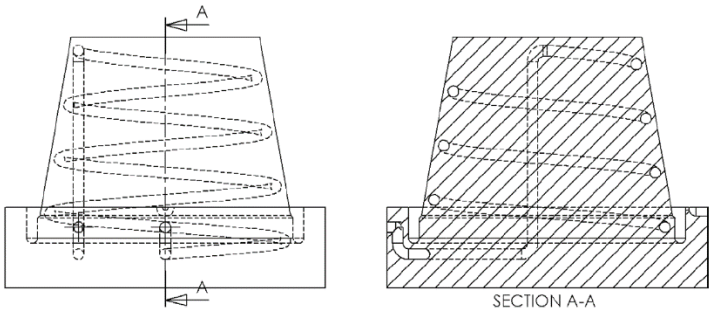

Figure 2-8 – Conformal cooling insert [14].

2.1.5. Injection moulding cycle

The whole injection moulding process is based on a moulding cycle, which can be explained by an operational cycle, as shown in figure 2-9.

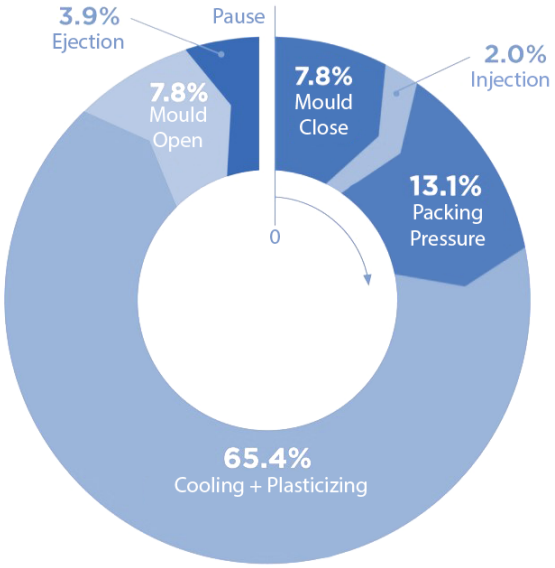

Figure 2-9 – Simplified cycle steps of the injection moulding process with exemplary percentual extent of each [17].

The injection moulding process starts when the mould closes, this is the phase that will allow for the impression of the part to happen between the cavity and the core. After this phase, the mould cavity is filled. Due to the cooling of the material, which is caused by

contact with the metal surface at a lower temperature, the material will undergo a shrinkage process. To compensate for the shrinkage a second pressure, also known as packing pressure, is required. This pressure will be exerted on the molten injection material for a defined period. Before the material is ready to be extracted, it will have to cool down, the so-called cooling phase. In this phase, the injected material will rest until it reaches a sufficiently low temperature to be extracted from the mould. While the cooling phase takes place, due to the need of reducing cycle time, the plasticisation of the pellets inside the cylinder happens, so that the material is prepared for the following injection. With the part solidified, the mould opens, and the part is ejected through the ejectors and accessory movements. With the part out of the mould, a waiting time is given to allow complete removal of the part and/or the use of robotic arms to remove the component(s) and/or by other unexpected occurrences, and the next injection is started.

2.2. Structural foam

Structural foam is an alternative process to injection moulding which started to be used in the early 1960s. In this process, it is possible to create parts with a cellular core and a solid outer shell in one operation. The process consists of using an inert gas, which is dispersed through the material. This can be done in two ways, physically where the gas is forced directly into the melted material, or chemically where the resin is preblended with a chemical blowing agent that will release the inert gas under heating. In both cases the process has the same objective, to create gas bubbles that will expand within the melt. This expansion allows to fill of the mould and creates the cellular structure core, when these bubbles collapse against the mould surface, they create solid skin around the foamed core [18,19].

This process, as is with conventional injection moulding, obtains quality parts from the correct combinations of a parameter such as temperature, pressures, injection speed, and mould design, among others. The difference in this process lies in the uniformity in which the blowing agent is dispersed in the melt. Another parameter that should be carefully controlled is the temperatures in the feed zone, this must be kept at lower temperatures and gradually increased towards the nozzle. This temperature control minimizes the decomposition of the blowing agent prematurely [18]. The size of the bubbles created by the blowing agent highly impacts the moulded part, therefore the rate at which the bubble grows is a factor to be accounted for to obtain the desired mechanical and physical properties of the component. The following processing variables should be carefully chosen to establish

the final cell size: pressure and temperature gradients, injection speed, and injection melt temperature which determines melt viscosity and elasticity. The temperature gradients in the mould slow the bubble growth near the wall of the mould, it is this parameter that facilitates the creation of the outer shell [18,19].

Due to the petroleum crisis in the 1980s, and because the traditional foaming process highly reduces mechanical properties such as strength, a new technology was introduced by the MIT, which was named microcellular foam injection moulding. This technology brings two clear advantages to the industry since it allows obtaining lighter, hence less material, and reasonably strong parts [20].

The microcellular foam process (Mucell®), as in the traditional physical foaming process, follows the premises of injecting a gas into the melt. The main difference in this process is that the injected gas is a supercritical fluid (SCF). The agents usually used are CO_2 and N_2. The process goes through four steps: gas dissolution, nucleation, cell growth and shaping. All these steps must occur on the injection machine to allow the microcellular foam to be created [20,21]. Step 1 of the foaming process is a polymer-SCF single-phase generation, where the supercritical fluid is injected into the injection barrel and dissolved into the melt. The saturation, microcellular process pressure (MPP) and temperature determine the concentration of SCF and the final bubble size. When the polymer-SCF single-phase mixture is injected into the mould cavity (step 2), its pressure will change from MPP to atmospheric pressure. This provokes a rapid pressure unloading which leads to the separation of the SCF from the single-phase mixture, hence generating many nuclei. This incites the growth of the nucleus, and when the size of the nucleus is higher than the critical it will become stable. Consequently, the final nucleus density and nuclei process is affected by mixture temperature, MPP and SCF concentration. It is after the nucleus stabilizes that the bubble growth starts (step 3). The bubbles will continue to grow until one of two happens, either the melt freezes due to temperature or the SCF concentration of the mixture is higher than the SCF concentration inside the bubbles. Step 4 of the process is called bubble typing, and this is when mould cooling leads to the decrease of the melt temperature and consequently the freeze of the material. This conjunction of parameters stops bubble growth and subsequent final part shape [20–22]. Figure 2-10 represents the phases and steps of the microcellular foam injection moulding process.

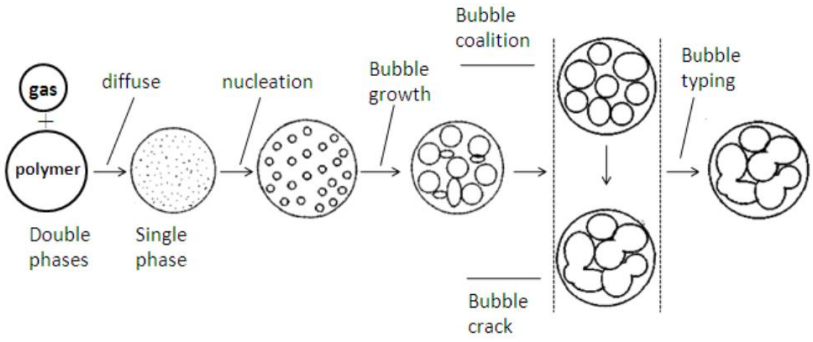

Figure 2-10 – Representation of microcellular foaming process in polymers [20].

The introduction of this technology brings changes to both processing parameters and part properties such as the decrease in polymer melt viscosity, process cycle time and part weight reduction, it also greatly affects the mechanical properties and surface finish quality [20].

2.3. Welding lines

Many criteria are used to evaluate the quality of an injected moulded part, one of them being its appearance. One of the defects that appear on plastic parts is the appearance of welding lines [23]. Welding lines arise from the presence of an obstacle in the flow front that leads to the separation into multiple fronts, whenever these merge after the obstacle, a weld line is formed [23,24]. Usually, these are identified as mechanically weak regions making them undesirable in some cases. Weld lines have two identifiable types depending on the meeting angle of both (figure 2-11). A cold weld line or knit line is the point where two streams of plastic material meet and merge in opposite directions during the injection moulding process. Knit lines can be a source of weakness in the moulded part and can also be visible as a line or mark on the surface of the part. To minimize knit lines, it is important to properly design the mould and control the flow of plastic material during the injection moulding process. A hot weld line or meld line, on the other hand, is a visible line or mark that is formed when two stream fronts converge parallel to each other during the injection moulding process. Meld lines can be cosmetic defects, but they do not affect the strength or function of the part [23,25,26].

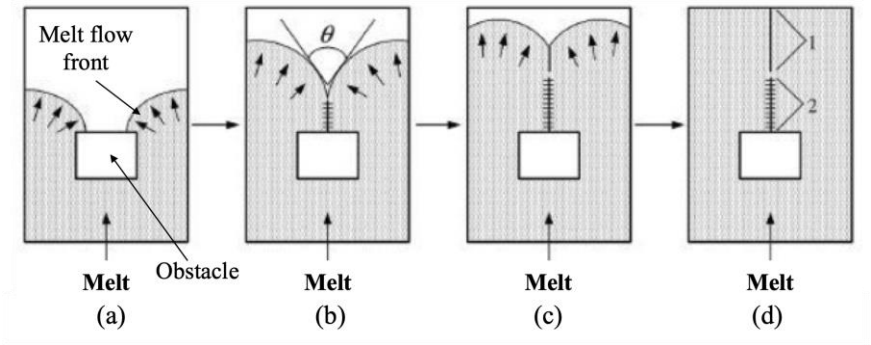

Figure 2-11 – Weld line formation process and identification of types of welding line. (a) Separation of melt fronts; (b) weld (knit) line formation; (c) meld line formation; (d) filled cavity with weld line (1) and meld line (2) [5].

As mentioned before weld lines are considered a cosmetic defect and can also affect the appearance of the moulded part. To minimize weld lines, proper mould design and control of the plastic flow are crucial in the injection moulding process. Techniques such as gate location and design, balanced filling, and reducing the filling time can help reduce the occurrence of weld lines.

2.4. Rapid heating/cooling

Injection moulding is a temperature dependant process, as shown by the multiple cooling channels and temperature-related defects such as shrinkage and warpage. Since the cavity's thermal level and distribution is a very important factors in obtaining good-quality parts, heat transfer control becomes the most important process to control.

For an injection process to be controlled correctly, after cycle heat balance is achieved, the global heat that is going into the system must be equal to the heat removed from it [27]. The heat exchange present in the mould is mainly conducted through the cooling system, nevertheless, for correctly studying thermodynamics in this process, other additional mechanics must be contemplated due to heat losses from the metal to the machine's plate.

The cooling phase of the injection process, not only accounts for up to 60% of cycle time but drives the cooling process of the parts. It is in this phase that an improvement in heat transfer efficiency can lead to economic feasibility, this is achieved by reducing cooling time to the minimum possible [27]. Thermal and geometric features on the mould and part have major effects on heat transfer between the injected material and the coolant. To control heart transfer, factors like steel and coolant conductivity, coolant flow rate, location, diameter and/or shape of cooling channels, among others must be taken into consideration [14,27,28].

Heat transfer from the part to the cooling system can be divided into two consecutive steps. The first happens from the inside of the part where the heat is transferred through conduction to the outer surface of the part, and the second from the part surface to the environment around it which is divided into heat exchange with the cooling system and with the environment.

Part thickness has been identified as the highest impactor in cooling time surpassing coolant flow, temperature or even 3D cooling [7,12,13,27,28]. A highly efficient cooling system should withdraw heat quickly and homogeneously.

The continuous growth in quality requirements for technical injected components has led to the development of new technologies like sequential injection, in-mould label (IML), etc. [29,30].

One of the most recent, that has engaged designers and manufacturers to implement, is the heat and cool process (H&C), or rapid heat and cooling moulding (RHCM) [31]. This novice technology, conceptually, allows for full temperature control of the process, since it states that throughout the filling phase, the cavity is quickly heated before the material enters the mould to allow improved melt front advance, and when the packing phase starts, the coolant flow starts to reduce mould temperature. This allows for better and more homogeneous temperature distribution, since the frozen layer becomes thinner, improving the filling of the impression. Reduction of the mould temperature at the end of packing grants it to rapidly reach ejection temperature which translates into reducing cycle time. With this technology, aesthetical defects such as weld lines become scarcely perceptible [32], because of the thin frozen layer.

The use of this technology promotes a highly polished and high-quality texturized surface, permitting the so-called appearance of “piano black” [27]. Nevertheless, it comes with the economical downside of requiring additional time and operational processing costs for the heat exchanges to occur, and augmentations in energy and additional investments in required equipment. It also diminishes the tool’s lifetime due to constant temperature variations which in turn requires better materials for the tool. To overcome these weaknesses, a careful design based on the combination of materials and heat transfer optimization designs is usually the methodology used.

Sanchez [27], states that some of the design factors that are strongly involved in solving the drawbacks of RHCM may be:

- The material volume under the thermal cycle: the time necessary for heating and cooling until the desired temperature is highly related to its global mass.
- Selected tool material: usually steel, good thermal conductivity, good thermal stress, and corrosion behaviour but other options could be considered, such as aluminium alloys.
- Heat and cold system design: channels closer to the surface improve heat flow and reduce cycle time but this choice affects the mechanical mould strength.
- Heating technology efficiency: induction coils, water steam or resistor elements.

Due to the drawbacks, several variants of this technology have been developed such as heat and cool (H&C), variotherm, rapid temperature cycling (RTC), weldness moulding and others, where they mostly differ in the heating technology used. Three main strategies have been identified for heating strategies: convective heating, induction heating moulding (IHM), and electricity heating mould (E-mould) [27].

Convective heating uses the channel wall and some fluid to establish convective heat flow, employing the cooling lines for both heating and cooling operations. Oil was utilized in the early phases of development but was later abandoned due to its low boiling point and low heat conductivity [33]. . Hot gases and combustion gases were employed concurrently, but in the end, the process developed organically to use steam water as the heat source [34,35].

IHM employs the Joule effect using a high-frequency electromagnetic field which directly heats the cavity surface [36–38]. In the channels or cavities present in the mould, coils are installed, when necessary, between the cooling channels and the cavity surface. This method combines the effectiveness of convective steam with high temperatures that are not feasible at saturated steam logic pressures. Induction heating costs must be carefully considered if project feasibility is to be maintained.

E-mould generates heat using Joule's first law when a low-frequency current is applied to resistors. For this strategy, a crucial design factor is the power density [39]. The key benefits are simplicity, affordability, and operation temperature up to roughly 250 °C.

Nonetheless, the identifiable drawbacks are low efficiency and slow response time, which are major factors in the process and should not be neglected.

2.5. Computational Numeric Simulation

Since the 1970s injection moulding simulation tools have been used to allow a better understanding of whether the process parameters and moulding functional systems were correct or not. These tools provide a cognizance of part and gate design, runner and cooling layout, moulding materials, and process conditions, among others [40,41]. The main advantage of using such tools is the time and money saved throughout the design phase of a project. In addition to conventional injection moulding, other innovative processes have appeared and been included in these tools, such as the G/WAIM (Gas-/Water-Assisted Injection Moulding) and MuCell® processes.

Moulding issues have become more and more difficult with the introduction of new technologies. Fortuitously, CAE tools are provided with the capacity to solve new types of innovative processes, allowing the detection of possible problems in the injection process and tool design. The key criteria for solving moulding issues are plastics rheology, and the designs of parts and moulds since these will highly affect the property variations inside the mould [40].

Wang [40], , references that the difficulty in the process is that the adjustment of a single parameter can influence the whole process in different ways. For example, by increasing the injection speed, material temperature, or mould temperature it is possible to mitigate the appearance of a short shot. Nevertheless, the intensification in speed can also induce an exaggerated shear rate and intensify moulding stress or residual stress. Conversely, an increase in material or mould temperature can result in additional cooling time and thus lengthen the moulding cycle and induce production costs. By using CAE tools for simulating the process, these are mitigated and some of the possible mould production errors can be detected much earlier in the manufacturing process.

Usually, the problem of these tools is the time restrictions imposed by the simulation itself or the limitations of the hardware used. These limit the number of iterations possible for a specific problem. When using these simulations, it is necessary to obtain the maximum information in each iteration, so it is possible to solve the causes of the existing problems [42].

The main goal of using moulding simulations is to understand the possibility of the manufacturability of moulded parts [41]. This is achieved by using software such as Autodesk's Moldflow, CoreTech's Moldex3D, SOLIDWORKS Plastics, SIGMASOFT Virtual Molding and Vero VISI Flow to analyse design verification and optimization of parts and moulds, and optimization of process conditions. These are achieved by using a general workflow for simulation, depicted in figure 2-12.

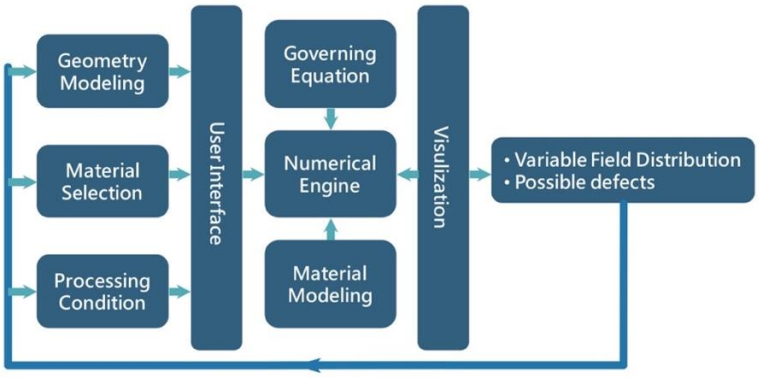

Figure 2-12 – Computer-assisted engineering simulation general workflow [40].

2.6. Recycling

As shown in the previous sections the injection moulding process is one of the main plastic transformation processes, and this has made the use of plastic a necessity throughout the years. Consequently, this increasing need of using plastics in one's daily lives has led to an exponential growth in plastic waste [3,4].

From 2009 until 2022 a substantial increase of 18.2% in plastic waste was registered in the European Union (EU) [43]. This means that talking about plastics is synonymous with its recycling. In the same span 2009-2022, recovery and recycling volumes increased even more, by 25.2% and 21.5%, respectively. This need of reducing plastic waste and the adoption of the circular economy action plan (CEAP) by the European Commission (EC) in March 2020 made plastic recycling one of the building blocks of the European green deal [2]. The full implementation of this plan will achieve the prerequisites of the EU's 2050 climate neutrality plan.

The main reason plastics have received such special attention is that they are hydrocarbons, meaning most types rely on crude oil for their manufacture. This makes them less than sustainable materials with large carbon footprints. In addition, through processes such as incineration, plastic waste is easily converted into carbon dioxide and other

greenhouse gases, which harm the climate. The other reason lies in their environmental degradation resistance and the majority of these are not biodegradable. Hence, they can last a long time once they are no longer useful. This makes the disposal of plastics burdensome since they take a long time to break down in the environment. Plastics are extremely difficult to recycle, economically, since there are various variations in their type, grades within family groups and the possible additives that can be added to them.

The recycling of plastics was divided into four categories, primary, secondary, tertiary, and quaternary recycling when ASTM D7209-06 [44] was active. Nonetheless, this division is still present in three categories used in the ISO 15270:2008 [45], which is still in use. The ISO standard divides plastic recycling into mechanical recycling which makes up primary and secondary recycling, chemical recycling which corresponds to tertiary recycling, and energetic valorisation which makes up quaternary recycling. Goodship [3] refers that mechanical recycling is one of the most common ways of recycling in the plastic industry. As priorly noted, mechanical recycling is divided into two categories primary and secondary recycling, the main difference between both is the material quality. Primary recycling is a closed-loop process, *i.e.*, the processing history is known to the company and focuses on grinding down and reprocessing the material without mixing it with others, the whole process is controlled inside the same corporation. On the other hand, secondary recycling, although based on the same concept, is an open-loop process meaning that the main difference to primary recycling lies in the fact that the recycled material is acquired from other sources and might require pre-processing the material through some or all the steps presented by Goodship [3] and Santos [46] which are summarized into size reduction, cleaning, sorting, and re-granulating to a suitable pellet size as detailed in the process' scheme in figure 2-13. In this type of recycling, there may exist some difficulties due to the unknown history of the raw material.

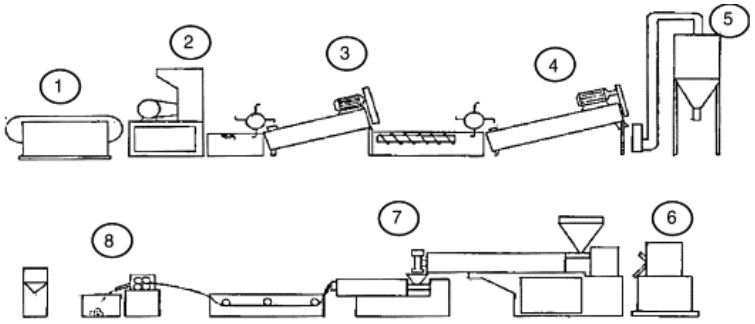

Figure 2-13 – Scheme of plastic recycling process with each detailed phase. (1) identification, separation, and classification of different types of plastics; (2) grinding; (3) washing with or without the addition of cleaning agents; (4) drying; (5) silos; (6) agglutination (films and products with fine thick); (7) extrusion; (8) granulation [46].

The lack of history in secondary recycling makes the use of these plastics demanding since reprocessing might affect the materials' properties. The reason for secondary recycling's lower implementation does not lie in the process complexity, but rather in the fact that these materials are more susceptible to plastic contamination and plastic combinations with changeable compositions when originating from industrial sources, for example.

As already established, recycling plastics comes at a cost, this means that for companies to ultimately invest in recycling as well as use recycled materials it is of utmost importance to understand the behaviour of plastic materials.

3. Experimental work

The present chapter introduces the experimental work performed with the aim of studying the injection parameters and recycling effects on plastic properties. To achieve this, three case study are proposed. The first is the study of a laboratorial technical part, the second is an industrial technical component which is a part of the project S4PLAST, and the last is a mechanical recycling study for the comprehension of property variation after recycling. In the first two case studies the experimental procedure is explained throughout this chapter, from part design to the mould design and CAE simulations, as well as the respective injection tests and the mechanical behaviour of the injected parts. The software used for the numerical simulations was Moldex3D 2021R4OR. Regarding the third case study, the procedure used for the mechanical recycling approach is detailed.

3.1. Laboratorial case study

The laboratorial case study is comprised of a technical component to explore the effects of weld lines on part aesthetics, the effects of using foams in injected parts, and the effects of high thickness variation in a part. These studies are industrially relevant, namely the high thickness variation and the welding lines since they cause visual defects that decrease the quality of a part, both aesthetically and in its mechanical properties.

As a first approach to this case study, a conceptual model, shown in figure 3-1, was sketched with specific zones designed for evaluation of the features mentioned above, it also intends to provide a better visualization of the component to be produced and understand some of the details that must be considered for mould design.

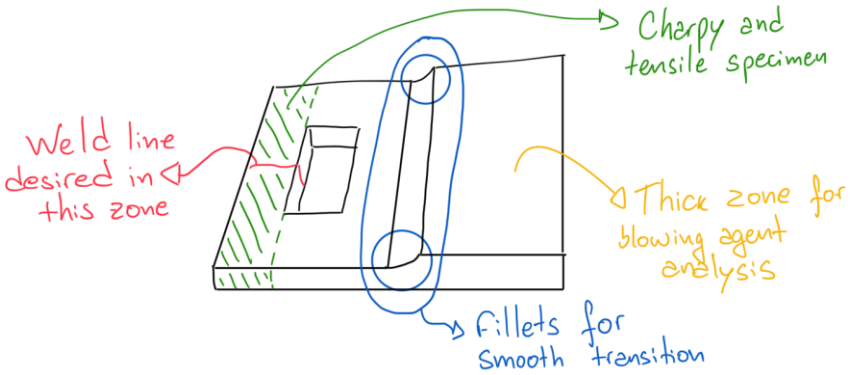

Figure 3-1 – Conceptual part of laboratorial case study.

After this definition, the part was further developed to understand dimensions and supplementary necessities such as placement of gates and runners, and flow direction prediction, resulting in concept A and concept B, presented in detail in Appendix A. Due to the high thickness variation in concept A after the middle gate, a second concept, concept B was developed, in this one, the part's hole was move so that it would not create a problem in this zone, since polymers solidify more rapidly in thinner places, and this does not allow for filling the part. According to Wang [40], as the thickness of a part is thinner the faster its cooling, the higher the viscosity and injection pressure, there is an increase in resistance, and short shots are more likely to happen.

As previously explained, the part designed for the laboratorial case study has two zones, the green zone and the blue one, as shown in figure 3-2, intending to analyse the use of foam injection moulding, the high thickness transition, and the appearance of knit and/or weld lines that appear during the injection process.

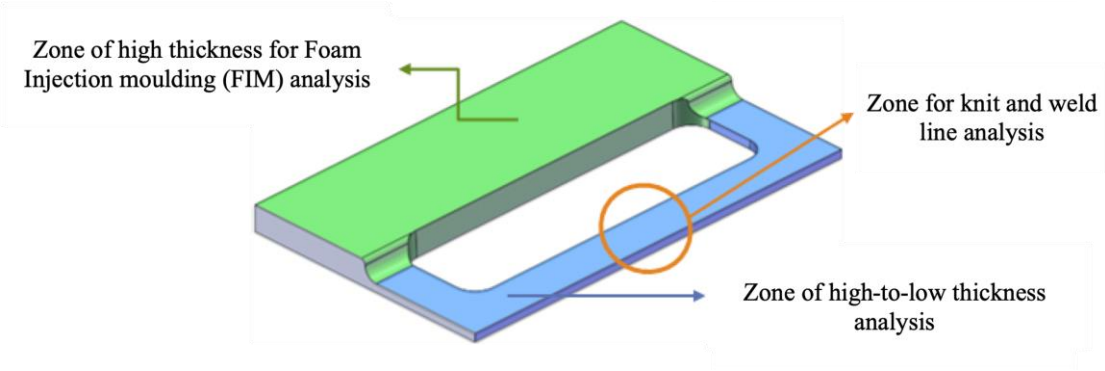

Figure 3-2 – Identification of study zones of the laboratorial case study.

The part in the case study has the main dimensions presented in figure 3-3 and the technical drawing of this component is presented in Appendix B.

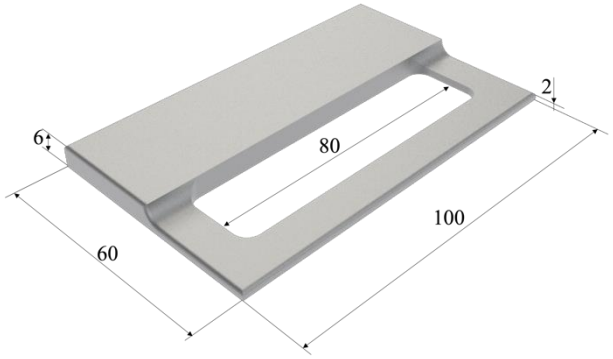

Figure 3-3 – Geometry and main dimensions of the part for the laboratorial case study.

3.1.1. Mould design of the laboratorial case study

In this case study, the mould developed is of a two-plate typology, due to the simplicity of the part. For the possibility of reutilizing the structure of the mould, a core insert was developed. In this mould, both the cavity and core side hold conventional cooling channels for temperature control.

The initial geometry of the mould (Appendix C) was made to be used on a BOY 22A injection machine which has 254 mm between the tie-bars, and 200 and 400 mm as the minimum and maximum height of the mould. These limitations allowed for setting the dimensions of the mould. This first iteration, represented in Appendix D, was defined for a part with a draft angle of 2º and a shrinkage factor of 1.2% due to the materials to be injected using in this mould. After locating the part inside the mould plates, a 25 mm distance from the impression to the core insert edges and 50 mm from the latter to the mould edge were used, making the final dimensions of the mould 190×246×232.

The ejection system on this mould consists of nine ejector pins, three for the extraction of the runner system and six for the ejection of the part itself.

Due to needing a change on the injection machine to a Demag NCIII 150, the mould required major changes in order to be used in this machine. Hence, the mould developed possesses two moulding inserts, the core and the cavity, on both sides of the mould, with a similar layout. Nonetheless, the core insert's cooling channel layout was rearranged to move some of the ejectors to provide a better equilibrium during the extraction of the part. Since the injection machine is bigger than previously intended, the structure was also modified. The final mould (Appendix E) used in this laboratorial case study, presented in figure 3-4 has as its main dimensions 296×296×236 mm and was manufactured in a 1.2311 steel.

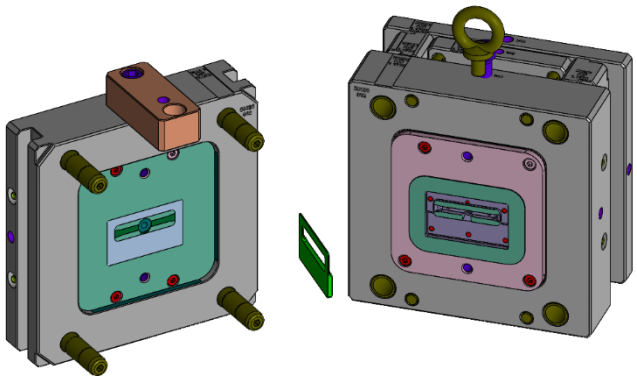

Figure 3-4. – Final injection mould CAD model: Injection side (left); Part (middle); Ejection side (right).

As shown in figure 3-4, this mould allows the exchange of moulding inserts without removing the mould structure from the machine. This flexibility allows an easy and quick exchange of moulding inserts, depending on the geometry of the part to be injected or if alternative materials are needed for the moulding inserts, namely, to produce small series of plastic parts.

3.1.2. Computational numeric simulation

In the present work, computational numeric simulations were made to understand the filling, packing and cooling phases during the injection moulding cycle. With this, it is possible to define the placement of the gates, understand the influence of its dimensions, as well as understand the efficiency of the cooling channels and the moulding surface temperature distribution. It is with the simulations that the effects of part thickness, welding line location and temperature were predicted.

For these studies, the used software was Moldex3D 2021R4OR. When resorting to a software such as the one priorly stated, it is important to know some concepts [47]:

Filling time. It is defined as the time required to fill the cavity with the chosen material in its entirety. A volumetric flow rate is forwarded to the Moldex3D flow solver based on filling time and cavity volume, considering both part and cold runner(s).

Injection Pressure. Is defined as the maximum available injection pressure.

Injection pressure profile. It is related to the process and details how the filling process will vary during the filling phase of the process. It is given as a pressure variation through time (Pressure vs. time).

Packing time. Specifies the time of the packing stage.

Holding Pressure. This is the maximum holding pressure the machine can deliver.

Packing pressure profile. Like the injection pressure profile, it defines the profile of packing pressure used in the packing stage.

VP Switch-over. This value indicates when the switch-over point from filling to packing should occur, *e.g.*, if it is defined as 98% it means that when that percentage of the cavity's volume is filled the process changes from the filling stage to the packing stage.

Cooling time. This value is used to define the necessary time to guarantee that the part is ready to be ejected. Its efficiency can be used to determine the quality of the mould.

Volumetric shrinkage. It is a result that shows the distribution of part volume change percentage as the part is cooled from high temperature and pressure to ambient temperature and pressure. Its calculation is based on the PVT relationship of the plastic material. The volumetric shrinkage between two points indicates the degree of linear shrinkage and warpage of a part. This property allows for a quantitative study on warpage.

Before using the software, the CAD files were prepared in Solidworks 2021-22 student edition. This preparation consisted in modelling the part, the runner layout, and the cooling channels layout (figure 3-5).

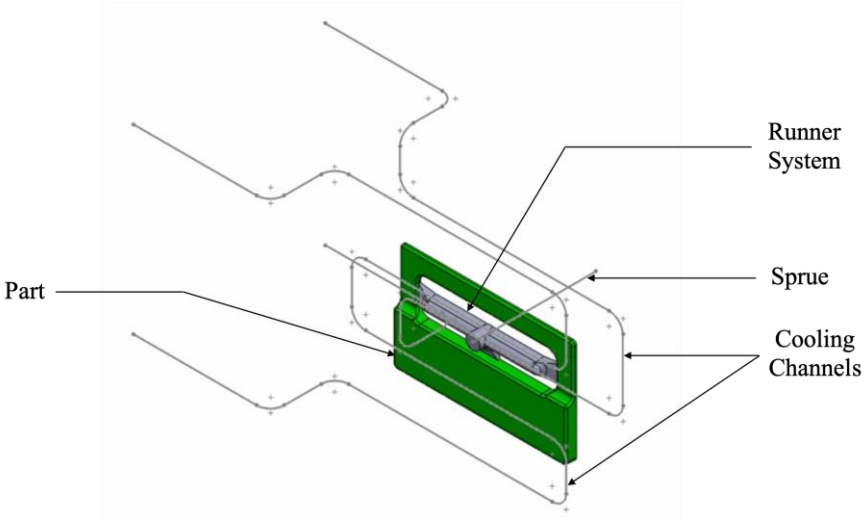

Figure 3-5 – Imported geometries from Solidworks. CAD models of part (green) and runner system (grey); centrelines of cooling channels and sprue.

After this procedure, the part and the runner system were saved in STEP format, and the sprue and layout of the cooling system were saved as IGES files. The previously stated files were then imported to Moldex3D Studio Designer where the geometries were identified as part, sprue, cold runner, gate, and cooling channels according to what was desired for each, as shown below. The diameters were then specified for the sprue and cold runner and cooling channels (figure 3-6).

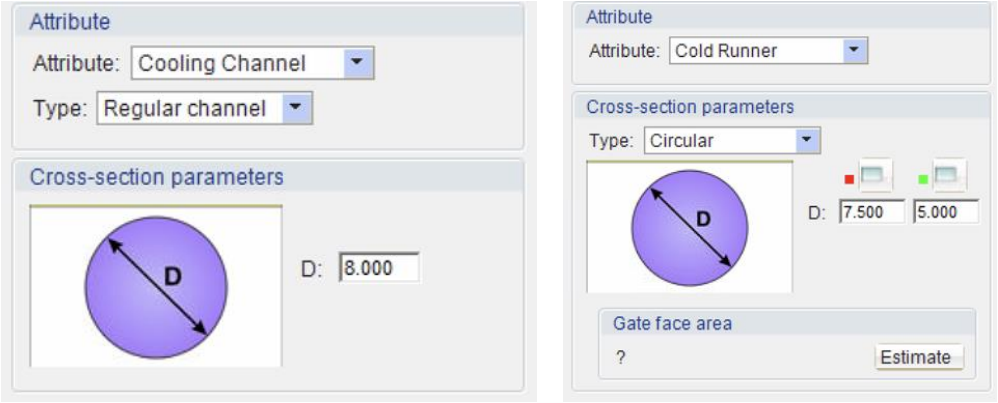

Figure 3-6 – Attributed geometries to cooling channels and sprue in Moldex3D.

After the identification of the geometries, the melt inlet was specified, followed by the definition of the mould base dimensions which are the primary dimensions of the mould. With these steps concluded, the last stage in preparing the model is to define the boundary conditions, which in this case were the inlet and outlet of the cooling system, as shown in figure 3-7.

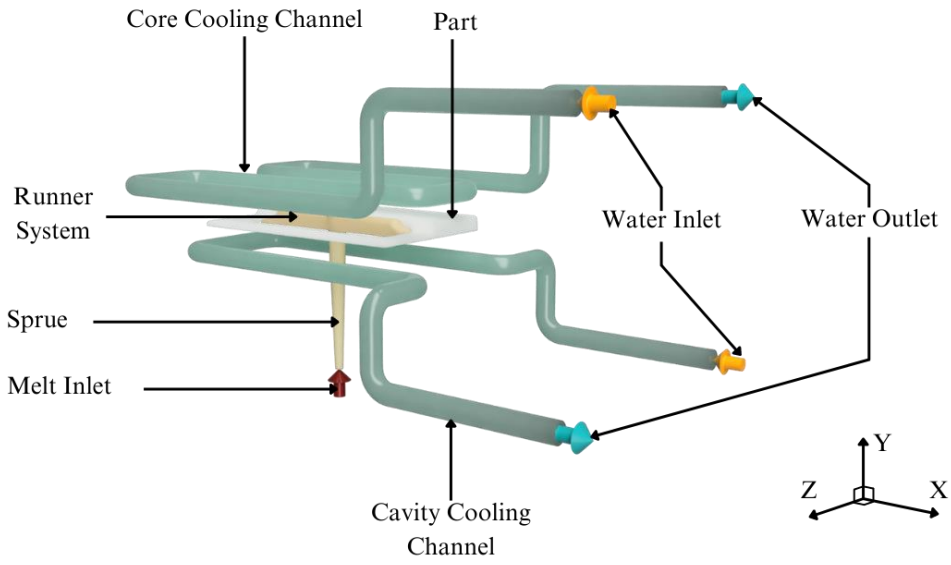

Figure 3-7 – Imported setup of injection system, cooling system and part layout of the laboratorial case study mould.

With the geometries defined, it is necessary to define a mesh, which in this case was made with boundary layer mesh (BLM), a hybrid type of mesh convenient for building grid models and can be used for any shape. According to Wang [40], BLM's "main feature is that the prisms are used on the surface of the product, and the inside is created by tetrahedrons". This allows for a better resolution at the walls and a medium number of elements which in turn allows for better predictions in a relatively short calculation time.

In figure 3-8 the settings used for the simulation's BLM mesh are presented for the geometry, curve and hybrid meshing of part, runner, and cooling channels.

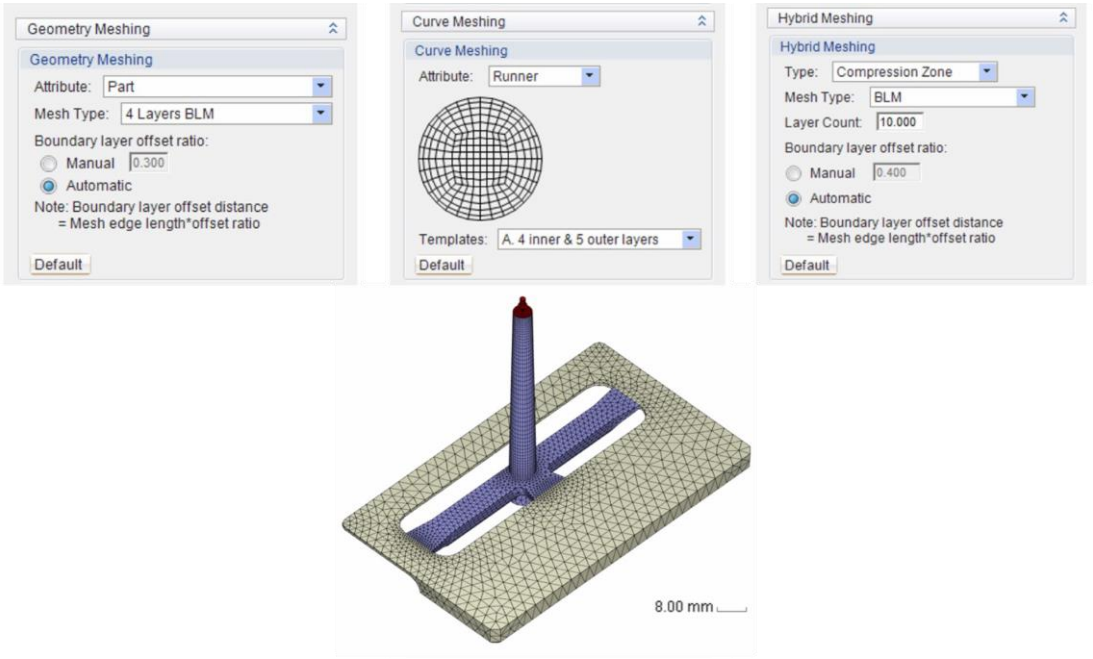

Figure 3-8 – Setup of BLM mesh settings in Moldex3D.

The resulting mesh summary data is presented in table 3.1, which shows the mesh type, the number of elements used, as well as the dimensions of the mould and part, and the volumes of the part and cold runner system.

Table 3.1 – Summary of the mesh used in the Moldex3D simulations on the laboratorial case study.

Item Name	Item Data
Mesh Type	Tetrahedral
Solid Mesh Element Count	815463
Part Elements	22524
Cold runner Element	38260
Part Dimension (mm)	60.72x101.20x6.07
Mould Dimension (mm)	296.00x296.00x243.00
Part Volume (cm^3)	20.78
Cold runner Volume (cm^3)	5.48

After this procedure, the subsequent steps are the selection, in the software's database, of the material to be injected and the processing conditions used to inject the selected material. The processing conditions established when using polypropylene and polystyrene are shown in table 3.2. In this case, the materials used were polypropylene (PP) named

Moplen HP500N (Appendix F) manufactured by LyondellBasell (Rotterdam, Netherlands). Regarding the polystyrene, since the material used for the injection moulding tests is not available in Moldex3D's database, a general-purpose polystyrene was used entitled Polystyrol 143E (Appendix G) from BASF (Ludwigshafen, Germany) which has similar properties to the one used in the injection tests, named Styrolution PS 124N/L (Appendix H) from INEOS Styrolution (Frankfurt am Main, Germany).

Table 3.2 – Process conditions used in Moldex3D simulations.

Filling	**Item Data**	**Unit**
Filling Time	1.05	sec
Melt Temperature	230.00	°C
Mould Temperature	20.00	°C
Max Injection Pressure	240.00	MPa
Injection Volume	26.26	cm^3
Packing		
Packing Time	5.00	sec
Max Packing Pressure	240.00	MPa
Cooling		
Cooling Time	20.00	sec
Mould Open Time	5.00	sec
Ejection Temperature	84.00	°C
Air Temperature	25.00	°C
Cycle Time	31.05	sec

To simulate the process, three profiles must be defined which are the flow rate profile shown in figure 3-9, the injection pressure profile which was defined as 100% of the pressure available and the packing pressure profile expressed as 75% of the injection pressure.

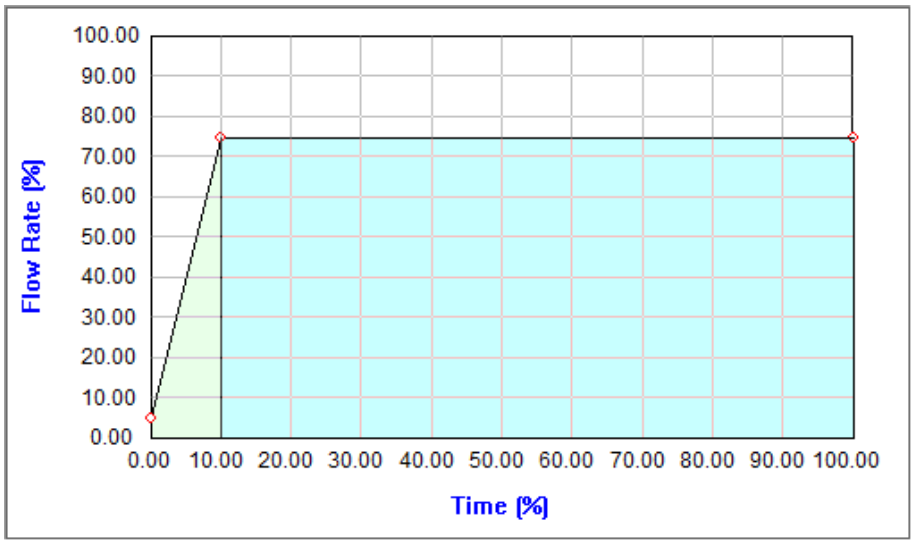

Node	Node-1	Node-2	Node-3
Time (%)	0	10	100
Flow Rate (%)	5	75	75

Figure 3-9 – Profile used for flow rate in the Moldex3D simulations.

3.1.3. Injection moulding tests

The injection tests for this case study were made in a Demag NC III 150 (figure 3-10). This machine has a maximum clamping force of 150 tons and the distance between tie-bars is 460×460 mm.

Figure 3-10 – Injection machine DEMAG NC III 150.

The tests were made using a polystyrene (PS) named Styrolution PS 124N/L from INEOS Styrolution (Frankfurt am Main, Germany), and a polypropylene (PP) named Moplen HP500N manufactured by LyondellBasell (Rotterdam, Netherlands). For the structural foam, a chemical endothermic blowing agent (Appendix I) named Hydrocerol™ ITP 822 from Clariant Plastics and Coatings (Muttenz, Switzerland) was selected. The

injection tests were made using different percentages of blowing agent mixed with both PS and PP all above the degradation temperature of the blowing agent so that the chemical reaction could happen. The injection tests were performed in the mould cavity presented in figure 3-11.

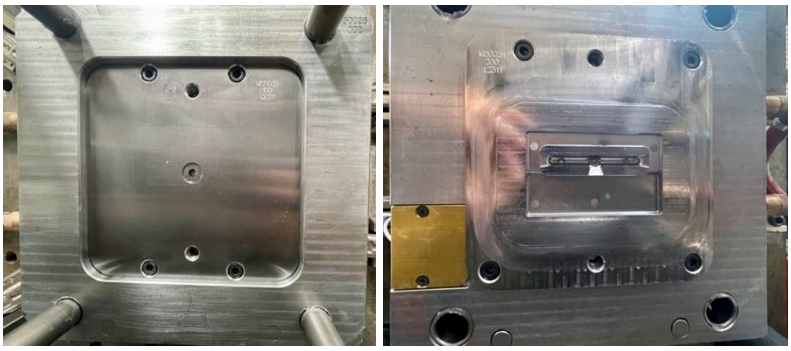

Figure 3-11 – Mould core and cavity used for the injection tests: cavity (left); core (right).

To assess the existing welding lines, the parts were injected with (PS and PP) and without (PS_{BA} and PP_{BA}) blowing agent as shown in table 3.3. The parts were injected with four percentages of blowing agent, namely 0.5% (BA0.5), 0.8% (BA0.8), 1% (BA1.0), and 1.5% (BA1.5), respectively.

Table 3.3 – Process conditions used for the injection process in laboratorial case study (PS and PP).

Var. / Cod.	T_{inj} (°C)	T_{mould} (°C)	P_{inj} (bar)	P_{pack} (bar)	t_{pack} (s)	t_C (s)	Polymer (%)	Blow Agent (%)
BA0.0	210-230	20	50	40	5	25	100	0
BA0.5				–	–		99,5	0.5
BA0.8							99,2	0.8
BA1.0							99	1
BA1.5							98,5	1.5

To evaluate the effects of introducing the blowing agent, the injected components were weighted to understand the amount of mass reduction and further visually compared to understand the blowing agent's effects on the decrease of shrinkage and warpage of the parts, flow marks, burns (black spots), dark spots, and weld lines.

3.1.4. Mechanical tests

For the mechanical tests, the injected parts were cut as depicted in figure 3-12 to provide a test specimen. These specimens were then subjected to Charpy and tensile tests to evaluate these mechanical properties. The machine used for Charpy tests was a RESIL pendulum impact tester from CEAST (Torino, Italy) with a pendulum hammer of 4 Joule with an angle of 140˚. The tensile tests were made using a Zwick Z100 from Zwick Roell (Ulm, Germany) at a speed of 10 mm/min with a distance between grips of 65 mm, and the load cell used was a 10 kN maximum load. These tests were made as a comparison study, meaning that no standard parameters were used.

Figure 3-12 – Example of specimen geometry used in Charpy and tensile tests.

3.2. Industrial case study (S4Plast)

To develop the industrial case study, the consortium of the project S4Plast developed a part (figure 3-13) that possessed multiple thickness steps and some characteristics normal in plastic products such as ribs and clamping pins. To compare with the laboratorial case study, which possesses high thickness variation and the appearance of weld lines, allowing the evaluation of the material behaviour in plastic parts with this type of geometry, this industrial case study was used to further understand and broaden the information about these two subjects. To understand the behaviour of the material and possible ways to mitigate defects, the mould for this part comprises, as a temperature control strategy, conformal cooling channels to implement in parallel with the variotherm technology of RHCM.

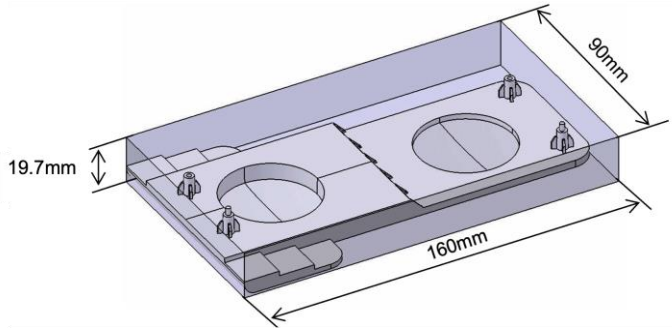

Figure 3-13 – Part developed for the industrial case study from the S4Plast project.

The specifications of the part (figure 3-14) were developed to enable the analysis of different variables and their effects on the visual characteristics of the part. This component

has three zones, the opaque zone, that was divided into high gloss and textured surface finish, and the zone in which transparency required a high gloss finish was defined, as shown in figure 3-14(b).

Initially, it was also intended to evaluate the use of FIM and analyse the effects of thickness variation, however, the latter was the only one that was kept. For this objective, the part processes three thickness zones which are 8 mm, 3 mm, and 1 mm as presented in figure 3-14(a).

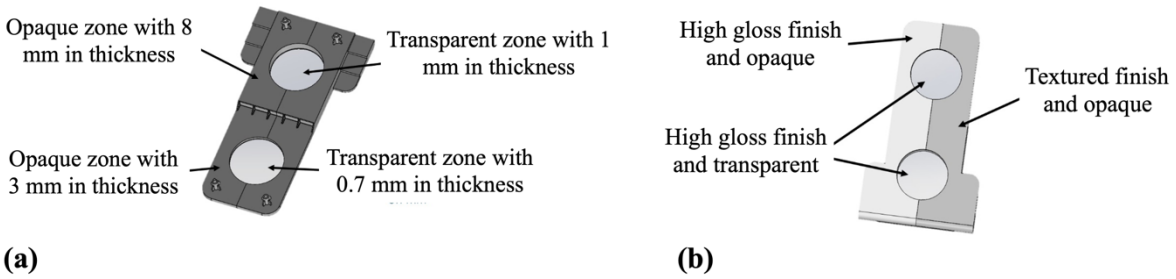

Figure 3-14 – Industrial component specifications for: (a) thickness, and (b) surface finish.

3.2.1. Mould design of the industrial case study

The mould used in this case study follows the same structure as the laboratorial one, the main difference here is the inserts needed to achieve the visual characteristics desired. For density control of the part, which will present itself as changes in transparency, the inserts were manufactured through SLM technology to include the presence of complex cooling channel geometries, as it is possible to see in figure 3-15.

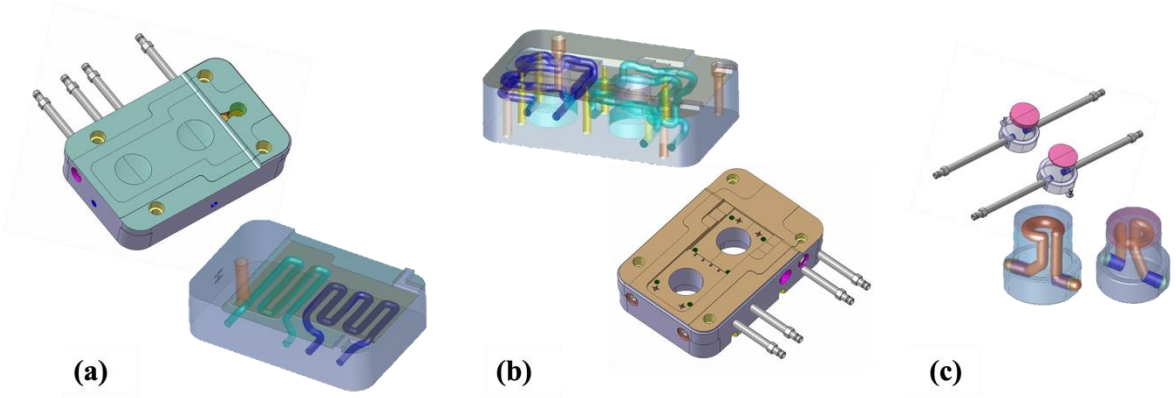

Figure 3-15 – Inserts produced through SLM for heat transfer control and respective inner channels. (a) cavity insert, (b) core insert, (c) core lens inserts.

Through the presence of such channels associated with the use of the variotherm technology, it is possible to have better control of the heat transfer during the injection process. The mould used in this project has the main dimensions of 246×296×290 mm.

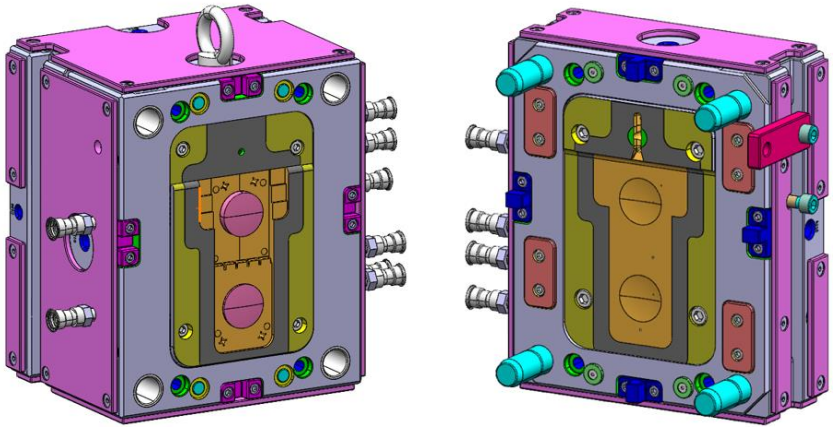

Figure 3-16 – Mould developed for the industrial case study: Core (left) and cavity (right).

This tool uses one cold runner to inject the part and because of it, the sprue is not placed at the centre of the mould. Due to the use of the variotherm technology, this mould uses insolation plates to avoid heat transfer between the mould and the machine's plates. The material selected to make this mould is a 1.1730 steel.

To evaluate some parameters during processing, this mould possesses six PRIAMUS sensors, three temperature sensors of type N (type 4004D1.2-101) and three pressure sensors (one of type 6002B1.2-102 and two of type 6006BC1.2-102). The temperature sensors are placed in the lens and close to the gate, while the pressure sensors are present near the weld lines and in the cold runner.

3.2.2. Computational numeric simulation

As explained for the laboratorial study, CAE simulations were made by resorting to the same software, Moldex3D 2021R4OR, for this case study. Nonetheless, these had a different objective which lies in the evaluation of the layout of the channels and further confirming the decisions on the geometries of the channels, while also aiding in the positioning of the sensors.

To correctly perform the numerical simulations, the feed system must be defined, figure 3-17 presents the selected feed system. Following the same methodology used in the laboratorial case study, the setup of the conformal cooling channels was imported to the software and their diameters were defined, resulting in the setup presented in figure 3-18.

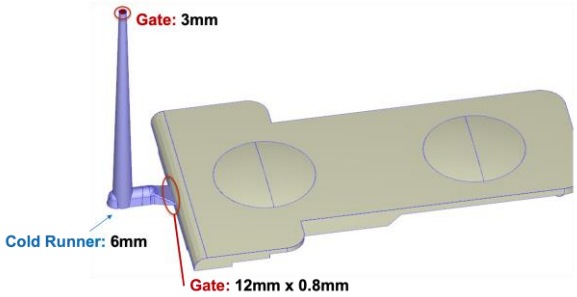

Figure 3-17 – Definition of the sprue, runner, and gate dimensions of the industrial case study.

For better temperature control of the mould, conformal channels were manufactured onto two SLM inserts, which were placed on the rheological simulation software as shown in figure 3-18.

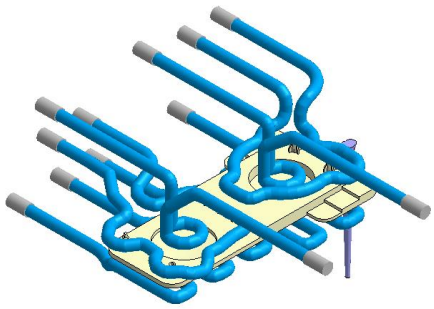

Figure 3-18 – Setup of the conformal cooling channels used in the industrial case study.

The resulting mesh summary data is presented in table 3.4, which shows the mesh type, the number of elements used, as well as the dimensions of the mould and part, and the volumes of the part and cold runner system.

Table 3.4 – Summary of the mesh used on the Moldex3D simulations for the industrial case study.

Item Name	Item Data
Mesh Type	Tetrahedral
No. cooling channel	6
Part dimension (mm)	90.20 x 160.10 x 19.80
Mould dimension (mm)	246 x 296 x 290
Cavity (Part) volume (cm^3)	46.66
Cold runner volume (cm^3)	3.01
Element number	271223
Part elements	185138

Since the material to be used in the case study was not available, a similar one was chosen from Moldex3D's database, resulting in the material presented in Table 3.5.

Table 3.5 – Summary of the material selected for the simulations in the industrial case study.

Item Name	Item Data
Material type	Thermoplastic
Generic name	SAN
Supplier	Trinseo
Trade name	TYRIL 905
MFI (230 ˚C, 3.8 kg) (g/10min)	5
Melt temperature range (˚C)	200 – 250
Mould temperature range (˚C)	25 – 60
Ejection temperature (˚C)	101
Freeze temperature (˚C)	121

The profiles used in this simulation were the same used in the laboratorial case study. The differences were the process conditions (Table 3.6), since the machine used possesses a 180 MPa of maximum injection pressure, the profile was made with 50% of this pressure and the applied packing pressure was 40 MPa.

Table 3.6 – Process conditions used in Moldex3D simulations.

Filling	Item Data	Unit
Filling Time	1.30	sec
Melt Temperature	225.00	℃
Mould Temperature	40.00	℃
Max Injection Pressure	180.00	MPa
Injection Volume	49.67	cc
Packing		
Packing Time	6.00	sec
Max Packing Pressure	180.00	MPa
Cooling		
Cooling Time	25.00	sec
Mould Open Time	5.00	sec
Ejection Temperature	100.85	℃
Air Temperature	25.00	℃
Cycle Time	37.30	sec

3.2.3. Injection moulding tests

Similarly, as made in the laboratorial case study, the injection tests for this case study were injected, although with some differences. The injection machine (figure 3-19) used was a VC 330/80 Tech from Engel (Schwertberg, Austria). This machine possesses a maximum clamping force of 80 tons, this machine does not possess tie-bars due to its mechanisms and has a plate maximum dimension of 670×477 mm. For the variotherm system a setup of two TT-137 temperature controllers from Tool-Temp® (Concord, NC, USA) with a maximum service temperature of 160˚C and a switch-box TT-SB2C from the same brand.

Figure 3-19 – Injection machine VC 330/80 Tech.

The tests were made using styrene acrylonitrile (SAN) resin named TYREL™ 875 (Appendix J) from Trinseo (Wayne, Pennsylvania, USA). The injection tests were performed with different mould temperatures to test the variotherm effects of the injection process. The industrial case study possesses a pair of cylinders above the mould to guarantee an even clamping force during the injection process due to the mould being off-centre with the injection machine (figure 3-20). For the variotherm process, the mould used a temperature for heating and one for cooling, while having another temperature set in the lens, the process parameters are presented in table 3.7.

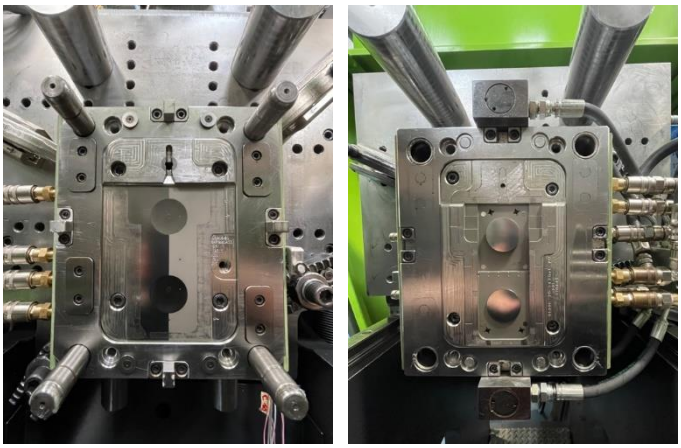

Figure 3-20 – Industrial case study mould assembled into the injection machine.

Table 3.7 – Process conditions used for the injection process in the industrial case study.

Var. / Cod.	T_{inj} (°C)	$T_{mould\ heat}$ (°C)	$T_{mould\ cool}$ (°C)	T_{lens} (°C)	P_{inj} (bar)	P_{pack} (bar)	t_{pack} (s)	t_C (s)
$SAN_{Variotherm}$	220-240	120	20	60	1000	500	20	60
$SAN_{Conventional}$	220-240	60	60	60	1000	500	20	60

To evaluate the effects of the variotherm technology and the other objectives of this case study throughout the injection of the parts a visual analysis was performed to evaluate shrinkage, warpage, weld lines, air gaps, and internal stresses in the part using polarized light.

3.3. Recycling study

The laboratorial and industrial case studies have the main interest in the evaluation of defects and improving the quality of plastic parts. Quality control induces the number of scrap parts, even when high-quality control systems are applied. Together with the number of generated scraps, there is the waste that comes from the injection moulding process, which increases the amount of plastic waste generated by the plastic industry. As stated in section 2.6, the introduction of a circular economy and the objectives established by the EU, demand more knowledge about the effects of recycling on plastic properties.

To address the previous statement a study on mechanical recycling was developed. The main objective of this study is to understand how some types of polymeric materials are affected through the successive use of mechanical recycling. The ultimate goal is to evaluate the variation in thermal and mechanical properties that occur after each cycle of processing while trying to understand to what extent the performance of each of the materials is affected or not. Thus, samples of virgin and recycled materials (polycarbonate, polystyrene, glass fibre reinforced polyamide 6, and polyethylene terephthalate) were obtained by injection moulding to evaluate their thermal behaviour (differential scanning calorimetry), flowability (melt flow rate), and mechanical properties (hardness and tensile tests) [48–54].

The virgin materials used in the present work were two amorphous polymers—polycarbonate (v-PC) named Lexantm Healthcare Resin HP3REU and supplied by SABIC (Riyadh, Saudi Arabia), and polystyrene (v-PS) provided by INEOS Styrolution (Frankfurt am Main, Germany) named Styrolution PS 124N/L—and a semicrystalline one, namely, glass-fibre-reinforced polyamide 6 (v-PA6-GF30) named Ultramid B3EG6 Polyamide 6

from BASF SE (Ludwigshafen, Germany). Since there was interest in also analysing two semicrystalline materials, polyethylene terephthalate (v-PET) was selected due to its high use in the packaging industry, which is associated with a high volume of solid residues. However, although there was the availability of this material, there was not any information about its source. To confirm the presence of the functional groups of PET, Fourier-Transform Infrared Spectroscopy (FTIR) analysis was carried out.

FTIR analysis was performed with an Alpha-P ATR FTIR from Bruker (Billerica, MA, U.S.A.) using a KBr disk. The spectra were collected from 400 to 4000 cm^{-1} with a 2 cm^{-1} resolution on three samples of each virgin material.

3.3.1. Injection moulding

The processing method to obtain the recycled materials was the injection moulding process through a EUROINJ D80 injection machine from LienYu Machinery Co., Ltd. (Tainan, Taiwan) with a clamping force of 80 tons (Figure 3-21).

Figure 3-21 – EUROINJ D80 injection machine.

The materials were injected into a cavity/core with the geometry of tensile and flexural specimens according to ASTM D790-02 and ASTM D638-02A standards [55,56], respectively (figure 3-22). To obtain the first cycle of the recycled specimen (referred to as r1-PC, r1-PA6-GF30, r1-PS, and r1-PET) the virgin material was initially injected. A part of the specimen was kept for density analysis and mechanical testing (hardness and tensile tests), and another was mechanically recycled by grinding. A portion of the recycled granules was saved to evaluate thermal behaviour and the melt flow rate, and the other portion was used to repeat the grinding and injection process to obtain the second cycle of the recycled specimen (referred to as r2-PC, r2-PA6-GF30, r2-PS, and r2-PET).

Figure 3-22 – Example of the geometry of the injected geometry.

The injection moulding processing conditions are presented in table 3.8. Since the materials may degrade or change their properties, such as their melt flow rate, the premise of the setup parameters was to maintain the injection and mould temperatures the same for each group of materials (virgin, cycle 1 recycled, and cycle 2 recycled).

Table 3.8 – Injection moulding processing conditions in recycling study.

Injection Parameters	**PC [1]**	**PS**	**PA6-GF30 [2]**	**PET [3]**
Injection Temperature (°C)	270 ± 15	230 ± 15	225 ± 15	255 ± 15
Mould Temperature (°C)	85	40	65	70
Injection Pressure (MPa)	10	10	10	10
Packing Pressure (MPa)	8	8	8	8.5 [4] / 8 [5]
Packing Time (s)	5	4	3	20 [4] / 4 [5]
Cooling Time (s)	50	25	35	50

[1] Material previously dried for 4 hours at 120 °C. [2] Material previously dried for 4 hours at 83 °C. [3] Material previously dried for 12 hours at 140 °C. [4] Parameters for v-PET. [5] Parameters for r1-PET and r2-PET.

3.3.2. Density

Density measurements were obtained through a Mettler Toledo's AG204 (Greifensee, Switzerland) scale and performed according to the ISO 1183-1:2019 standard [57] by using the immersion method. The temperature of the distilled water was 23 °C for the PS samples and 24 °C for the rest of the materials. To understand if there was any variation in density after each recycling process, five tests were performed for each material.

3.3.3. Differential Scanning Calorimetry

Differential Scanning Calorimetry (DSC) analysis was carried out to evaluate the thermal behaviour of the virgin and recycled samples, namely glass transition and melting and/or crystallisation temperatures, using a DSC 124 Polyma from NETZSCH (Selb, Germany) equipment. The samples (11–15 mg) were placed on metal crucibles, and then the

measurements were performed in two runs in an inert gas atmosphere (N2) at a heating rate of 10 °C/min from 20 °C to 300 °C, the second run was intended to delete the material's thermal history, and this is where the value for Tg (glass transition temperature) was taken from.

3.3.4. Melt-Mass Flow Rate

The melt-mass flow rate (MFR) was determined by a Ray-Ran 6 MBA by the DKSH Group (Zurich, Switzerland), where the same conditions were used for each type of virgin and recycled samples. PC samples were tested with a load of 1.2 kg at 300 °C, PA6-GF30 samples were subjected to a 2.16 kg load at 235 °C, PS samples were tested with 5 kg at 200 °C, and PET samples were tested with 2.16 kg at 260 °C. All tests followed ASTM D1238-13 [58].

3.3.5. Hardness (Shore D)

The Shore D hardness measurements of each material followed the ISO 868:2003 standard [59]. The measurements were taken at the 15 s mark. The equipment used for the analysis was the Shore D Härteprüfer HP series by Bareiss (Oberdischingen, Germany). To execute the test, a 5 kg.f weight was applied at room temperature.

3.3.6. Mechanical Analysis

To perform the tensile tests, the machine used was a Zwick Z100 from Zwick Roell (Ulm, Germany). The tests were performed at room temperature without drying the samples.

The system recorded both the load applied and the displacement of grips automatically. The tests were performed through the application of displacement-controlled loading. The test speed used in all materials was 5 mm/min with a distance between grips of 100 mm, and the load cell used was a 10 kN maximum load. The mould cavity used for injecting the samples followed the basis of the ASTM D638-02A standard [56], and therefore the specimens used were of type I.

To obtain the stress–strain curve, the tensile stress was calculated as the force related to the initial cross-section area of the gauge length of the tested sample. The standard also defines tensile strength as the maximum recorder tensile stress and elongation at break as the gauge length deformation at break. For these tests, the effect of transverse deformations of the sample during the test was not considered.

4. Results and discussion

4.1. Laboratorial case study

4.1.1. CAE results

The objective of the Moldex3D simulations is to predict the way that the part will be filled. With these results, is possible to gain a better insight in what concerns the gate placement, particularly if it will create the expected weld line and predict at which angle and temperature this will form. Another objective of using these simulations is to understand the efficiency of the cooling channels and, if needed, changing the layout. This efficiency will affect the amount of material above the melting temperature and the ways that the part will warp and shrink. It is possible to visualise how the cavity will be filled and the time necessary to achieve a complete fill.

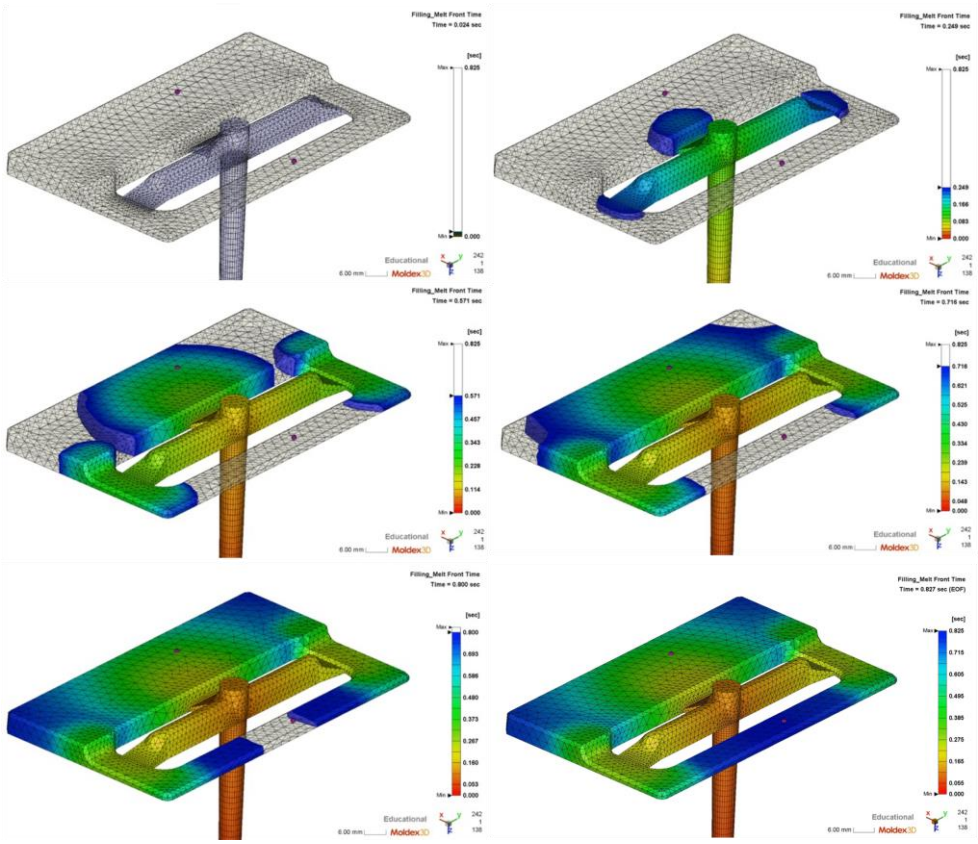

Figure 4-1 – Filling melt front time progression along the injection process processing.

As it is possible to see in figure 4-2, the central gate will allow for filling around 67% of the part which is important for the use of the blowing agent, since the interest is that this gate fills most of the 6 mm zone. The side gates were designed to create a weld line in the area where red and blue regions intersect.

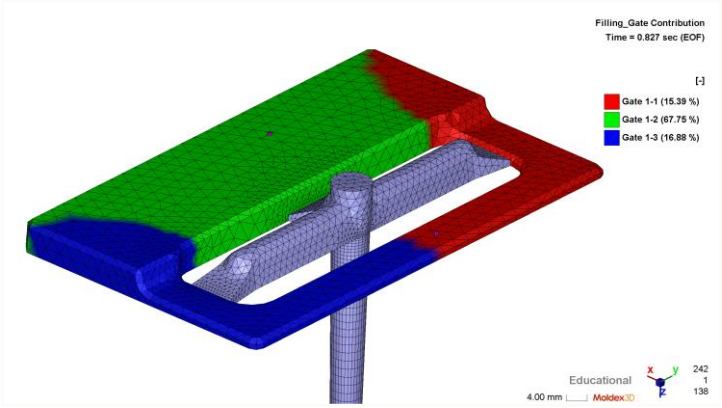

Figure 4-2 – Percentage of contribution from each gate for filling the part.

The simulation results show the formation of three weld lines, as presented in figure 4-3. These show that the intended purpose of creating a weld line in the middle of the lower thickness zone is achieved close to the 90° angle as envisioned and will be created at an average temperature of 230°C (table 4.1) which will be close to the injection temperature.

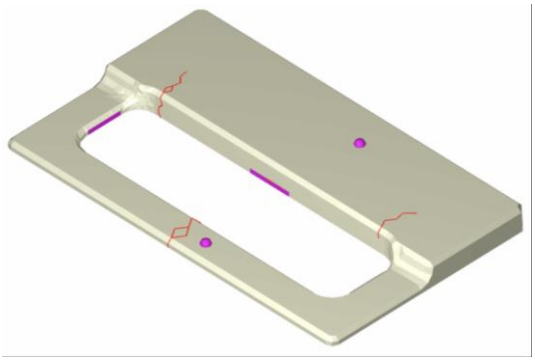

Figure 4-3 – Simulation prediction of weld lines' location.

Table 4.1 – Weld lines formation angle and temperature for the simulation setup.

	PS		**PP**	
	Minimum	**Maximum**	**Minimum**	**Maximum**
Formation angle (deg.)	49.4	142.3	61.8	136.4
Temperature (˚C)	228.1	230.4	226.2	229.9

When analysing the efficiency of the cooling channels (figure 4-4) it is possible to see that the core channel has a higher (~50%) efficiency than the cavity's (~41%), this happens due to the location of the sprue, which does not allow for a better layout of the conventional channels. However, this difference is not meaningful enough to change the way the part cools down, and the way it will warp and shrink.

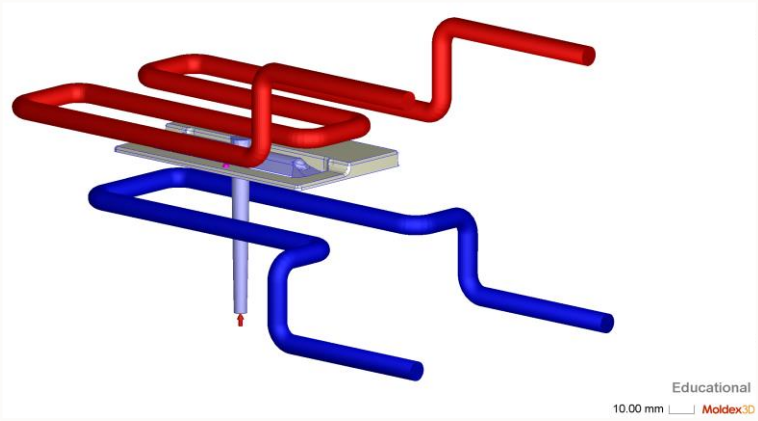

Figure 4-4 – Conventional cooling channels efficiency for mould temperature control.

One of the extracted results is the amount of material which is still above the melt temperature. Parts with high differences in thickness will have a variation in injection and cooling conditions throughout the process, since the properties of the flow change as well as cooling time, for example. The results in this study show, due to a high thickness zone, at the end of the cooling phase there will still exist a high volume of molten material in the 6 mm zone, as seen in figure 4-5.

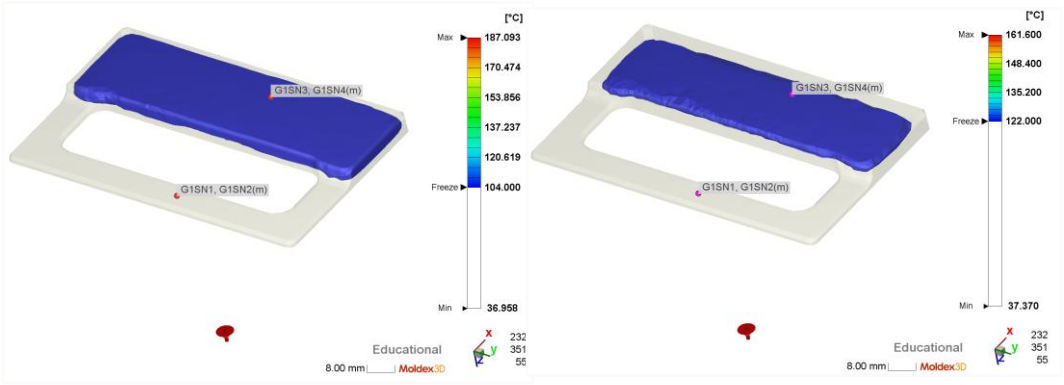

Figure 4-5 – Molten core at the end of the cooling phase. Polystyrene (left); Polypropylene (right).

After the cooling phase, there is still an analysis which is important for defect detection, the warpage analysis. This analysis allows an understanding of the degree of shrinkage and the direction of the part warpage. The results show a maximum volumetric shrinkage of 9% and a minimum of 1% in PS and 13% and 5% in PP, respectively. It is also possible to understand that the part will have a warpage in the x, y, and z directions, as shown in figure 4-6, and that this will have a higher magnitude in the injection of polypropylene.

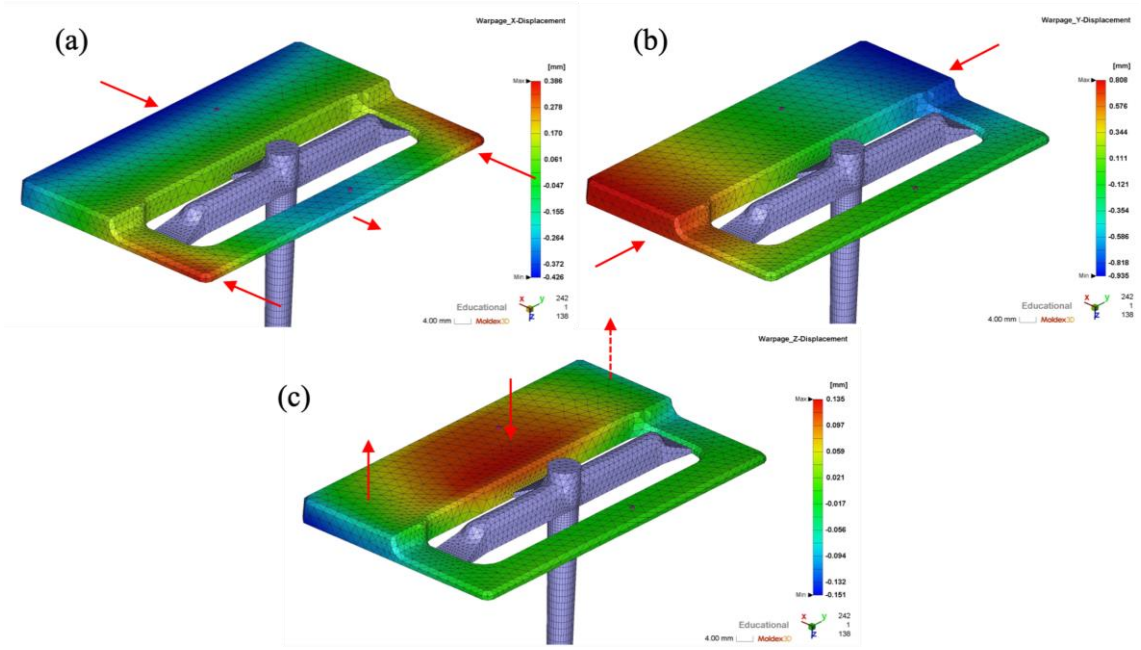

Figure 4-6 – Warpage results in: (a) x-direction; (b) y-direction; and (c) z-direction.

To provide a better comparison and understanding of the pressure and temperature progression throughout the injection moulding process, sensor nodes were placed in the zones where the sensors were machined in the mould, the pressure sensor in the thicker zone and the temperature sensor near the centre weld line. With these sensor nodes, it was possible the obtain the temperature and pressure progression throughout the injection process for both PS (figure 4-7) and PP (figure 4-8).

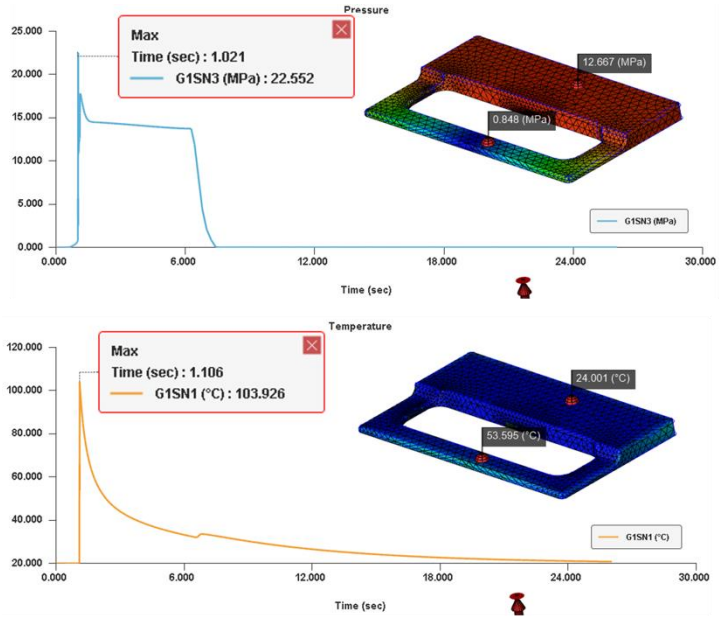

Figure 4-7 – Moldex3D plots for sensor node pressure (blue) and temperature (orange) for the PS simulation.

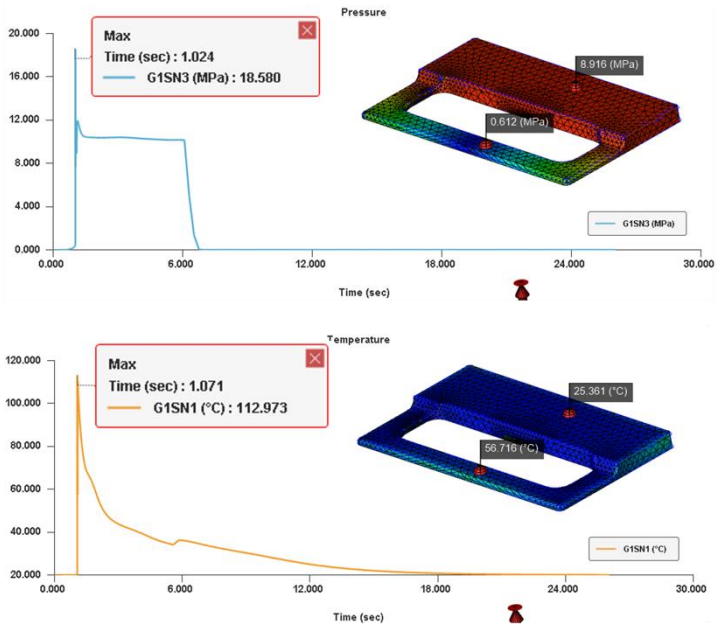

Figure 4-8 – Moldex3D plots for sensor node pressure (blue) and temperature (orange) for the PP simulation.

CAE simulations use mesh nodes to obtain the values for both pressure and temperature, while experimentally the sensor used is of type piezoelectric for pressure and thermocouple for temperature. This means that the type of response is very different. However, the pressure maximum value obtained from the simulations is very close to the experimental value as it is possible to see in Figure 4-12 and Figure 4-19. Nevertheless, in the case of temperature, the values differ from the simulation to the experimental values. Usually, it is assumed that perfect contact with no thermal resistance between neighbouring objects occurs which simplifies the cooling simulations. In most real cases, microscopic gaps always exist which cause resistance. The contact between plastic and mould is complex and can vary along the moulding process. To mitigate this Moldex3D uses a tool called HTC (Heat Transfer Coefficient), which allows to easily consider the thermal resistance of the interfaces, which accounts for the existing air gaps on the interface due to the high viscosity of polymer melt (figure 4-9). However, this tool does not completely solve the real sensors issue since the thermocouple has a contact diameter and the sensor node uses a mesh point in the 3D model.

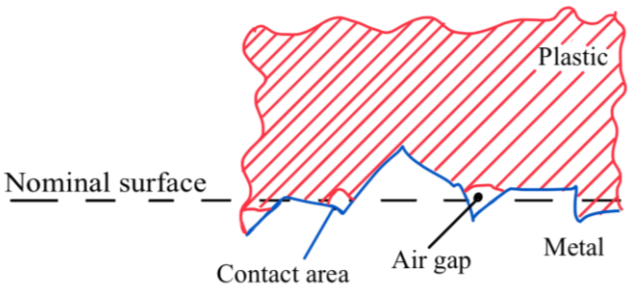

Figure 4-9 – Schematic example of plastic and mould contact interface

4.1.1. Injection moulding tests

As mentioned in sub-section 3.1.3, the plastic parts were produced in PS and PP with and without the addition of a blowing agent.

The results from the injected polystyrene show a high degree of shrinkage and warpage, as already detected in the simulations while resulting in a reduction of time cycle due to the non-existent packing pressure. Due to the high thickness of 6 mm, the first injected parts exhibit two voids near the gate, as shown in figure 4-10a. This was solved by changing the injection speed resulting in its extenuation (figure 4-11). As expected, it is also possible to identify the three weld lines due to the melt front interception due to the presence of the three gates (figure 4-10b,c).

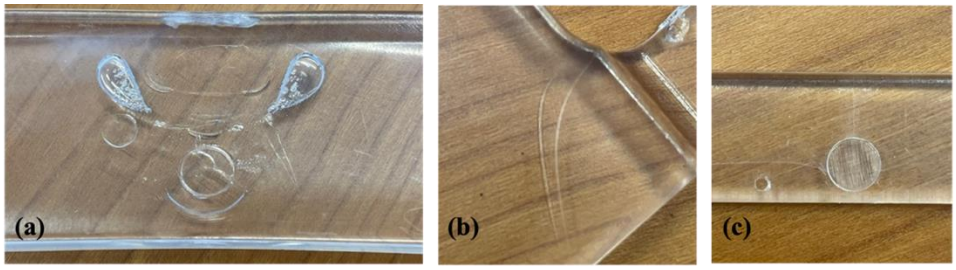

Figure 4-10 – Defects detected in the first injection tests of PS.

Figure 4-11 – Parts injected in PS and effects of changing injection speed. Voids (left) and their mitigation (right).

The injection process of the PS parts shown above were evaluated through the pressure and temperature sensors, figure 4-12. As already explained, the temperature sensor does read an extremely low temperature as the maximum melt temperature, this might be explained by the fact that the sensor used is a thermocouple which tends to "effectively measure the mould surface temperature rather than the melt bulk temperature" [60].

The literature identifies that in-mould temperature reading is a challenging task, mainly when using thermocouples. The justification for this is that the temperature sensor is embedded in the metal of the mould which results in heat being transferred from the nearby metal to the sensor head. Consequently, heat transfer may result in significant phase lag and steady-state error in the measurement of the melt bulk temperature.

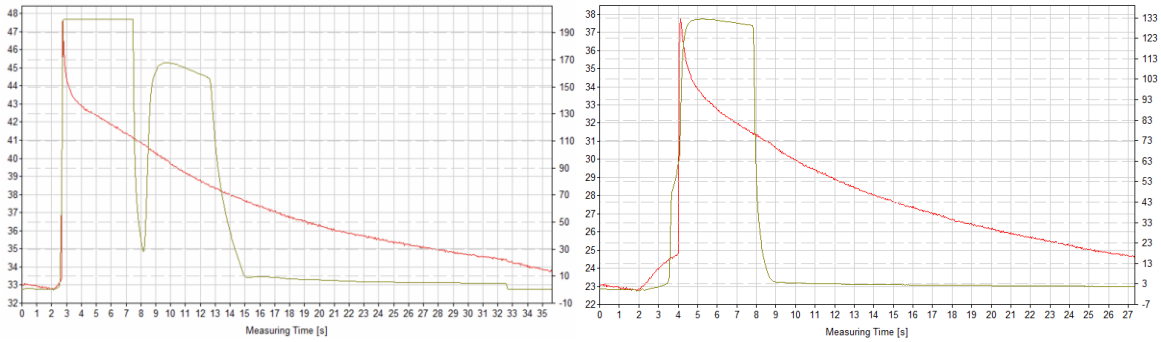

Figure 4-12 – Example of a plot of the injection process of PS (left) and PS-BA (right). Temperature (maximum of 40.4 ˚C and 37.6 ˚C) reading in red and pressure (maximum of 199.3 bar and 130.0 bar) in green.

By analysing the pressure curve in figure 4-12, it is also possible to detect a drop followed by a new peak in pressure, this may be a result of the 6 mm thickness gate not freezing which results in material entering the mould when the plasticizing occurs. The introduction of the blowing agent shows a decrease in the cycle time of 9 seconds per injection.

The introduction of the blowing agent to create a foam is immediately noticeable in PS, since the addition of 0.5% of the blowing agent, the material loses all transparency/ translucency. It is also possible to conclude that the blowing agent decreases the effect of shrinkage and warpage with the increase in the blowing agent (figure 4-13).

Figure 4-13 – Top view of PS parts with and without blowing agent. PS, PS-BA0.5, PS-BA0.8, PS-BA1.0, and PS-BA1.5 (shown left to right and top to bottom).

Polarized light allows an understanding of the internal stresses on the part after ejection (figure 4-14). By analysing these results, it is possible to understand the internal stresses that come from the transition from gates to part, the 2 mm zone also identifies accumulated stress on the 90˚ transition. It is possible to visualise the location where the flow merges, which is placed in the middle of the part, and the merge of both melt fronts creates the weld line. Both PS and PS-BA0.5 identify similar stresses.

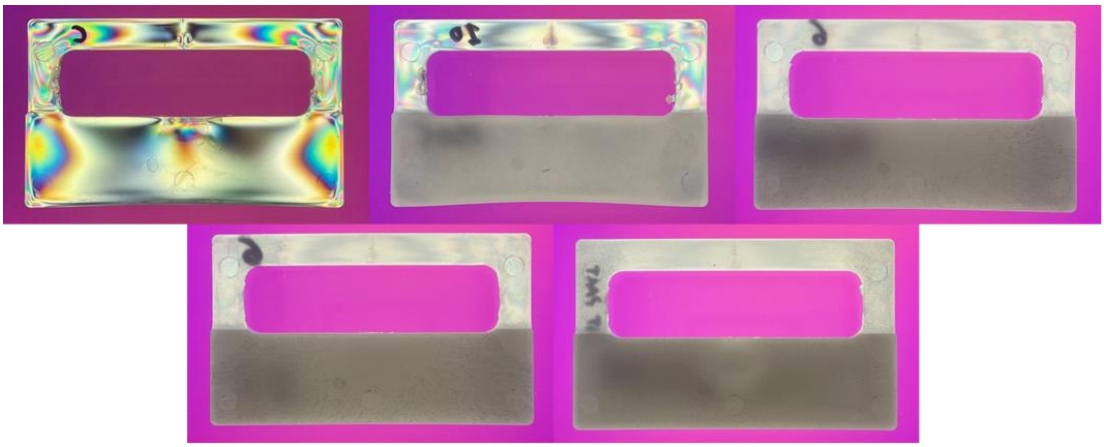

Figure 4-14 – PS parts subjected to a polarised light filter for the identification of internal stresses.

When analysing the polypropylene injected parts, two things are immediately identified, the degree of shrinkage and warpage in the 6 mm zone (figure 4-15), it is also possible to locate the weld lines in the same regions of the polystyrene parts (figure 4-16).

Figure 4-15 – Parts injected in PP and resulting shrinkage and warpage.

Figure 4-16 – Welding lines zones of parts injected in PP.

To obtain the structural foam, a mixture between PS or PP and the blowing agent was made using a scale and mixing the blowing agent by hand before placing it into the injection unit as shown below in figure 4-17.

Figure 4-17 – Mixing process of the blowing agent.

When the PP part is backlit, there is a noticeable darker smudge in the thicker zone, as seen in figure 4-18. This smudge is the result of non-uniform cooling due to its high thickness. Since cooling is non-uniform, when the material starts to shrink, the outer surface will be cooled down much faster than the core which creates a vacuum zone.

As is the case in PS, in PP the same phenomenon of pressure drop occurs when plasticizing starts, and the same for the temperatures registered by the temperature sensor (Figure 4-19). The curve of blowing agent addition also shows a decrease in the cycle time of 9 seconds.

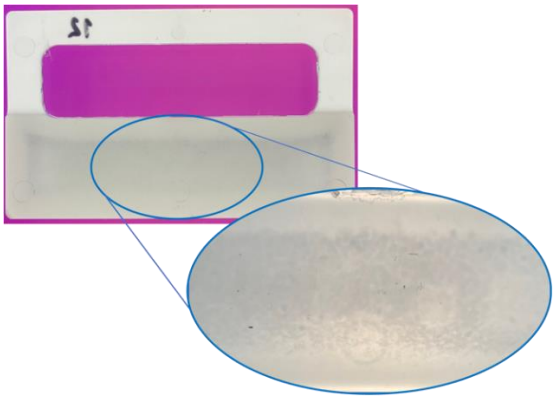

Figure 4-18 – PP part's smudge with air bubbles

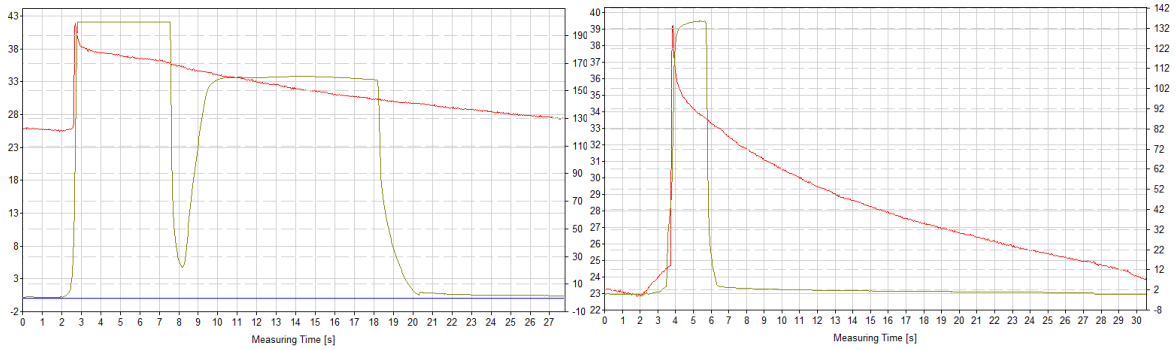

Figure 4-19 – Example of a plot of the injection process of PP (left) and PP-BA (right). Temperature (maximum of 41.8 ˚C and 36.2 ˚C) reading in red and pressure (maximum of 199.3 bar and 136.0 bar) in green.

The analysis of the introduction of the blowing agent to PP is almost non-noticeable for the 0.5% mixture (figure 4-20), and since this part was not injected with packing pressure the sink marks become more evident than the ones present at the PP part (figure 4-20).

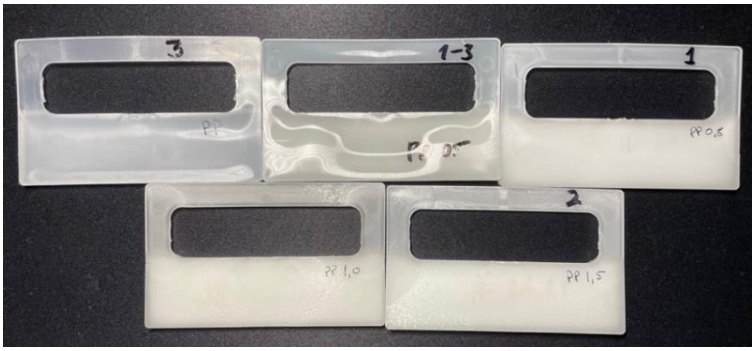

Figure 4-20 – Top view of PP parts with and without blowing agent. PP, PP-BA0.5, PP-BA0.8, PP-BA1.0, and PP-BA1.5 (shown left to right and top to bottom).

Although all the other three mixtures (0.8%, 1% and 1.5%), are evident on the part, one thing that must be identified is the percentage increase, by using the polarised light as a back-light, it is possible to understand the increase in air in the 6 mm zone due to its opacity (figure 4-21). Just as with the PS injection, the mixture of 1.5% shows the presence of over effect of the blowing agent, creating a non-flat surface in the 6 mm zone.

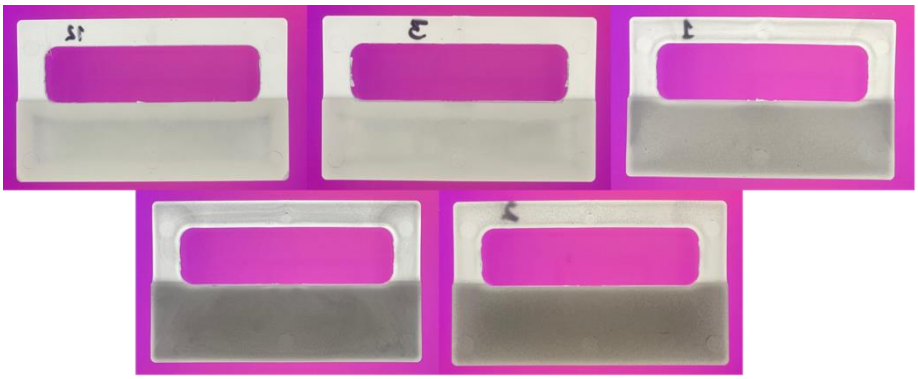

Figure 4-21 – PP parts subjected to a polarised light filter for the identification of internal stresses.

The effects of the blowing agent onto the parts were analysed in two ways, by weighting three parts of each mixture, which in theory should decrease with the increase in blowing agent percentage (table 4.2 and table 4.3), and through the measurements, using a micrometre, in each part in three different locations, named BE1, BE2, and BE3, as shown in figure 4-22.

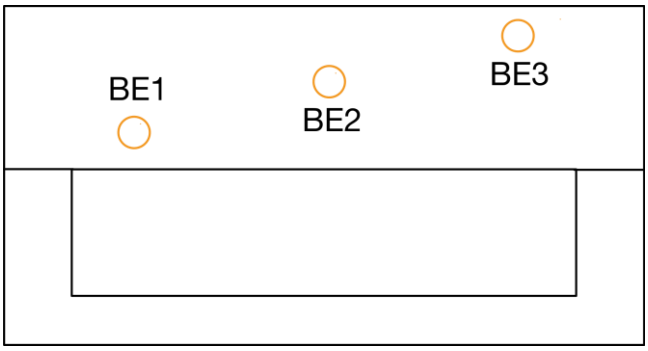

Figure 4-22 – Location for measuring the effect of the blowing agent on the thickness and flatness of the part surface.

The weight evaluation of the parts shows a decrease in weight with the addition of the blowing agent as expected. Nonetheless, the degree of weight reduction is very similar for each of the percentages used. This means that the advantage of a specific percentage, in this case, is related to the effect on the part finish.

Table 4.2 – Weight reduction evaluation in the PS parts.

		PS	***PS-BA0.5***	***PS-BA0.8***	***PS-BA1.0***	***PS-BA1.5***
Mass (g)	**m1**	21.16	20.82	20.85	20.85	21.30
	m2	21.17	20.81	20.83	20.91	20.92
	m3	21.22	20.79	20.86	20.89	20.94
	Mean	**21.18**	**20.81**	**20.85**	**20.88**	**21.05**
	SD	**0.03**	**0.01**	**0.01**	**0.02**	**0.17**

Table 4.3 – Weight reduction evaluation in the PP parts.

		PP	***PP-BA0.5***	***PP-BA0.8***	***PP-BA1.0***	***PP-BA1.5***
Mass (g)	**m1**	17.06	16.40	16.54	16.69	16.50
	m2	17.08	16.43	16.47	16.50	16.51
	m3	17.02	16.48	16.41	16.41	16.50
	Mean	**17.05**	**16.44**	**16.47**	**16.53**	**16.50**
	SD	**0.02**	**0.03**	**0.05**	**0.12**	**0.00**

The analysis of the effects of the blowing agent on the thickness of the parts (table 4.4), shows that when comparing the PS parts with the respective blowing agent equivalents, the effects on part thickness are not beneficial above 0.5%, since the part does not maintain its flat surface in the 0.8, 1.0 and 1.5 % mixtures. In the case of PP, the results differ greatly due to the high degree of shrinkage in this material. The results of the PP and blowing agent mixture show that to obtain a flat surface the mixture of 0.8 allows for a better finish.

Table 4.4 – Blowing agent effect on part thickness (mm).

Blowing agent (%)	*PS*			*PP*		
	BE1	**BE2**	**BE3**	**BE1**	**BE2**	**BE3**
0	5.94	6.17	5.94	5.75	5.88	6.07
0.5	6.07	6.35	6.04	5.85	5.71	5.87
0.8	6.03	6.74	6.51	6.19	5.77	5.95
1	6.48	6.62	6.47	6.30	6.45	6.43
1.5	6.31	7.40	6.38	7.27	8.05	7.32

4.1.1. Mechanical tests

4.1.1.1. Charpy tests

Besides the visual comparison of defects mitigation, to understand the differences between not-using and using blowing agents the specimens were then submitted to Charpy tests, enabling an understanding of the effects of the welding lines in parts. Due to the excessive effect of the blowing agent with a mixture of 1.5% (PP-BA1.5 and PS-BA1.5) on both PP and PS, these were neglected for the Charpy tests. Moreover, since the parts obtained with the 0.8% (PP-BA0.8 and PS-BA0.8) mixture were very similar to the 1% (PP-BA1.0), they first were not accounted for. The tests were made to pure PS and PP and the 0.5% (PP-BA0.5) and 1% mixtures of blowing agent to these materials.

The test specimen was assembled onto the CEAST impact tester by aligning the hammer with the weld line and with the straight surface against the jig walls, as shown in figure 4-23.

Figure 4-23 – Charpy test specimen setup onto the CEAST impact tester.

Table 4.5 – Charpy tests results of energy absorbed using a 4 J hammer in both PS and PP with and without the addition of the blowing agent.

Specimen / Material	Energy absorbed (J)						
	1	**2**	**3**	**4**	**5**	**Mean**	**SD**
PS	0.112	0.096	0.104	0.104	0.096	0.102	0.004
PS-BA0.5	0.104	0.104	0.104	0.128	0.112	0.110	0.010
PS-BA1.0	0.112	0.120	0.104	0.112	0.112	0.112	0.006
PP	1.104	1.264	1.040	1.040	0.520*	1.112	0.129
PP-BA0.5	0.296*	0.262*	0.664	0.552	0.424	0.547	0.072
PP-BA1.0	0.616	0.544	0.488	0.576	0.536	0.552	0.032

*Due to being too discrepant, these values were not considered in the mean calculation.

As shown in table 4.5, the results of the Charpy impact test show that the introduction of the blowing agent to PS introduces a slight increase in the resistance to impact, nonetheless, this increase is so trifling that it is considered neglectable. The same does not apply to PP, which shows a decrease in resistance to impact, as expected. This happens due to the presence of air bubbles inside the plastic part, which reduces the mechanical resistance.

4.1.1.2. Tensile tests

The tensile tests (figure 4-24) show a slight decrease in strength from PS and PP when compared to the respective mixtures of the blowing agent with 0.5 and 1%. This reduction occurs due to the existence of air bubbles inside the plastic part originating, therefore, an easier propagation of fracture, hence slightly reducing Young's modulus and tensile stress. However, this reduction is so slight, that for the 2 mm thickness, it would not become problematic. Table 4.11 shows a summary of the results obtained for Young's modulus and tensile stress for each tested material.

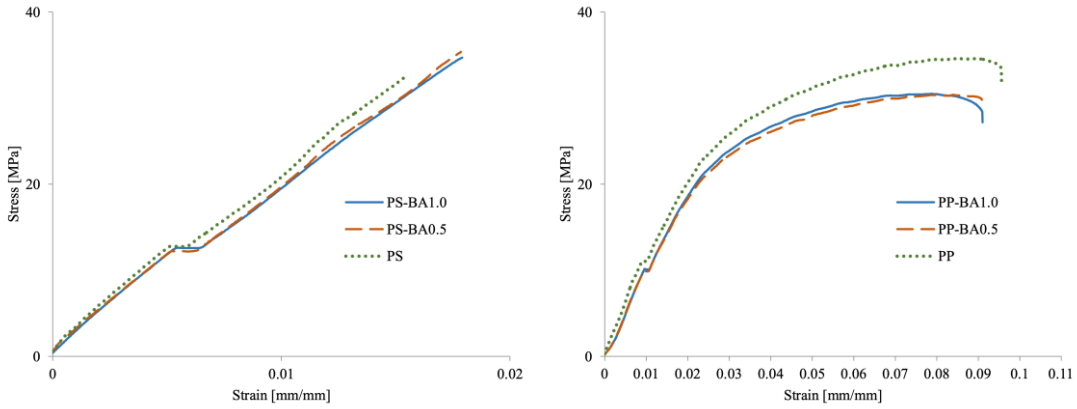

Figure 4-24 – Stress-strain curves for PS, PS-BA0.5, and PS-BA1.0 (left); and PP, PP-BA0.5, and PP-BA1.0 (right).

Table 4.6 – Mechanical properties of polystyrene and polypropylene with and without addition of a blowing agent.

Material	Young's Modulus (MPa)	Tensile Stress (MPa)
PS	2379.3 ± 92.4	12.4 ± 0.3
PS-BA0.5	2291.8 ± 17.6	12.3 ± 0.9
PS-BA1.0	2317.8 ± 21.2	12.1 ± 0.4
PP	1266.8 ± 109.3	11.3 ± 0.2
PP-BA0.5	1044.8 ± 54.9	10.0 ± 0.4
PP-BA1.0	1031.1 ± 55.8	10.0 ± 0.1

4.2. Industrial case study (S4Plast)

4.2.1. CAE results

In this case study, the intent of doing simulations is to predict defects, air traps, weld lines, sink marks and warpage directions. It is also important to understand the way the cavity is filled (figure 4-25).

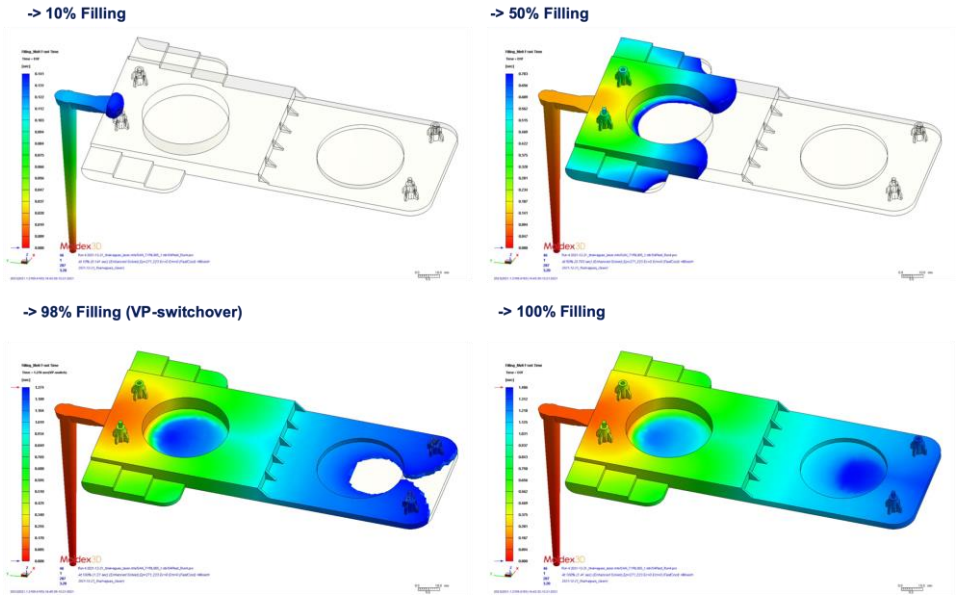

Figure 4-25 – Melt front-time development throughout the filling process.

Due to the thickness difference in the lens, the melt will create problematic air traps since it is not possible to place air vents in these zones (figure 4-26). This is a troublesome defect that appears in parts such as this. Since this part will use the variotherm technology, it is expected that if a certain temperature is reached, the air bubbles will disappear. It is also possible to identify that right after the lens there will be the formation of weld lines.

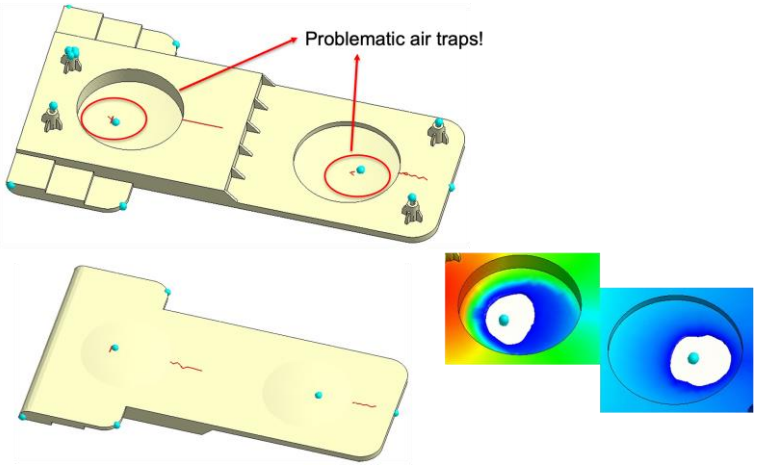

Figure 4-26 – Identification of the problematic air traps and weld lines.

As explained in the laboratorial case study, parts with high thickness will have the presence of sink marks. This fact is related to the non-uniform cooling that happens from the surface to the core of the part. These sink marks will not reach the desired surface finish. In this case, the sink mark displacement will be 0.14 mm which will be noticeable when injected (figure 4-27).

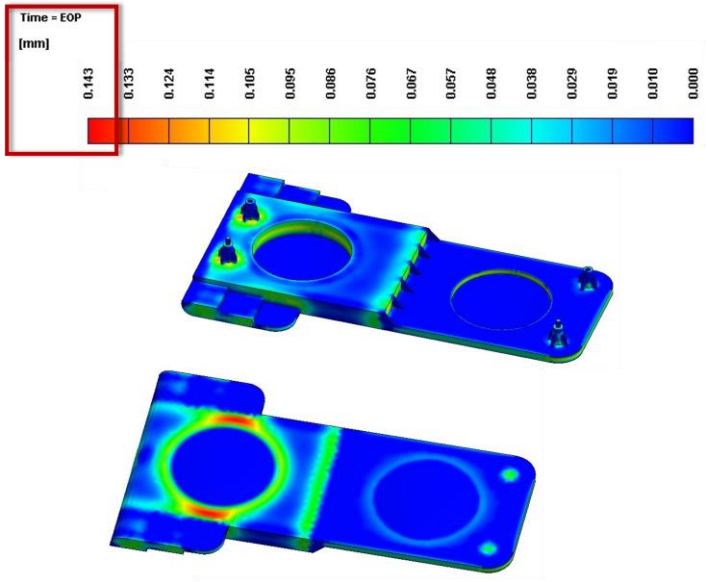

Figure 4-27 – Sink mark displacement in the industrial case study.

To understand the direction in which the part will warp, a warpage study was also performed. With this study, it was concluded that a maximum warpage of 0.26, 0.51, and 0.45 will occur in the x, y, and z directions, respectively (figure 4-28).

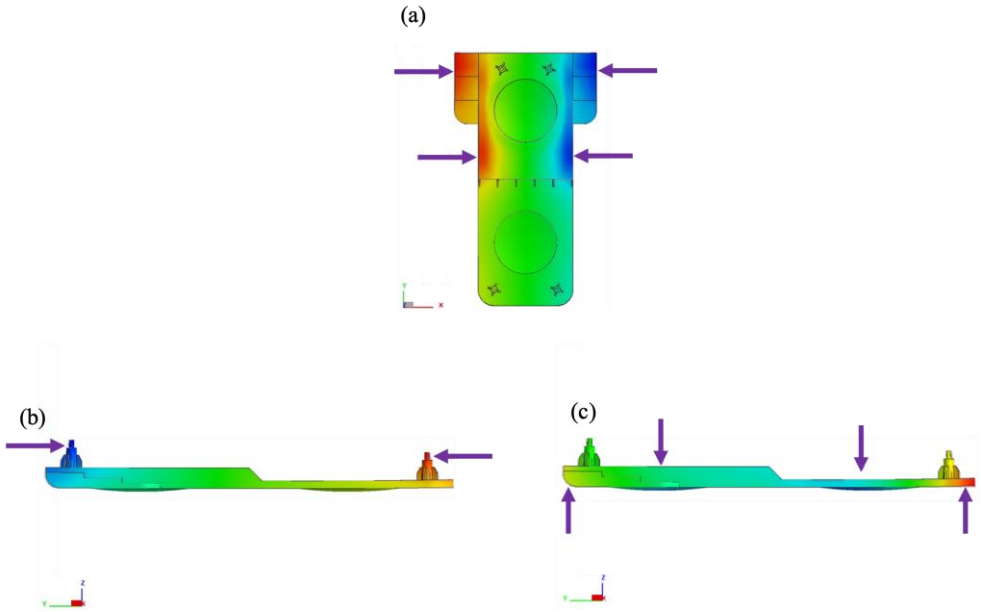

Figure 4-28 – Warpage results in: (a) x direction; (b) y direction; and (c) z direction.

With the results from this simulation, the sensor placement was defined as shown in figure 4-29. The temperature sensors (in blue) in the lens zone allow to understand the effects of temperature variation at this location, and the pressure sensors (in green) enable the study of pressure variation along the part.

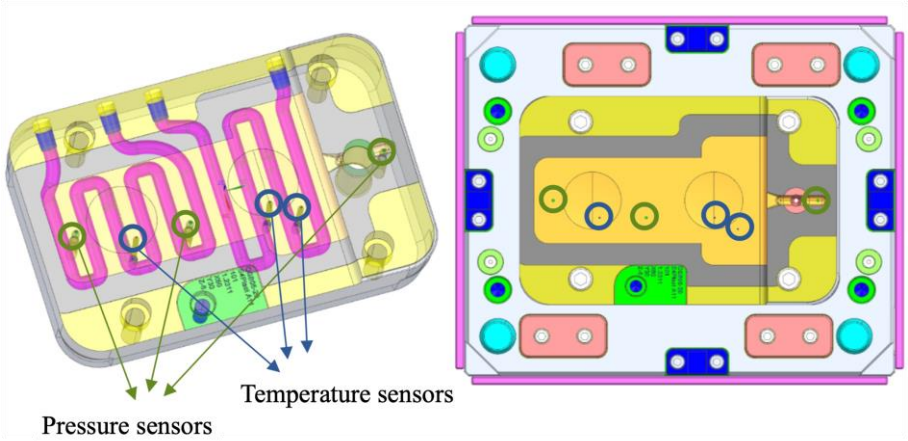

Figure 4-29 – Pressure and temperature sensor placement in the industrial case study.

4.2.1. Injection moulding tests

To assess the variotherm process, the part was evaluated in terms of the existence and lack thereof sink marks. The parts were also submitted to a polarised light to understand the differences in internal stresses between using a constant temperature and the variotherm process.

The results show that the temperatures used in the variotherm process worsen the sink marks due to the high thermal shock in the material when the water switch occurs. Nonetheless, with the help of air vents, the variotherm process allows for the air traps to disappear (figure 4-30).

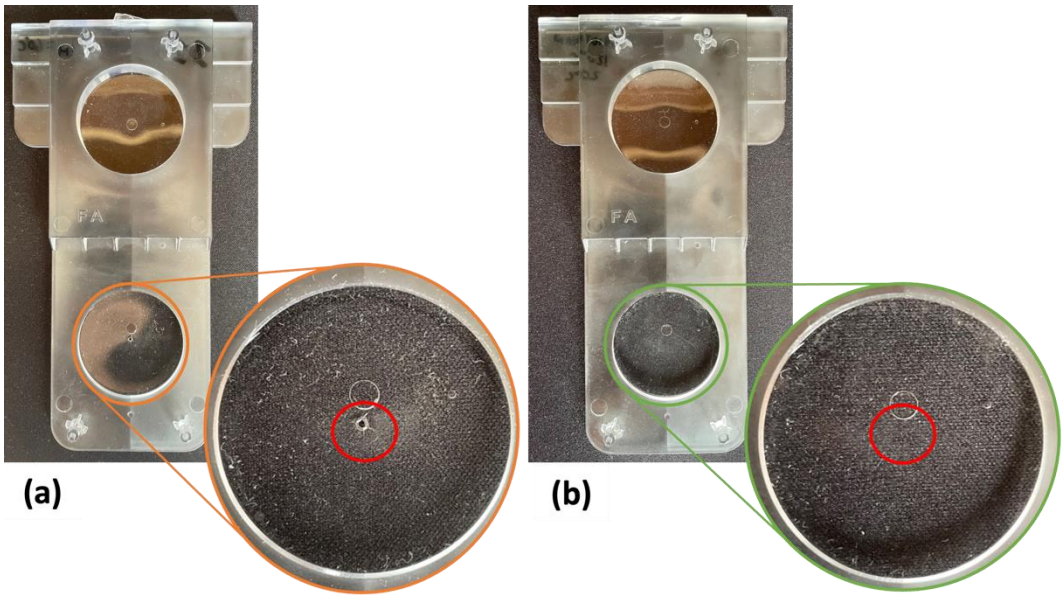

Figure 4-30 – Elimination of the air gap present in the part with conventional injection moulding (a), and its elimination with variotherm (b).

The variotherm process is mainly used to solve defects, however, this comes at the cost of having a longer process cycle, which occurs in this case (~ 60 sec). To allow for the mould surfaces to reach both injection and ejection temperatures, the processing time increases exponentially. Nevertheless, the injection plot results obtained from the sensors (Figure 4-31 and figure 4-32), show that after heating the cavity to the desired temperature, there is a high capacity for heat removal from the cavity using the variotherm process, which allows for reducing the injection pressure and for a longer packing time leading to the elimination of sink marks.

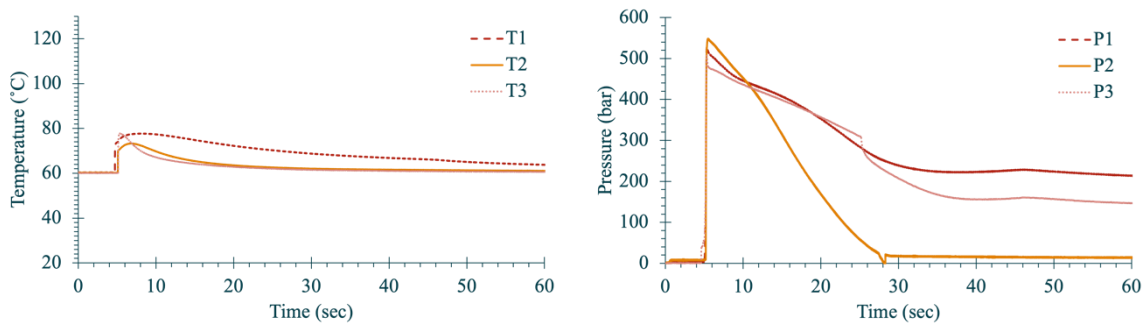

Figure 4-31 – Temperature (left) and pressure (right) sensors plots for conventional injection process using conformal cooling in the industrial case study.

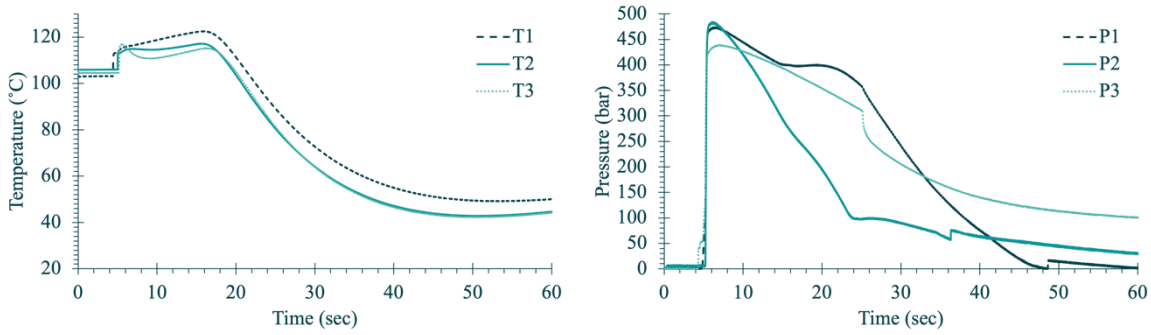

Figure 4-32 – Temperature (left) and pressure (right) sensors plots for the variotherm process combined with conformal cooling in the industrial case study.

Still, there is an interesting result from the exposing of both parts to the polarised light (figure 4-33) which shows that the internal stresses will be magnified with the use of the variothem process. This can be observed through the increase in colour variation of the patterns, which become more evident and closer to each other, mainly on the lens location. The changes might be associated with the thermal shock from switching the temperatures in the variotherm process.

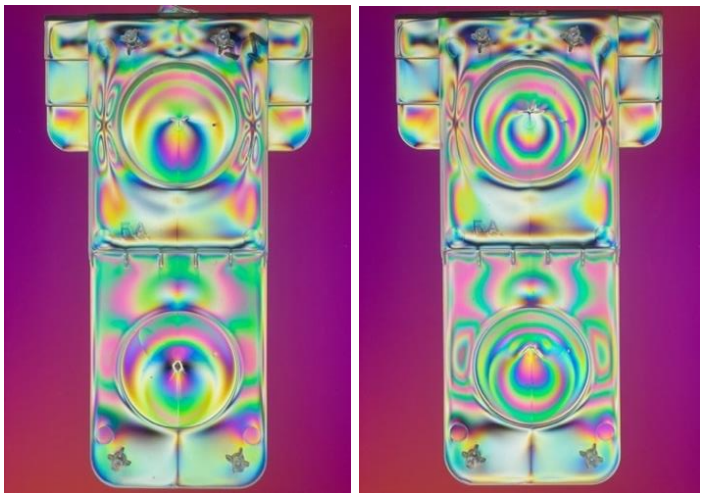

Figure 4-33 – Qualitative birefringence measurement results for SAN parts injected with constant mould temperature (left) and with the variotherm process (right).

The variotherm process must be revaluated in terms of insert cooling channels efficiency, and process time. These are two of the challenges of using this process and must continue to be studied.

4.3. Recycling study

The work developed on the subject of recycling, already mentioned in section 3.3, is analysed and discussed throughout the present section. Each of the results of the analysis and tests executed in this study is shown and analysed in this section. This work resulted in the documents presented in Appendix K.

4.3.1. Injection Moulding

With the injected samples, the first analysis to be done was the optical characteristics of each material. Thermoplastic materials can be of two types: amorphous or semicrystalline. In this work, there are two of each type: PC and PS on the amorphous side, and PA6-GF30 and PET as the semicrystalline ones.

Due to their disorganized chains, amorphous materials are either transparent or translucid materials, which makes one of the desired properties when used in injection moulding. Figure 4-34a,b shows the variability in optical properties in PC and PS, which show a loss of transparency after each cycle and a visible degradation of the material that can be identified through its increased opacity.

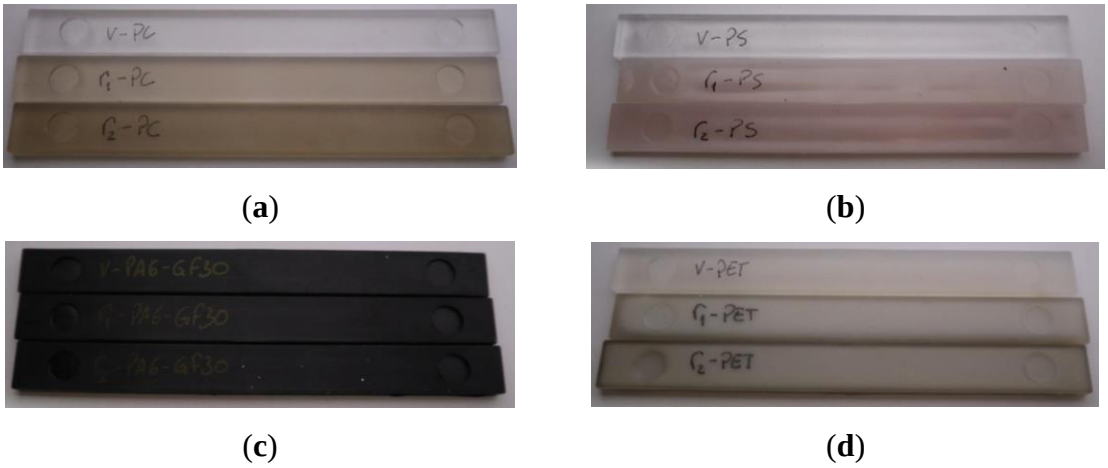

(**a**) (**b**)

(**c**) (**d**)

Figure 4-34 – Examples of the injection-moulded specimens: (a) PC; (b) PS; (c) PA6-GF30; (d) PET.

When looking at semicrystalline materials, the optical characteristics look for is the appearance of a yellowish tone, which may indicate degradation. On the one hand, in PA6-GF30 (figure 4-34c), there is no clear variability by observing the specimens; on the other hand, PET (figure 4-34d) has a particular optical analysis to be done. When looking at the recycled materials, it is possible to see that there is some degradation after each reprocessing cycle through the appearance of a yellow tone and that with the successive processing of the material, this ends up having high changes in its morphology. When looking at the virgin material, is similar to the amorphous material, but when recycled, it starts to lose its transparency, mainly at its core. As described by Lin [61], this may be justified by the fact that PET exhibits a moderate crystallization rate, and when cooled too quickly it will retain its amorphous state since the chains do not have enough time to reorganize. Meanwhile, the recycled materials appear to have time for this reorganization in their core, which might be related to the property found in the DSC analysis defined as “cold crystallization”.

4.3.2. Density Analysis

Table 4.7 shows the density results for each material. As it is possible to understand, there is little variation in density between recycling cycles in PC and PS. In the case of PA6-GF30, due to the shortening of the glass fibres triggered by the mechanical recycling process, an increase in density is expected, which happens because of the decrease in fibre length, resulting in an increase of the fibre weight ratio, i.e., a higher volume of fibres that are denser than polyamide. It is also possible to observe a slight increase in density between each cycle of PET, which may happen due to the decrease in the ability to absorb humidity, as stated by Nadali [62].

Table 4.7 – Density of the studied materials was tested according to the guidelines in ISO 1183-1:2019 [57].

Material	Density (kg/m^3)
v-PC [1]	1199.1 ± 1.6
r1-PC [1]	1196.9 ± 0.5
r2-PC [1]	1197.7 ± 0.4
v-PS [2]	1043.9 ± 0.2
r1-PS [2]	1043.3 ± 0.3
r2-PS [2]	1043.8 ± 0.6
v-PA6-GF30 [1]	1295.8 ± 14.8
r1-PA6-GF30 [1]	1337.3 ± 18.6
r2-PA6-GF30 [1]	1346.3 ± 2.8
v-PET [1]	1331.7 ± 2.6
r1-PET [1]	1346.2 ± 1.5
r2-PET [1]	1359.4 ± 2.0

[1] H_2O density @ 24 °C: 997.5 kg/m^3; [2] H_2O density @ 23 °C: 997.3 kg/m^3.

4.3.3. DSC Analysis

The differential scanning calorimetry results shown in figure 4-35 were performed to understand the eventual degradation in thermal properties. This study tries to understand if it is possible to reuse the material when it is mechanically recycled, only considering thermal properties. In other words, if the processability of the material remains intact or if it has meaningful changes.

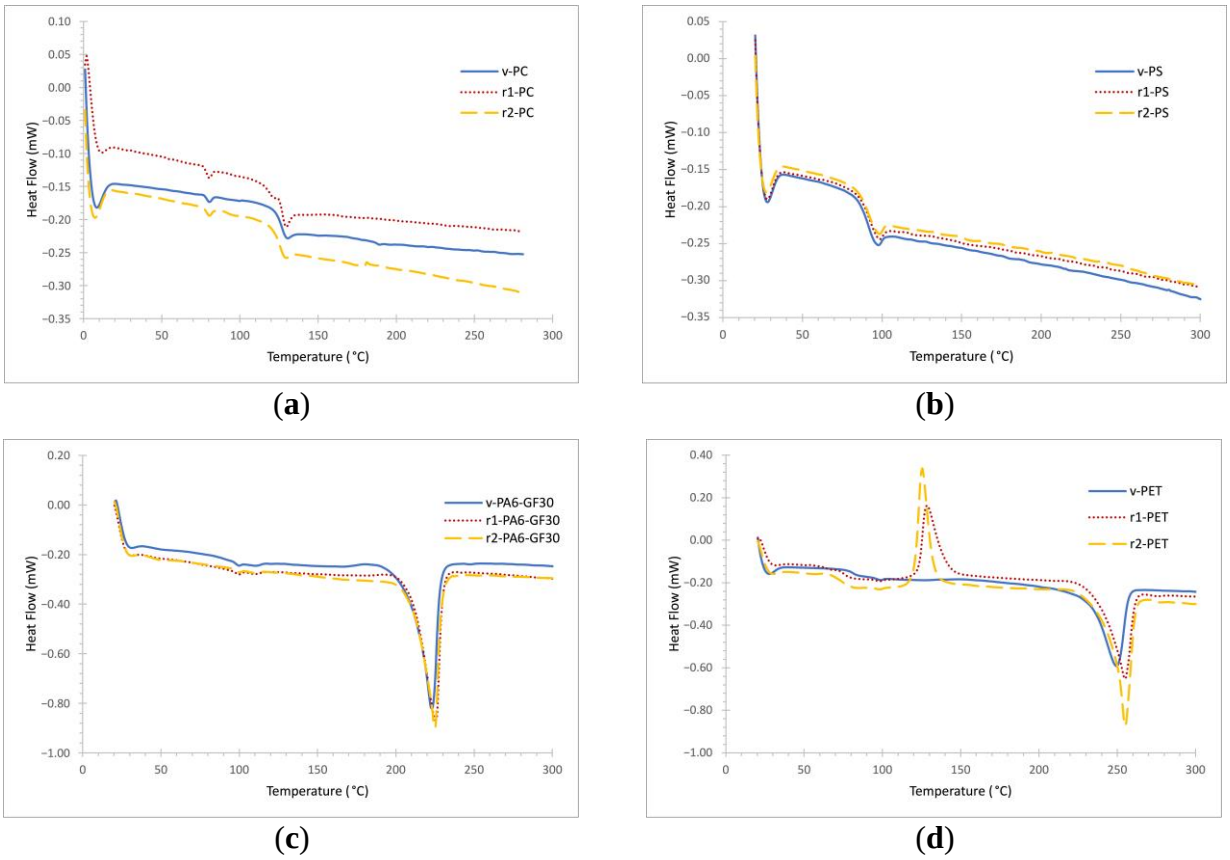

Figure 4-35 – DSC analysis of the virgin and recycled materials: (a) PC; (b) PS; (c) PA6-GF30; and (d) PET.

In the case of amorphous materials, it is only possible to observe the glass transition temperature (Tg), since in these types of polymers the macromolecules are randomly organized. For semicrystalline materials, due to the presence of crystallites, along with Tg, it is possible to observe an endothermic peak that corresponds to the melting temperature (Tm). Table 4.8 summarizes the DSC results for virgin and recycled materials.

Table 4.8 – Glass transition and melting temperature for virgin and recycled materials.

Material	Glass Transition Temperature (°C)	Melting Temperature (°C)
v-PC	144.3	-
r1-PC	143.7	-
r2-PC	142.8	-
v-PS	89.3	-
r1-PS	89.7	-
r2-PS	89.2	-
v-PA6-GF30	44.0	221.6
r1-PA6-GF30	42.5	225.6
r2-PA6-GF30	43.5	222.7
v-PET	79.7	249.4
r1-PET	72.2	254.9
r2-PET	73.7	255.0

When comparing v-PC to r1-PC and r2-PC, as shown in figure 4-35a, it is possible to detect that Tg does not suffer significant variation, meaning that reprocessing does not affect this property. In the case of PS, another amorphous polymer (figure 4-35b), there are no significant changes in Tg values.

Regarding PA6-GF30, presented in figure 4-35c, there is almost no change in Tg, but there is a slight increase in melting temperature from the virgin to the recycled materials.

Finally, figure 4-35d shows that for PET there is little variation in Tg and Tm between processing cycles. In this case, it is important to highlight the presence of an exothermic peak during heating. This peak, defined as "cold crystallization" temperature (Tc), appears at 128.4 °C and 126.7 °C for r1-PET and r2-PET, respectively, but not in v-PET. Although the temperatures are similar, the appearance of this cold crystallization peak might explain the differences in optical properties mentioned in Section 4.3.1.

Similar behaviour for PET is reported by Torres [49] and Cañadas [63], who state that the exothermic peak arises from the "crystallization of the amorphous phase" and is typical in polymers such as PET, PPS, and PEAK. According to Torres [49], this phenomenon "arises from the weak mobility of planar benzenic nuclei and can easily be explained: chains being frozen, the heating involves a critical mobility leading to the reorganization of the structure."

4.3.4. MFR Analysis

The MFR is a property of plastic materials that allows an understanding of the ease of flow of the material at a specific temperature. Throughout this work, measurements were made to compare the ease of flow between the virgin and recycled samples. In some cases, as shown in Table 4.9, the reprocessing completely changes the flowability of the material. Although a high MFR can benefit the injection moulding process, if this value is too high it can lead to the appearance of defects in the injected components.

Table 4.9 – Melt mass flow rate results for virgin and recycled materials tested according to the guidelines in ASTM D1238-13 [64].

Material	Melt Mass Flow Rate (g/10 min)
v-PC [1]	17.1 ± 1.2
r1-PC [1]	18.9 ± 0.9
r2-PC [1]	25.1 ± 0.8
v-PS [2]	15.7 ± 0.5
r1-PS [2]	18.3 ± 0.8
r2-PS [2]	18.3 ± 0.9
v-PA6-GF30 [3]	9.6 ± 0.8
r1-PA6-GF30 [3]	20.5 ± 0.7
r2-PA6-GF30 [3]	28.8 ± 0.9
v-PET [4]	23.1 ± 1.1
r1-PET [4]	112.4 ± 4.7
r2-PET [4]	126.0 ± 3.7

[1] 300 °C–1.20 kg; [2] 235 °C–2.16 kg; [3] 200 °C–5.00 kg; [4] 260 °C–2.16 kg.

As expected, all materials present an increase in melt mass flow rate after successive mechanical recycling processes. Nonetheless, two materials are deserving of some more critical analysis, namely PA6-GF30 and PET, since they present a significant increase after recycling.

4.3.5. Hardness Tests

Hardness evaluation allows an understanding of the resistance towards the indentation of a material. The results of the hardness tests (Shore D) are shown in table 4.10.

Table 4.10 – Shore D hardness results of virgin and recycled materials were tested according to the guidelines in ISO 868:2003 [59].

Material	Hardness (Shore D)
v-PC	68.6 ± 1.9
r1-PC	72.4 ± 1.6
r2-PC	72.5 ± 1.2
v-PS	79.4 ± 0.7
r1-PS	76.0 ± 0.8
r2-PS	73.9 ± 1.1
v-PA6-GF30	71.1 ± 1.5
r1-PA6-GF30	71.3 ± 1.6
r2-PA6-GF30	70.4 ± 1.7
v-PET	62.9 ± 1.8
r1-PET	68.8 ± 1.4
r2-PET	69.7 ± 1.7

As it is possible to realize in table 4.10, there are minimal changes in hardness between the virgin and recycled materials.

4.3.6. Tensile Tests

One of the most representative test to evaluate mechanical properties is the tensile test. In this work, the test was carried out according to the guidelines in ISO 527:2019 [65], with the objective of understanding if the ability to deform elastically would change with the recycling process and if tensile strength would suffer any significant modification. The results of the tensile tests for the PC, PS, PA6-GF30, and PET virgin and recycled specimens are shown in Figure 4-36–Figure 4-39. The corresponding values of Young's modulus (E) and tensile stress (σy) are shown in table 4.11.

The results for polycarbonate (PC), as shown in figure 4-36, indicate a minimal loss in strength between each recycling cycle while maintaining its value for Young's Modulus (E).

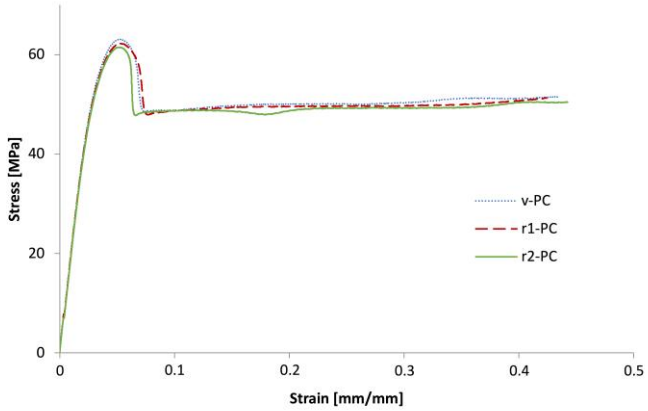

Figure 4-36 – Stress–strain curve of virgin and recycled of PC.

The tensile properties of polystyrene (figure 4-37) show a reduction in its strength after recycling while observing a slight variation in the elasticity modulus.

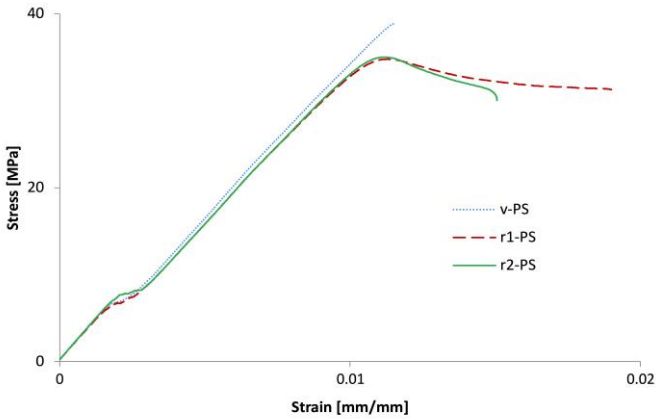

Figure 4-37 – Stress–strain curve of virgin and recycled of PS.

By analysing the mechanical properties of PA6-GF30 (figure 4-38), it is possible to observe that there is not a significant change. This means that after recycling the material twice, it can still resist similar tensile loads.

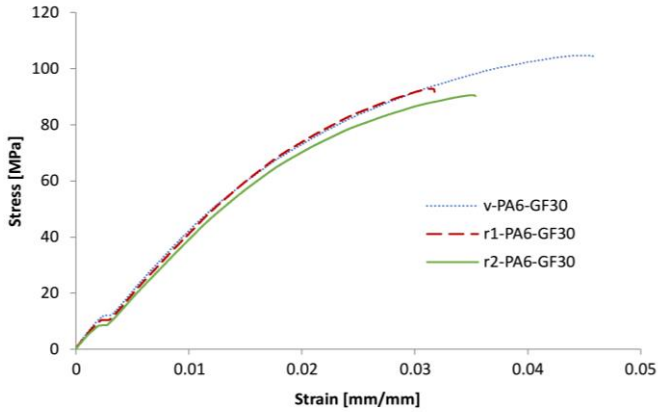

Figure 4-38 – Stress–strain curve of each processing cycle of PA6-GF30.

The changes in mechanical properties (figure 4-39) from v-PET to r1-PET can be related to the higher melt flow rate, as shown in table 4.11, which might promote higher molecular orientation. After a second recycling cycle, the results show that there is a notorious loss of properties, displaying the characteristics of a fragile material.

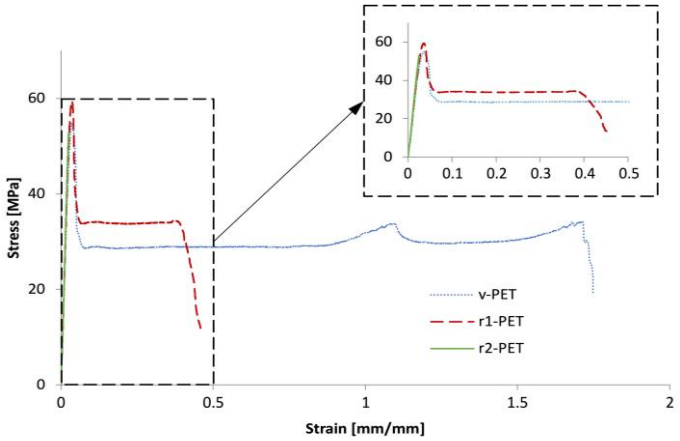

Figure 4-39 – Stress–strain curve of each of processing cycle of PET.

Table 4.11 – Mechanical properties for virgin and recycled materials tested according to the guidelines in ISO 527:2019 [65]

Material	Young's Modulus (MPa)	Tensile Stress (MPa)
v-PC	1992.7 ± 48.3	63.3 ± 1.9
r1-PC	1957.2 ± 25.9	61.9 ± 0.6
r2-PC	1953.4 ± 15.5	61.8 ± 0.4
v-PS	2707.6 ± 23.6	38.6 ± 0.6
r1-PS	2664.3 ± 25.6	35.1 ± 1.1
r2-PS	2621.5 ± 46.9	34.9 ± 0.7
v-PA6-GF30	4049.6 ± 61.1	103.1 ± 1.0
r1-PA6-GF30	4271.7 ± 54.9	101.5 ± 1.6
r2-PA6-GF30	4086.5 ± 21.1	91.5 ± 1.5
v-PET	1847.3 ± 19.6	53.8 ± 1.0
r1-PET	2103.8 ± 69.6	60.8 ± 1.7
r2-PET	2269.7 ± 11.5	49.7 ± 1.0

5. Conclusions

The work develop in this project thesis highlights the importance of addressing several issues in what concerns injection moulding plastic parts. With this aim, three distinct case studies were proposed and solved.

The first case study intended to improve the quality of a plastic part with thickness variations, that although not ideal when considering the design for mouldability rules, sometimes is required, by reducing both shrinkage effects and weld lines. The latter were accomplished using blowing agents, which shown a reduction of the shrinkage effects, such as sink marks in the polypropylene parts, and that there are interesting results on the mass reduction of the parts, such as the negative impact that increasing the percentage too much bring. This study has shown that weld lines are zones of fragility and should be avoided whenever possible. However, when this cannot be achieved, the solution lies in the temperature control of the mould to try and mitigate it. The introduction of blowing agents in parts with weld lines will reduce their mechanical behaviour due to the air bubbles present on the core of the part.

The comparison between the results obtained in Moldex3D and the readings of the thermocouple sensors have not shown positive relation, resulting in different readings. This does not allow to predict the temperature at which the weld line will appear. In turn, an understanding of the effects that temperature can have on this subject was not found. This incorrect relation and the literature have shown that thermocouples are not the best solution for melt temperature surface readings.

Following the achievements of the first case study, the second one was an industrial part that not only presented thickness variations, but also some requirements in what concerns weld line aesthetic marks, therefore, the use of a variotherm was envisaged. The variotherm process has shown to be an efficient and interesting tool in mould temperature control, nonetheless, if not well implemented it might provoke worst results than the conventional process. This means that the mould should be carefully designed for the variotherm process. The variotherm process has shown that the cooling phase can be much better controlled.

Lastly, and considering the growing discussion of moving towards a greener planet, a recycling study has proposed, intending to further increase the knowledge on plastic

recycling. This study has shown that some properties change between virgin and recycled materials. Amorphous materials do not present significant variations in their thermal and mechanical properties, the latter indicates a 2–4% decrease in tensile stress. Semicrystalline materials have shown an increase in their flowability after reprocessing, however, PET shows the highest variability in the properties, where a high MFR and complete change in mechanical behaviour are the main changes detected. The results of this work allow understanding that recycled materials may come with some compromises depending on the objective of their use. In conclusion, this has shown that when designing plastic components, the recycling of these materials should be considered for the success of the correct circular economy implementation.

6. Future Work

The work developed has shown that there are still some future studies that should be done, mainly in the laboratory and industrial case studies. The laboratory case study has shown interesting results for the implementation of blowing agents, nonetheless, it is still needed to improve the mixing process. In future work it is also suggested the implementation of the Mucell® process, to obtain a microcellular core, which would allow an improvement in both the surface appearance in the part and weight reduction, while having a better control of the process. Since the obtained surface finish obtained through the use of blowing agents is underperforming, another study that could not be developed, but it is still an interesting approach, is the use of over-moulding to try and improve the surface finish of the part with blowing agent.

In what concerns the industrial case study, it is suggested the implementation of different inserts with different conformal channels to improve the variotherm process, which may allow a reduction of defects such as the sink marks present at the high-thickness zone. Another interesting work that could not be completed in the timeframe of this thesis project, is the comparison of the variotherm process and the conformal cooling with inserts with conventional channels. Since this process has been shown to take a long time from cooling to re-heating the mould, it would be interesting to compare this process to other similar RHCM processes, such as the ones using water for cooling the mould and induction systems to heat it.

To further increase the understanding of the recycling influence on plastic properties it is important to continue these studies with other materials as well as complement the tests and evaluations performed in this project with other typologies of tests, such as thermogravimetric analysis which allows understanding the degradation of the recycled materials.

Bibliographic References

1. Al-Salem, S.M.; Lettieri, P.; Baeyens, J. The Valorization of Plastic Solid Waste (PSW) by Primary to Quaternary Routes: From Re-Use to Energy and Chemicals. *Prog Energy Combust Sci* **2010**, *36*, 103–129, doi:10.1016/J.PECS.2009.09.001.

2. Briassoulis, D.; Pikasi, A.; Hiskakis, M. Recirculation Potential of Post-Consumer /Industrial Bio-Based Plastics through Mechanical Recycling - Techno-Economic Sustainability Criteria and Indicators. *Polym Degrad Stab* **2021**, *183*, 109217, doi:10.1016/J.POLYMDEGRADSTAB.2020.109217.

3. Goodship, V. Plastic Recycling. *https://doi.org/10.3184/003685007X228748* **2007**, *90*, 245–268, doi:10.3184/003685007X228748.

4. Crawford, R.J.; Martin, P.J. *Plastics Engineering*; 4th ed.; Elsevier Publishing, 2020; ISBN 9780081007099.

5. Dzulkipli, A.A.; Azuddin, M. Study of the Effects of Injection Molding Parameter on Weld Line Formation. *Procedia Eng* **2017**, *184*, 663–672, doi:10.1016/j.proeng.2017.04.135.

6. Singh, G.; Verma, A. A Brief Review on Injection Moulding Manufacturing Process. *Mater Today Proc* **2017**, *4*, 1423–1433, doi:10.1016/j.matpr.2017.01.164.

7. Kazmer, D.O. *Injection Mold Design Engineering*; 2nd ed.; Carl Hanser Verlag GmbH & Co. KG: München, 2016; ISBN 978-1-56990-570-8.

8. Zheng, R.; Tanner, R.I.; Fan, X.-J. *Injection Molding*; Springer Berlin Heidelberg: Berlin, Heidelberg, 2011; ISBN 978-3-642-21262-8.

9. McCrum, N.G.; Buckley, C.P.; Bucknall, C.B. *Principles of Polymer Engineering*; 2nd ed.; Oxford University Press, 1997; ISBN 978-0-19-856526-0.

10. Martinho, P.G. Estudo Do Empeno Em Peças Moldadas Por Injeção. Tese para Obtenção do Grau de Mestre, Universidade do Minho: Braga, 2002.

11. Ebnesajjad, S. Injection Molding. *Fluoroplastics* **2015**, 236–281, doi:10.1016/B978-1-4557-3197-8.00010-9.

12. Bhandari, K.; Vihtonen, M. Designing Lego Brick and Its Mould for Manufacturing Title: Supervisor (Arcada), Arcada-University of Applied Sciences: Helsinki, 2016.

13. Bayer Corporation *A Design Guide Part and Mold Design Engineering Polymers*; Pittsburgh, 2000;

14. Kazmer, D.O. Cooling System Design. In *Injection Mold Design Engineering*; Carl Hanser Verlag GmbH & Co. KG: München, 2016; pp. 243–290 ISBN 978-1-56990-571-5.

15. Rosato, D.; Rosato, D.; Rosato, M. *Injection Molding Handbook*; 3rd ed.; Springer US, 2000; ISBN 978-0-7923-8619-3.

16. Khan, M.; Afaq, S.K.; Khan, N.U.; Ahmad, S. Cycle Time Reduction in Injection Molding Process by Selection of Robust Cooling Channel Design. *ISRN Mechanical Engineering* **2014**, *2014*, doi:10.1155/2014/968484.

17. Broeck, S. Guidelines on the Design and Implementation of Stereolithographic 3D Printed Moulds for Low Volume Injection Moulding, Ghent University: Ghent, 2017.

18. Villamizar, C.A.; Han, C.D. Studies on Structural Foam Processing II. Bubble Dynamics in Foam Injection Molding. *Polym Eng Sci* **1978**, *18*, 699–710, doi:10.1002/PEN.760180905.

19. Okoroafor, M.O.; Frisch, K.C. INTRODUCTION TO FOAMS AND FOAM FORMATION. *Handbook of Plastic Foams* **1995**, 1–10, doi:10.1016/B978-081551357-5.50003-6.

20. Guanghong, H.; Yue, W. Microcellular Foam Injection Molding Process. *Some Critical Issues for Injection Molding* **2012**, doi:10.5772/34513.

21. Xu, J.; Pierick, D. Microcellular Foam Processing in Reciprocating-Screw Injection Molding Machines. *Journal of Injection Molding Technology* **2001**, *5*.

22. Ding, Y.; Hassan, M.H.; Bakker, O.; Hinduja, S.; Bártolo, P. A Review on Microcellular Injection Moulding. *Materials* **2021**, *14*, doi:10.3390/MA14154209.

23. Ozcelik, B. Optimization of Injection Parameters for Mechanical Properties of Specimens with Weld Line of Polypropylene Using Taguchi Method. *International*

Communications in Heat and Mass Transfer **2011**, *38*, 1067–1072, doi:10.1016/J.ICHEATMASSTRANSFER.2011.04.025.

24. Tosello, G.; Gava, A.; Hansen, H.N.; Lucchetta, G.; Marinello, F. Characterization and Analysis of Weld Lines on Micro-Injection Moulded Parts Using Atomic Force Microscopy (AFM). *Wear* **2009**, *266*, 534–538, doi:10.1016/J.WEAR.2008.04.077.

25. Bociąga, E.; Jaruga, T. Experimental Investigation of Polymer Flow in Injection Mould. *Archives of Materials Science and Engineering* **2007**, *28*, 165–172.

26. Kagan, V.A.; Mazza, J.; Roth, C. Optimizing Mechanical Performance of Injection Molded Multiple Gated Rotating Thermoplastic Components: Part 2 - Knit Line/Weld Inter-Phase Integrity. *SAE Technical Papers* **2001**, doi:10.4271/2001-01-0439.

27. Sánchez, R.; Martinez, A.; Mercado, D.; Carbonel, A.; Aisa, J. Rapid Heating Injection Moulding: An Experimental Surface Temperature Study. *Polym Test* **2021**, *93*, 106928, doi:10.1016/J.POLYMERTESTING.2020.106928.

28. Dangel, R. *Injection Molds for Beginners*; Carl Hanser Verlag GmbH & Co. KG, 2020; Vol. 11;.

29. Martinez, A.; Castany, J.; Aisa, J. Characterization of In-Mold Decoration Process and Influence of the Fabric Characteristics in This Process. *http://dx.doi.org/10.1080/10426914.2010.536934* **2011**, *26*, 1164–1172, doi:10.1080/10426914.2010.536934.

30. Aisa, J.; Castany, J.; Fernandez, A. Sequential Injection Molding: Design Considerations. *SPE Injection Molding Division* **2011**, *89*, 15–20.

31. Huang, C.-T.; Hsieh, I.-S.; Tsai, C.-H. The Effects of Various Variotherm Processes and Their Mechanisms on Injection Molding. *Proceedings of the Polymer Processing Society 26th Annual Meeting* **2010**.

32. Wang, X.; Zhao, G.; Wang, G. Research on the Reduction of Sink Mark and Warpage of the Molded Part in Rapid Heat Cycle Molding Process. *Mater Des* **2013**, *47*, 779–792, doi:10.1016/J.MATDES.2012.12.047.

33. Hanemann, T.; Heckele, M.; Piotter, V. Current Status of Micromolding Technology. *Polymer News* **2000**, *25*, 224–229.

34. Rhee, B.O.; Kim, C.S.; Lee, K.; Kang, M.H. Evaluation of Momentary-Mold-Surface-Heating (MmSH) Process. *Annual Technical Conference - ANTEC, Conference Proceedings* **2005**, *3*, 35–38.

35. Kim, D.H.; Kang, M.H.; Chun, Y.H. Development of a New Injection Molding Technology: Momentary Mold Surface Heating Process. *Journal of Injection Molding Technology* **2001**, *5*, 229–232.

36. Chen, S.C.; Jong, W.R.; Chang, J.A. Dynamic Mold Surface Temperature Control Using Induction Heating and Its Effects on the Surface Appearance of Weld Line. *J Appl Polym Sci* **2006**, *101*, 1174–1180, doi:10.1002/APP.24070.

37. Kim, S.; Shiau, C.S.; Kim, B.; Yao, D. Injection Molding Nanoscale Features with the Aid of Induction Heating. *Polymer - Plastics Technology and Engineering* **2007**, *46*, 1031–1037, doi:10.1080/03602550701522344.

38. Johnson, R.J.; Pitchumani, R. Enhancement of Flow in VARTM Using Localized Induction Heating. *Compos Sci Technol* **2003**, *63*, 2201–2215, doi:10.1016/S0266-3538(03)00179-9.

39. Wang, G.; Zhao, G.; Li, H.; Guan, Y. Research of Thermal Response Simulation and Mold Structure Optimization for Rapid Heat Cycle Molding Processes, Respectively, with Steam Heating and Electric Heating. *Mater Des* **2010**, *31*, 382–395, doi:10.1016/J.MATDES.2009.06.010.

40. Wang, M.-L.; Chang, R.-Y.; Hsu, C.-H. (David) Molding Simulation: Theory and Practice. In *Molding Simulation: Theory and Practice*; Carl Hanser Verlag GmbH & Co. KG: München, 2018; pp. I–XVIII.

41. Zhou, H. *Computer Modeling for Injection Molding : Simulation, Optimization, and Control*; Wiley, 2013; ISBN 978-0-470-60299-7.

42. Beaumont, J.P. Shrinkage and Warpage Analysis of Plastic Injection Molded Parts. *SAE Technical Papers* **1989**, doi:10.4271/890626.

43. *Packaging Waste Statistics*; 2022;

44. ASTM *Standard Guide for Waste Reduction, Resource Recovery, and Use of Recycled Polymeric Materials and Products (Withdrawn 2015)*; West Conshohocken, PA, USA, 2006;

45. International Organization for Standardization *ISO - ISO 15270:2008 - Plastics — Guidelines for the Recovery and Recycling of Plastics Waste*; Geneva, Switzerland, 2008;

46. Santos, A.S.F.; Teixeira, B.A.N.; Agnelli, J.A.M.; Manrich, S. Characterization of Effluents through a Typical Plastic Recycling Process: An Evaluation of Cleaning Performance and Environmental Pollution. *Resour Conserv Recycl* **2005**, *45*, 159–171, doi:10.1016/J.RESCONREC.2005.01.011.

47. Moldex3D R16 Help: Filling and Packing Setting Tab Available online: http://support.moldex3d.com/r16/en/analysissetup_prepareanalysis_processwizard_fillingandpackingsettingtab.html (accessed on 1 March 2023).

48. Costa, A.A.; Potêncio, A.; Martinho, P.G.; Barreiros, F.M. Thermal and Mechanical Properties of Recycled Polystyrene. *Materials Proceedings 2022, Vol. 8, Page 88* **2022**, *8*, 88, doi:10.3390/MATERPROC2022008088.

49. Torres, N.; Robin, J.J.; Boutevin, B. Study of Thermal and Mechanical Properties of Virgin and Recycled Poly(Ethylene Terephthalate) before and after Injection Molding. *Eur Polym J* **2000**, *36*, 2075–2080, doi:10.1016/S0014-3057(99)00301-8.

50. Chen, T.; Mansfield, C.D.; Ju, L.; Baird, D.G. The Influence of Mechanical Recycling on the Properties of Thermotropic Liquid Crystalline Polymer and Long Glass Fiber Reinforced Polypropylene. *Compos B Eng* **2020**, *200*, 108316, doi:10.1016/J.COMPOSITESB.2020.108316.

51. Pedroso, A.G.; Mei, L.H.I.; Agnelli, J.A.M.; Rosa, D.S. The Influence of the Drying Process Time on the Final Properties of Recycled Glass Fiber Reinforced Polyamide 6. *Polym Test* **2002**, *21*, 229–232, doi:10.1016/S0142-9418(01)00074-5.

52. Hassan, M.M.; Badway, N.A.; Gamal, A.M.; Elnaggar, M.Y.; Hegazy, E.S.A. Studies on Mechanical, Thermal and Morphological Properties of Irradiated Recycled Polyamide and Waste Rubber Powder Blends. *Nucl Instrum Methods Phys Res B* **2010**, *268*, 1427–1434, doi:10.1016/J.NIMB.2010.01.021.

53. Pérez, J.M.; Vilas, J.L.; Laza, J.M.; Arnáiz, S.; Mijangos, F.; Bilbao, E.; Rodríguez, M.; León, L.M. Effect of Reprocessing and Accelerated Ageing on Thermal and Mechanical Polycarbonate Properties. *J Mater Process Technol* **2010**, *210*, 727–733, doi:10.1016/J.JMATPROTEC.2009.12.009.

54. Candal, M.V.; Safari, M.; Fernández, M.; Otaegi, I.; Múgica, A.; Zubitur, M.; Gerrica-Echevarria, G.; Sebastián, V.; Irusta, S.; Loaeza, D.; et al. Structure and Properties of Reactively Extruded Opaque Post-Consumer Recycled PET. *Polymers (Basel)* **2021**, *13*, doi:10.3390/POLYM13203531.

55. ASTM *Standard Test Methods for Flexural Properties of Unreinforced and Reinforced Plastics and Electrical Insulating Materials*; West Conshohocken, PA, USA, 2002;

56. ASTM *Standard Test Method for Tensile Properties of Plastics*; West Conshohocken, PA, USA, 2002;

57. International Organization for Standardization *ISO - ISO 1183-1:2019 - Plastics — Methods for Determining the Density of Non-Cellular Plastics — Part 1: Immersion Method, Liquid Pycnometer Method and Titration Method*; Geneva, Switzerland, 2019;

58. ASTM *Standard Test Method for Melt Flow Rates of Thermoplastics by Extrusion Plastometer*; West Conshohocken, PA, USA, 2013;

59. International Organization for Standardization *ISO - ISO 868:2003 - Plastics and Ebonite — Determination of Indentation Hardness by Means of a Durometer (Shore Hardness)*; Geneva, Switzerland, 2003;

60. Ageyeva, T.; Horváth, S.; Kovács, J.G. In-Mold Sensors for Injection Molding: On the Way to Industry 4.0. *Sensors 2019, Vol. 19, Page 3551* **2019**, *19*, 3551, doi:10.3390/S19163551.

61. Lin, Y.; Bilotti, E.; Bastiaansen, C.W.M.; Peijs, T. Transparent Semi-Crystalline Polymeric Materials and Their Nanocomposites: A Review. *Polym Eng Sci* **2020**, *60*, 2351–2376, doi:10.1002/PEN.25489.

62. Nadali, E.; Layeghi, M.; Ebrahimi, G.; Naghdi, R.; Jonoobi, M.; Khorasani, M.M.; Mirbagheri, Y. Effects of Multiple Extrusions on Structure-Property Performance of

Natural Fiber High-Density Polyethylene Biocomposites. *Materials Research* **2018**, *21*, doi:10.1590/1980-5373-MR-2017-0301.

63. Cañadas, J.C.; Diego, J.A.; Sellarès, J.; Mudarra, M.; Belana, J. Cold Crystallization Effects in Free Charge Relaxation in PET and PEN. *Polymer (Guildf)* **2000**, *41*, 8393–8400, doi:10.1016/S0032-3861(00)00192-0.

64. ASTM *Standard Test Method for Melt Flow Rates of Thermoplastics by Extrusion Plastometer*; West Conshohocken, PA, USA, 2013;

65. International Organization for Standardization *ISO - ISO 527-1:2019 - Plastics — Determination of Tensile Properties — Part 1: General Principles*; Geneva, Switzerland, 2019;

66. Marini, D.; Corney, J.R. A Methodology for near Net Shape Process Feasibility Assessment. *Prod Manuf Res* **2017**, *5*, 390–409, doi:10.1080/21693277.2017.1401495.

7. Appendix

Appendix A – Concepts for runner and gate placement of laboratorial case study

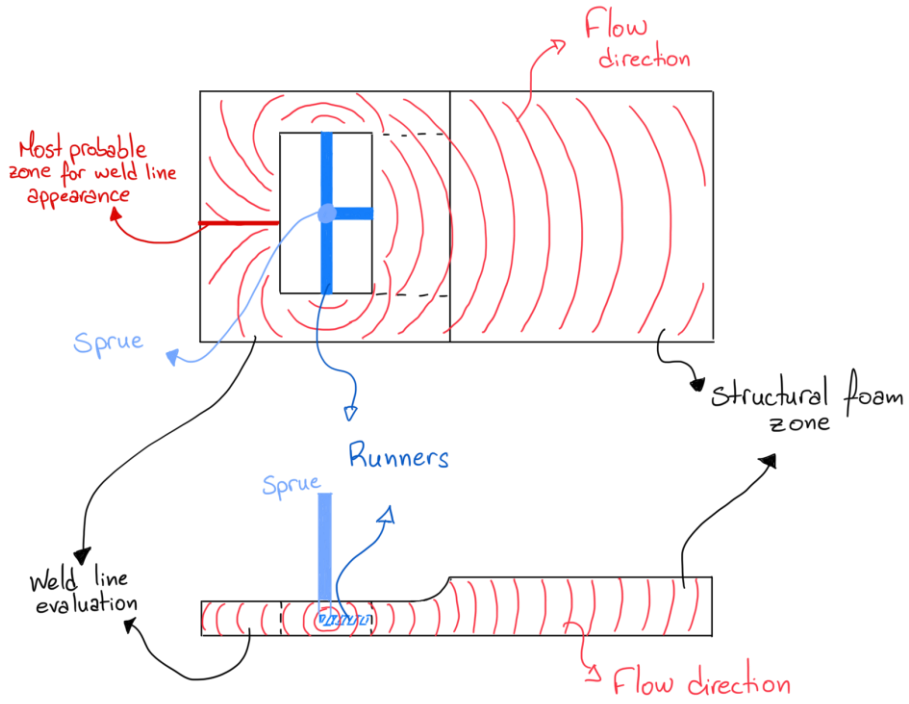

Concept A for placement of the runners and gates.

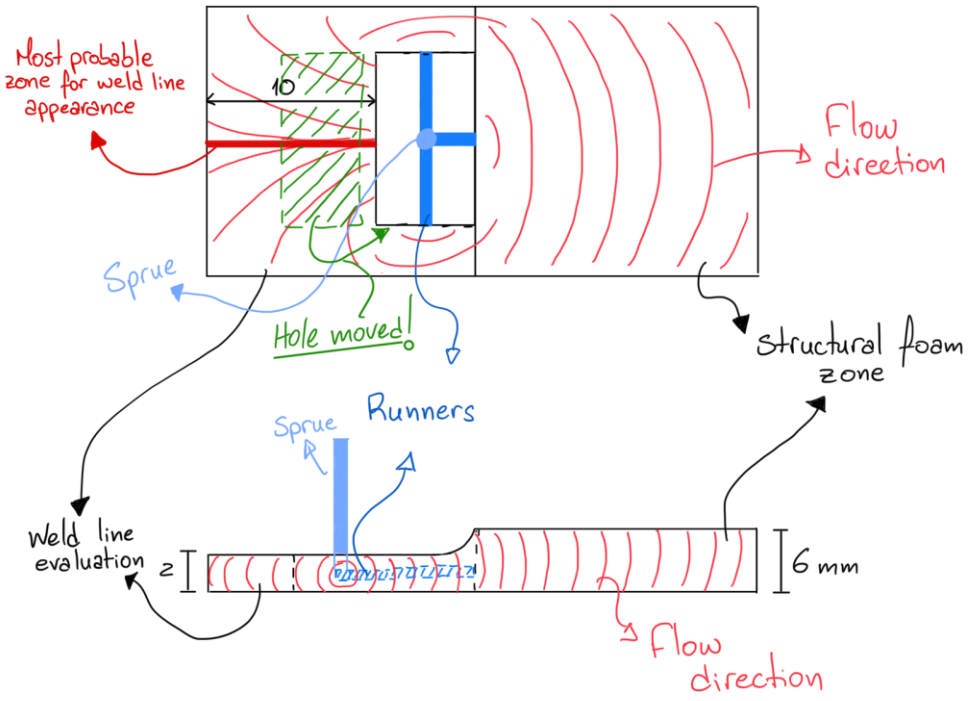

Concept B for placement of the runners and gates.

Appendix B – 2D drawing of the laboratorial case study's component.

Tabela de revisão/Revision Table			
Rev.	Descrição/Description	Data/Date	Aprovado/ Approved

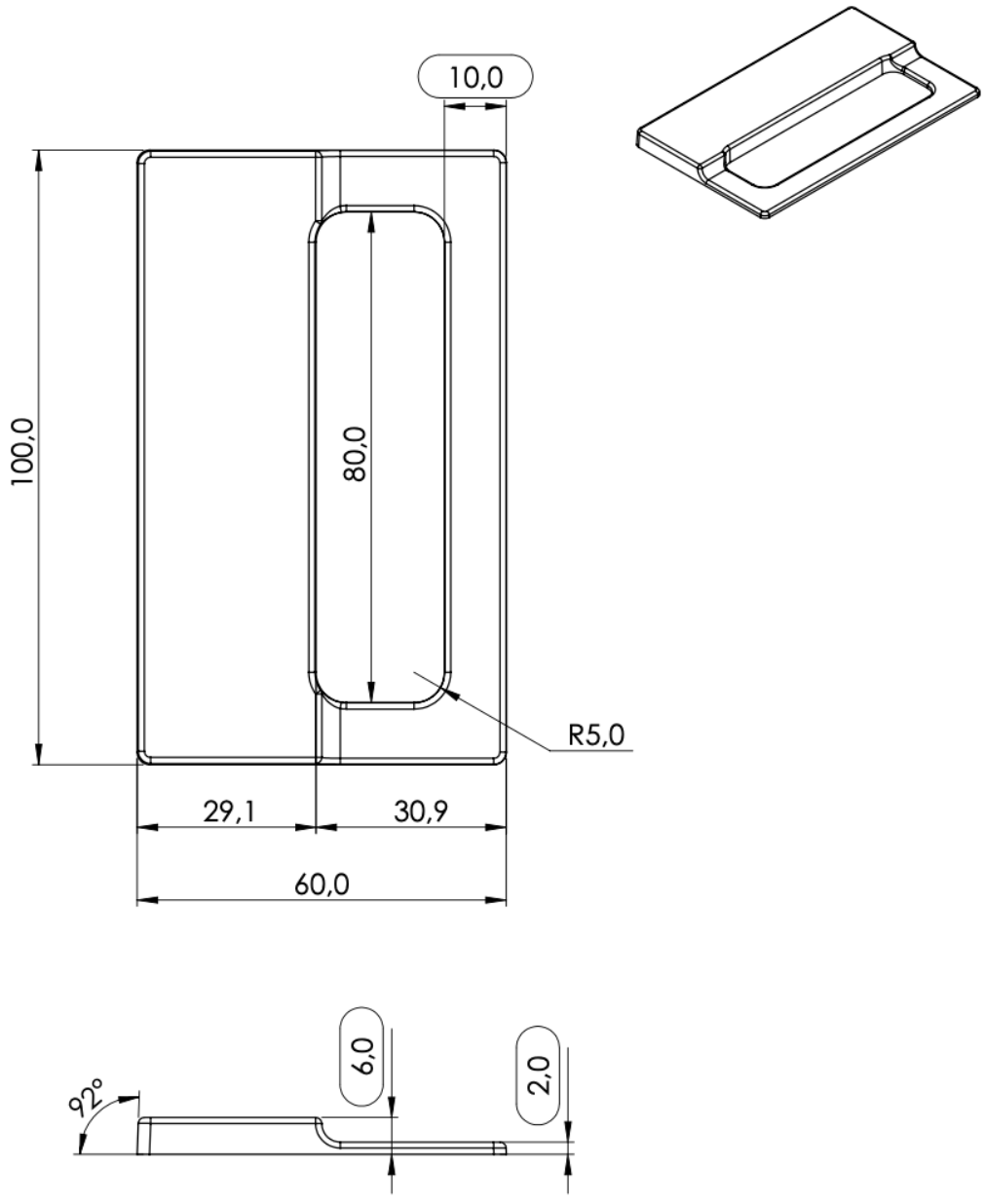

Projeto/ Project: S4Plast | Thesis Project

Observação/Observation:

	Data/Date	Nome/Name
Desenh./Drawn	10/01/2022	André Costa
Verifi./Checked	24/10/2022	André Costa
Proj.		

Projeto Nr./Project Nr.: 46089

Tolerâncias Gerais: DIN ISO 2768 mK
General tolerances: DIN ISO 2768 mK

Escala/Scale: 1:1

Título/Title: EXPERIMENTAL COMPONENT

Acabamento/Finishing

Peso/Weight (g)

Desenho nr./Drawing nr.: CDRSP-S4P-004

Revisão/ Version

Página/Sheet 1/1 Formato/Size: A

Appendix C – Preliminary mould request sent to the manufacturing company.

POLITÉCNICO DE LEIRIA | CDRSP CENTRE FOR RAPID AND SUSTAINABLE PRODUCT DEVELOPMENT | MANUFACTURING A BETTER FUTURE

Projeto do molde

Para a produção do artigo acima identificado é necessário o projeto e produção de um molde, assim, são definidos como requisitos deste molde:

Artigo a moldar :

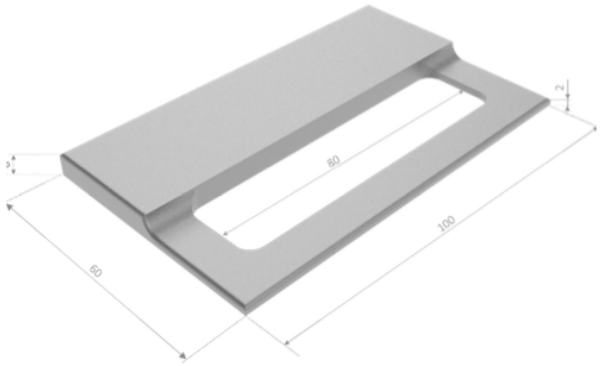

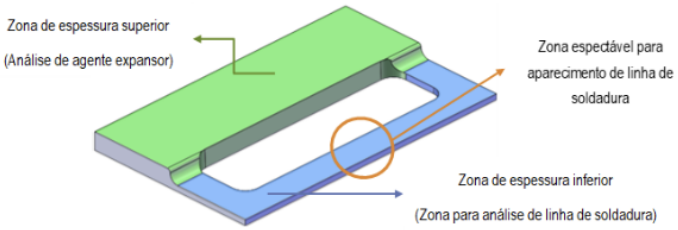

Materiais/Fabricantes:

GPPS | INEOS Styrolution 124N

PP | LyondellBasell Moplen HP500N

Contração:

1,2%

Ângulo de saída:

2°

Peso do artigo [g]:

21,00 g

18,17 g

Nº de cavidades:

1

Esquema de distribuição a utilizar :

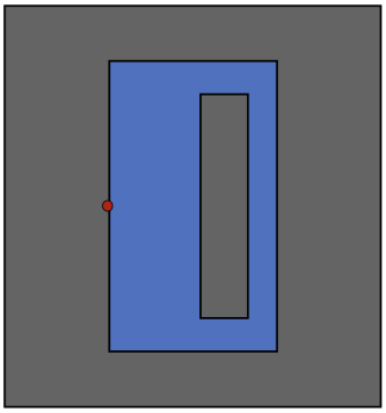

Elementos de desmoldação a utilizar:	Quantidade:
1. Elemento móvel atuado por mola de pressão	–
2. Elemento móvel atuado por guia/plano inclinada(o)	–
3. Elemento móvel atuado por cilindro hidraúlico	–
4. Balancé clássico / Balancé articulado / *Rack Lifter*	–
5. Buchas colapsíveis / Buchas expansíveis	–
6. Extrator elástico (aço mola)	–
7. Desenroscamento por veio sem-fim	–
8. Desenroscamento por cremalheira/cilindo hidraulico	–
9. Desenroscamento por motor hidraúlico/elétrico	–
10. Outro(s) elemento(s) de desmoldação:	–

Dimensões estimadas para o molde [mm]:

Comprimento:	Largura:	Altura:
246	196	232

Tipo de Sistema de injeção :

1. Distribuição e ataques "frios"	X
2. Distribuição por carburador (indicar 5. ou 6.) e ataques "frios"	
3. Bico quente direto (*single nozzle*)	
4. Bico quente direto valvulado (*single nozzle + valve gate*)	
5. Carburador + bicos diretos (*manifold + nozzles*)	
6. Carburador + bicos diretos valvulados (*manifold + valve gates*)	
7. Outro tipo de sistema de injeção:	

Tipo de Sistema de extração :

1. Extrator / Extrator laminar / Extrator respigado	X
2. Aro extrator / Chapa extratora	
3. Extração pneumática	
4. Extração atuada externamente	
5. Outro tipo de sistema de extração:	

Layout das chapas previstas para o molde :

Vista de topo

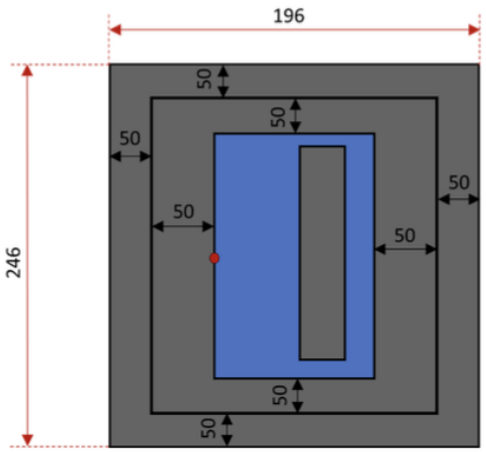

Curso de extração - CE

CE = 11mm

Z5=Z6=CE+12+17+3≥43

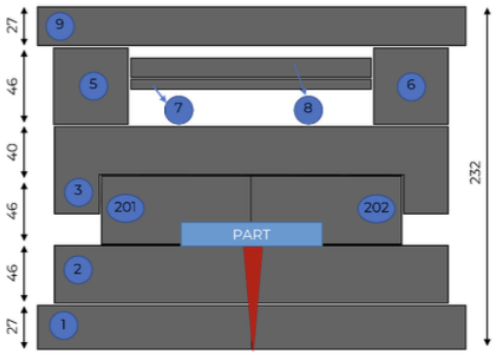

POLITÉCNICO DE LEIRIA | CDRSP CENTRE FOR RAPID AND SUSTAINABLE PRODUCT DEVELOPMENT | MANUFACTURING A BETTER FUTURE

Especificações mínimas da máquina de injeção :

Área projetada: 44,57 cm^2

Força de fecho mínima: 20 ton.f

Pressão de injeção: 170 $kg.f/cm^2$

Capacidade de plastificação: 105 g (PS)

Abertura mínima entre-pratos: 200 mm

Distância mínima entre colunas: 254 mm

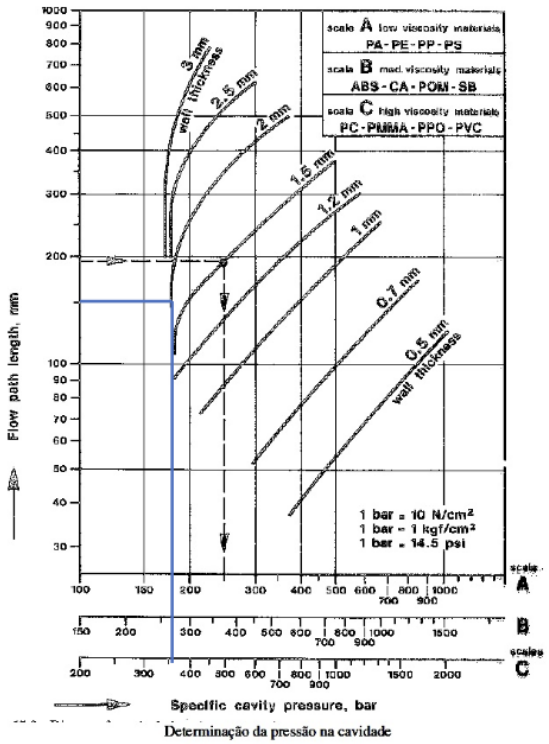

Determinação da pressão na cavidade

Equipamento de injeção sugerido: 150T

Appendix D – Preliminary design of the injection mould of the laboratorial case study

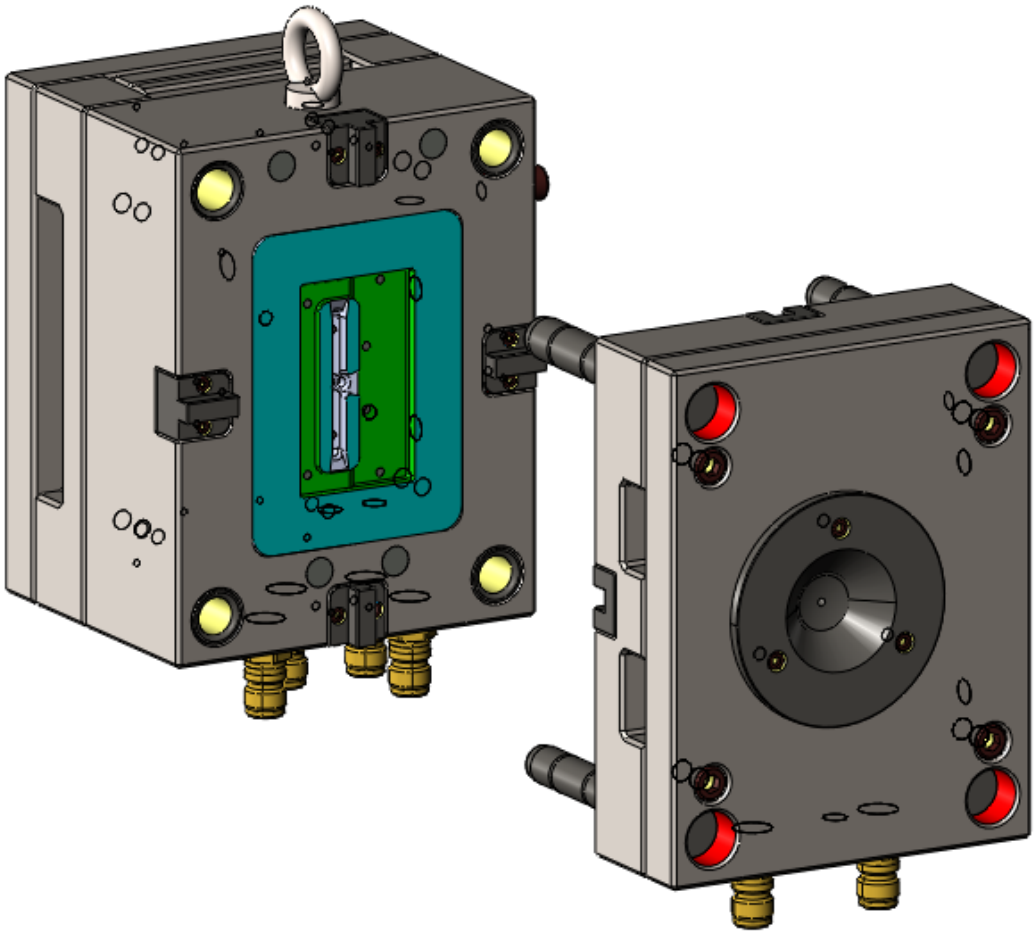

Tabela de revisão/Revision Table

Rev.	Descrição/Description	Data/Date	Aprovado/ Approved

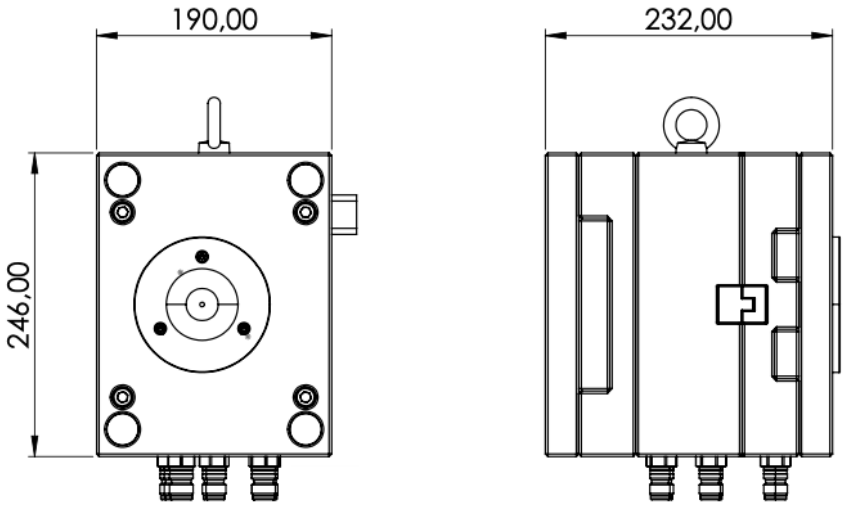

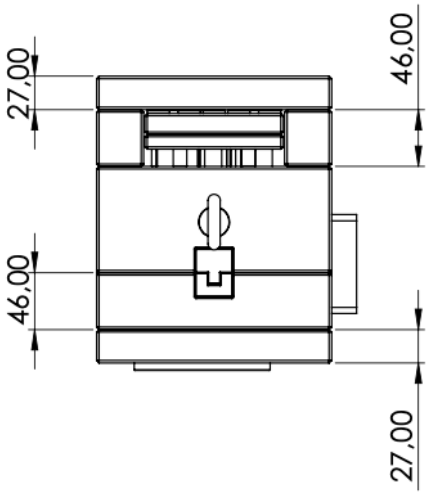

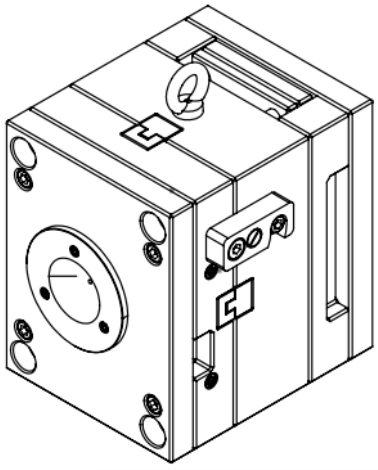

Projeto/ Project

S4Plast - Sustainable Plastics Advanced Solutions

POLITÉCNICO DE LEIRIA

Observação/Observation:

	Data/Date	Nome/Name
Desenh./Drawn	07 / 11 / 2023	André Costa
Verifi./Checked	07 / 11 / 2023	Moldetipo
Proj.		

Projeto Nr./Project Nr.: 41089

Acabamento/Finishing

Peso/Weight (g)

Tolerâncias Gerais: DIN ISO 2768 mK
General tolerances: DIN ISO 2768 mK

Escala/Scale 1:5

Título/Title

Mould S4Plast | Thesis

Desenho nr./Drawing nr. S4P-CDRSP-2023

Revisão/ Version A

Página/Sheet 1/1 Formato/Size: A4

Formato A4 - 10/2021 SolidWorks

Appendix E – Final design of the injection mould of the laboratorial case study

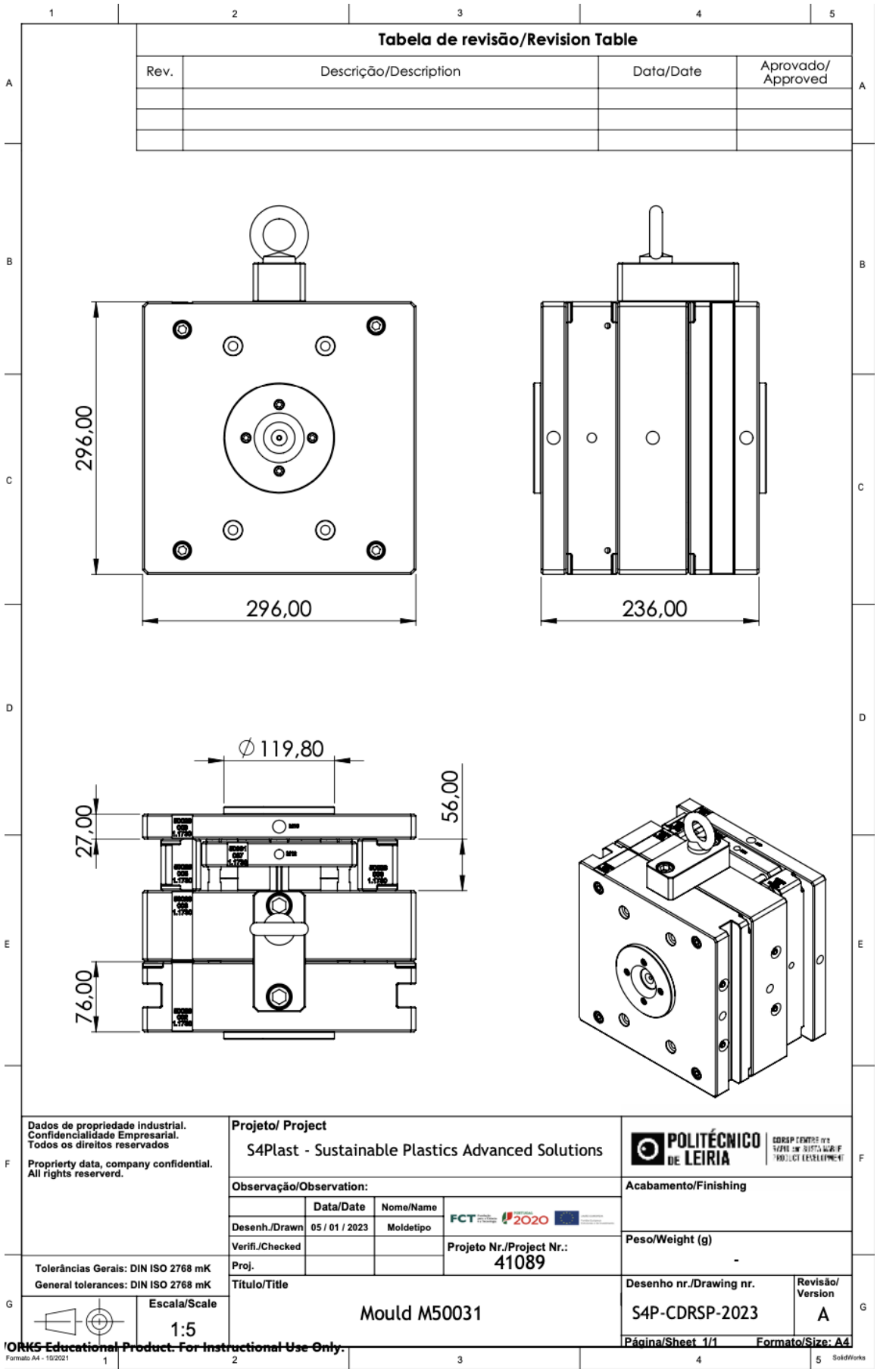

Appendix F – Technical datasheet of Polypropylene Moplen HP500N

Technical Data Sheet

Moplen HP500N

Polypropylene, Homopolymer

Product Description

Moplen HP500N is a homopolymer used for general purpose injection moulding applications. It exhibits good flow and stiffness. *Moplen* HP500N is suitable for food contact.
Moplen HP500N is UL listed under file E31765

Regulatory Status

For regulatory compliance information, see *Moplen* HP500N Product Stewardship Bulletin (PSB) and Safety Data Sheet (SDS).

Status	Commercial: Active
Availability	Africa-Middle East; Asia-Pacific; Europe
Application	Furniture; Housewares
Market	Compounding; Consumer Products; Rigid Packaging
Processing Method	Compounding; Injection Blow Molding
Attribute	Medium Flow; Medium Stiffness

Typical Properties	Nominal Value	Units	Test Method
Physical			
Melt Flow Rate, (230 °C/2.16 kg)	12	g/10 min	ISO 1133-1
Density	0.90	g/cm³	ISO 1183-1
Mechanical			
Tensile Modulus	1400	MPa	ISO 527-1, -2
Tensile Stress at Yield	35	MPa	ISO 527-1, -2
Tensile Strain at Break	> 50	%	ISO 527-1, -2
Tensile Strain at Yield	10	%	ISO 527-1, -2
Impact			
Charpy Impact Strength - Notched, (23 °C, Type 1, Edgewise, Notch A)	4	kJ/m²	ISO 179
Thermal			
Vicat Softening Temperature			
(A/50 N)	153	°C	ISO 306
(B50)	85	°C	ISO 306
Heat Deflection Temperature B, (0.45 MPa, Unannealed)	95	°C	ISO 75B-1, -2

Appendix G – Technical datasheet of Polystyrol 143E

Polystyrol 143 E

BASF
The Chemical Company

Typical values for uncoloured product at 23 °C[1]	Test method [2]	Unit	Values[3]
Mechanical Properties			
Tensile modulus	ISO 527-1/-2	MPa	**3300**
Stress at break	ISO 527-1/-2	MPa	**46**
Strain at break	ISO 527-1/-2	%	**2**
Flexural strength	ISO 178	MPa	**72**
Shear modulus	ISO 6721-2	MPa	**1350**
Charpy impact strength (23°C)	ISO 179/1eU	kJ/m²	**<25**
Charpy notched impact strength (23°C)	ISO 179/1eA	kJ/m²	**3**
Ball indentation hardness at 358 N/30 s	ISO 2039-1	MPa	**150**
Thermal properties			
Vicat softening temperature VST/B/50	ISO 306	°C	**84**
Vicat softening temperature VST/A/120	ISO 306	°C	**90**
HDT A (1.80 MPa)	ISO 75-1/-2	°C	**72**
HDT B (0.45 MPa)	ISO 75-1/-2	°C	**82**
Processing			
Melt volume-flow rate MVR 200 °C/5 kg	ISO 1133	cm³/10min	**10**
Processing: Injection moulding (M), Extrusion (E), Blow moulding (B)	-	-	**M.E**
Melt temperature, injection moulding	-	°C	**180 - 280**
Mold temperature, injection molding	-	°C	**10 - 60**
Melt temperature, flat film	-	°C	**200 - 240**
Electrical properties			
Relative permittivity (100Hz)	IEC 60250	-	**2.5**
Relative permittivity (1 MHz)	IEC 60250	-	**2.5**
Volume resistivity	IEC 60093	Ohm*m	**>1E16**
Surface resistivity	IEC 60093	Ohm	**>1E14**
Electric strength K20/P50	IEC 60243-1	kV/mm	**135**
Flammabillity			
UL 94 (d = 1.6 mm)	UL-94	class	**HB**
UL 94 (d = 3.18 mm)	UL-94	class	**HB**
Other properties			
Density	ISO 1183	kg/m³	**1043**
Water absorption, equilibrium in water at 23°C	similar to ISO 62	%	**<0.1**
Moisture absorption, equilibrium 23°C/50% r.h.	similar to ISO 62	%	**<0.1**

Footnotes
1) If product name or properties don't state otherwise.
2) Specimens according to CAMPUS.
3) The asterisk symbol '*' signifies inapplicable properties.

Product description

Polystyrol 143 E is a medium strength, easy flowing general purpose grade, suitable for blending with impact modified Polystyrol, Styrolux and for coextruded gloss layers.

Processing

Polystyrol 143 E can be injection molded at temperatures between 180 and 280°C. Recommended mold temperatures are between 10 and 60°C.
Extrusion melt temperature should not exceed 240°C.

Applications

In blends with high impact polystyrene or Styrolux: thermoformed articles like cups for cold beverages and lids. As easy flowing coextruded gloss layer on food packaging containers and vending cups.
Injection molded articles like razors, tooth brushes, packing articles.

Physical form and Storage

Polystyrol 143 E should be kept in its original containers in cool, dry place. Avoid direct exposure to sunlight. Polystyrol 143 E can be stored in silos.

Appendix H – Technical datasheet of Styrolution Polystyrene 124N/L

INEOS STYROLUTION

Styrolution PS 124N/L

General Purpose Polystyrene (GPPS)

TECHNICAL DATASHEET

DESCRIPTION

Styrolution PS 124N/L is a general purpose polystyrene grade with a good flow characteristic and an improved heat resistance.

FEATURES

- Excellent flow properties
- Good heat resistance
- UL 94 HB (Antwerp only)

APPLICATIONS

- Blending with HIPS in FFS thermoformed cups
- Injection molded articles
- Petri dishes, cuvettes, pipettes

Property, Test Condition	Standard	Unit	Values
Rheological Properties			
Melt Volume Rate, 200 °C/5 kg	ISO 1133	cm³/10 min	12
Mechanical Properties			
Charpy Unnotched, 23 °C	ISO 179/1eU	kJ/m²	10
Tensile Stress at Yield, 23 °C	ISO 527	MPa	50
Tensile Modulus	ISO 527	MPa	3200
Nominal Strain at Break, 23 °C	ISO 527	%	2
Flexural Strength, 23 °C	ISO 178	MPa	80
Flexural Modulus, 23 °C	ISO 178	MPa	3400
Hardness, Ball Indentation	ISO 2039-1	MPa	150
Thermal Properties			
Vicat Softening Temperature VST/B/50 (50N, 50 °C/h)	ISO 306	°C	87
Vicat Softening Temperature, B/1 (120 °C/h, 10N)	ASTM D 1525	°C	102
Heat Deflection Temperature A; (annealed 4 h/80 °C; 1.8 MPa)	ISO 75	°C	78
Coefficient of Linear Thermal Expansion	ISO 11359	10^{-6}/°C	80
Thermal Conductivity	DIN 52612-1	W/(m K)	0.16
Electrical Properties			
Volume Resistivity	IEC 62631-3-1	Ohm*m	$>10^{16}$
Surface Resistivity	IEC 62631-3-1	Ohm	$>10^{13}$

Property, Test Condition	Standard	Unit	Values
Optical Properties			
Refractive Index, Sodium D Line	ISO 489	-	1.56
Light Transmission at 550 nm	ASTM D 1003	%	91.4
Haze	ASTM D 1003	%	0.3
Other Properties			
Density	ISO 1183	kg/m³	1040
Processing			
Melt Temperature Range	ISO 294	°C	180 - 280

Typical values for uncolored products
Please note that all processing data stated are only indicative and may vary depending on the individual processing complexities.
Please consult our local sales or technical representatives for details.

SUPPLY FORM

Styrolution PS 124N/L can be supplied in two versions, without or with an external additive for improving pneumatic conveying. “L” as a suffix to the grade designation characterises the version with this agent, i.e. Styrolution PS 124L. Styrolution PS 124N/L is supplied as cylindrical or lens shaped pellets, packed in 25 kg bags or bulk.

PROCESSING

Styrolution PS 124N/L can be processed by all methods normally used for polystyrene. It is well balanced in its flow characteristic and heat resistance and is so used preferably for injection molding. It can be extruded as a blend component with high impact grades and as a gloss layer of thermoformed foils and sheets.

Appendix I – Technical datasheet of Hydrocerol™ ITP 822

Machine Translated by Google

Product data sheet

Hydrocerol® ITP 822 (blowing & nucleating agent)

General	Chemical substances that react under the influence of heat and split off gas during decomposition are referred to as "chemical blowing agents". In direct gassing processes, these "chemical blowing agents" can be used as nucleating agents in order to achieve particularly fine and uniform cell structures.
Description	- Hydrocerol® ITP 822 is an endothermic chemical blowing agent. Active ingredients: 20% - Non-toxic decomposition products - Good distribution in the melt - Paintable system
Suitable for	Especially for ABS, PC/ABS, PA, PBT, PET, PP. Other thermoplastics on request.
physical form	White granules
Packaging Unit	20 kg foil bag
More information	- Shut-off nozzle recommended (especially with the TSG) - Addition by hand or dosing device. - For mold plates or inserts: Steel grade 2083 ISO B (13% Cr) - Store the material in a cool and dry place. Do not expose to direct sunlight.

Purpose "Process optimizer"	Intended use Thermoplastic foam injection molding (TSG)
- Avoidance of sink marks, distortion, cavities - Shorter cycle times - Reduction of inner tensions - Advantages with long flow paths/better mold filling - Specific surface structures - Optimization of the locking forces - 2K technology	- Weight reduction - Material savings - Increase in the thermal and acoustic insulation effect - Good machinability (e.g. by sawing, cutting, drilling) - Increase in wall rigidity (sandwich effect) with the same use of materials
Recommended dosing to avoid sink marks: 0.5 - 1.5%	Recommended dosage for weight reduction: 0.8 - 3.0%

Processing information
Start of decomposition: 200°C. In order to avoid gas losses in the feed zone, the temperature should be as low as possible within the processing window of the plastic (e.g. 200 - 220°C). In order to achieve an optimal gas yield, the processing temperature should be at least 230°C.

temperature profile

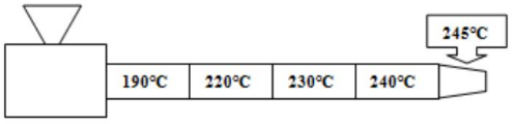

Note The temperature profile shown may deviate depending on the raw material.

The above information is based on our current technical knowledge and experience. Due to the large number of possible influences when processing and using the above-mentioned product, they do not release the processor from carrying out his own tests and trials. This does not constitute a guarantee of certain properties or suitability for a specific purpose and cannot be derived from the information. Laws and industrial property rights must be observed where applicable.

Appendix J – Technical datasheet of styrene acrylonitrile TYRIL™ 875

Technical Information

TRINSEO

TYRIL™ 875
SAN Resin

Overview

TYRIL* Styrene-actylonitrile (SAN) resins are designed to offer superior chemical resistance, strength, hardness and dimensional stability in a broad range of product applications. The key property of TYRIL 875 is specifically designed to provide good processability, good chemical resistance, heat resistance, very good strength and optimal aesthetics.

Applications

- Small appliances: transparent kitchen-robot parts

Physical	Nominal Value (English)		Nominal Value (SI)		Test Method
Density	1.08	g/cm³	1.08	g/cm³	ISO 1183/B
Apparent (Bulk) Density	0.69	g/cm³	0.69	g/cm³	ISO 60
Melt Mass-Flow Rate (MFR) (230°C/3.8 kg)	6.5	g/10 min	6.5	g/10 min	ISO 1133
Mechanical	**Nominal Value (English)**		**Nominal Value (SI)**		**Test Method**
Tensile Modulus	537000	psi	3700	MPa	ISO 527-2
Tensile Stress (Break)	10200	psi	70.0	MPa	ISO 527-2/5
Flexural Stress [1, 2]	14100	psi	97.0	MPa	ISO 178
Impact	**Nominal Value (English)**		**Nominal Value (SI)**		**Test Method**
Charpy Unnotched Impact Strength					ISO 179/1eU
73°F (23°C)	8.1	ft·lb/in²	17	kJ/m²	
Thermal	**Nominal Value (English)**		**Nominal Value (SI)**		**Test Method**
Heat Deflection Temperature					ISO 75-2/A
264 psi (1.8 MPa), Annealed	214	°F	101	°C	
Vicat Softening Temperature	232	°F	111	°C	ISO 306/A120
Flammability	**Nominal Value (English)**		**Nominal Value (SI)**		**Test Method**
Flame Rating [3] (0.06 in (1.5 mm))	HB		HB		UL 94

Notes

These are typical properties only and are not to be construed as specifications. Users should confirm results by their own tests.

[1] 0.079 in/min (2.0 mm/min)

[2] 3-points

[3] This rating not intended to reflect hazards presented by this or any other material under actual fire conditions.

Appendix K – Conference scientific papers redacted in the framework of this thesis

- A.A. Costa; A.C. Potêncio; P.G. Martinho; F.M. Barreiros. Thermal and Mechanical Properties of Recycled Polystyrene. – *Poster Session in the conference Materiais 2022.*

- A. A. Costa, P. G. Martinho, F. M. Barreiros. Mechanically recycled thermoplastics: thermal and mechanical analysis. – *Abstract submitted and accepted for presentation in the conference Materiais 2023 - Sustainability for a Future.*

- A. A. Costa, A. Mateus, T. Ruivo. Evaluation of high wall thickness variation on the properties of injected components through CIM and RHCM processes: A case study. – *Abstract submitted and accepted for presentation in the conference Materiais 2023 - Sustainability for a Future.*

Thermal and mechanical properties of recycled polystyrene

A. A. Costa[1,2], A. C. Potêncio[1], P. G. Martinho[1,2], and F. M. Barreiros[1,2]

[1] Centre for Rapid and Sustainable Product Development, Polytechnic of Leiria, Marinha Grande, Portugal
[2] School of Technology and Management, Polytechnic of Leiria, Leiria, Portugal

MATERIAIS 2022
Exploring a Better Future

INTRODUCTION

Motivated by legislation and environmental awareness, companies are looking for new materials or recycled ones. To understand which should be implemented, manufacturers need to know what differences occur when using a different material [1].

This study aims to evaluate the thermal and mechanical properties of recycled polystyrene, considering the high consumption of virgin raw material in the production of several plastic parts.

MATERIAL AND METHODS

The material used in this work was polystyrene (Styrolution PS 124N/L) which was recycled three times.

The polystyrene samples were obtained by injection molding. After the injection of the virgin material, some samples were saved for testing, and others were grinded and injected again, to obtain the first (Rec1) and second (Rec2) recycled samples. The injection tests were carried out using an injection molding machine (EUROINJ D80) of 80 tons of clamping force (Figure 1). The injection molding process conditions are presented in Table 1.

Figure 1: EUROINJ D80 injection machine

Table 1: Injection parameters used

Injection Temperature	230 °C
Mould Temperature	40°C
Injection Pressure	100 bar
Packing Pressure	80 bar
Packing Time	4 s
Cooling Time	25 s

The virgin and the recycled materials were characterized concerning thermal and rheological properties using differential scanning calorimetry (DSC) and melt flow index (MFI) tests, respectively. The DSC tests were carried out in a SETARAM DSC 131 equipment, using a heating rate of 10°C/min up to 300°C. The MFI tests were performed in a Ray-Ran equipment at 230°C (ASTM D1238 standard) [2].

The mechanical properties evaluated on the injected samples were obtained through tensile and shore D hardness tests, and dynamic mechanical analysis (DMA). The tensile tests were performed in a Zwick Z100 universal testing machine, equipped with a 10 kN load cell with a displacement rate of 1 mm/min, following the ASTM D638-02A standard [3]. The main dimensions of the samples are the following: thickness - 4.4 mm; length – 150 mm; width – 10 mm. The hardness tests were performed in a Bareiss Shore D Durometer (ISO 868 standard [4]). A Triton Tritec 2000 was used to perform dynamic mechanical analysis.

RESULTS AND DISCUSSION

The evolution of heat flow with the temperature for virgin and recycled polystyrene is presented in figure 1. According to the results, there are some differences between the virgin material and the recycled ones, but the glass transition temperature (Tg) of the polymer is almost the same, with a value of around 97°C.

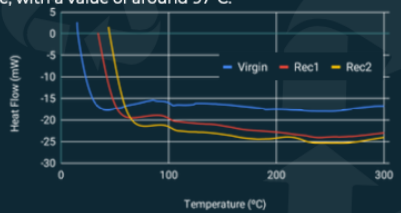

Figure 2: Differential Scanning Calorimetry (DSC) of virgin and recycled polystyrene

The results of melt flow index are summarized in Table 2. As expected the virgin material has a lower value compared to the recycled ones.

Table 2: Melt Flow Index (MFI) of virgin and recycled polystyrene

	Virgin	Rec1	Rec2
g/10 min	16.0	18.3	18.3

Figure 3 shows the results of the tensile tests. The values of yield strength, Young's Modulus, and hardness are shown in Table 3.

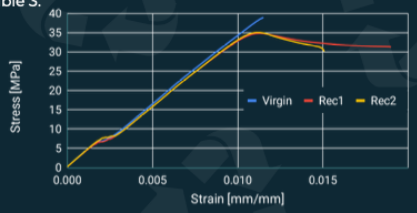

Figure 3: Tensile tests of virgin and recycled polystyrene

Table 3: Mechanical properties of virgin and recycled polystyrene

	Virgin	Rec1	Rec2
Yield Strength (MPa)	36.6	30.0	28.5
Young's Modulus (MPa)	3622.9 ± 37.6	3497.1 ± 33.7	3426.0 ± 66.4
Shore D Hardness	79.0 ± 0.7	76.2 ± 0.8	74.6 ± 1.1

The variation of stiffness with temperature for virgin and recycled polystyrene is presented in figure 4. The results show a slight decrease in stiffness in recycled polystyrene. However, the temperature at which there is a significant loss of stiffness occurs at approximately the same temperature.

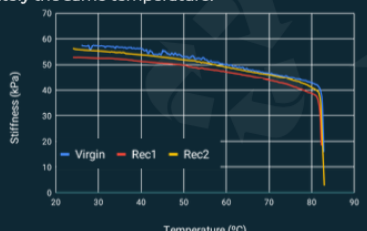

Figure 4: Dynamic mechanical analysis (DMA) of virgin and recycled polystyrene

CONCLUSIONS

The rheological and thermal analyses show slight differences between virgin and recycled material. Concerning mechanical properties, there is a noticeable decrease in yield strength of about 20% on recycled polystyrene. With this study, it is possible to understand that, depending on the function of the plastic part, the integration of recycled material in new components not only reduces waste but that it is a good option if mechanical performance is not a key requirement.

REFERENCES:

[1] S. Al-Salem, P. Lettieri and J. Baeyens, "The valorization of plastic solid waste (PSW) by primary to quaternary routes: From re-use to energy and chemicals", Progress in Energy and Combustion Science, vol. 36, no. 1, pp. 103-129, 2010. DOI: 10.1016/j.pecs.2009.09.001.
[2] *Standard Test Method for Melt Flow Rates of Thermoplastics by Extrusion Plastometer*, ASTM D1238-04, 2004.
[3] *Standard Test Method for Tensile Properties of Plastics*, ASTM D638-02a, 2002.
[4] *Plastics and ebonite — Determination of indentation hardness by means of a durometer (Shore hardness)*, ISO 868:2003, 2003.

ACKNOWLEDGMENTS:

This work was financially supported by the Fundação para a Ciência e a Tecnologia FCT/MCTES (PIDDAC) through the following Projects: UIDB/04044/2020; UIDP/04044/2020; Associate Laboratory ARISE LA/P/0112/2020; PAMI - ROTEIRO/0328/2013 (Nº 022158) and by the Portuguese National Innovation Agency through the following project: "S4Plast - Sustainable Plastics Advanced Solutions", project in consortium n. 046089.

POLITÉCNICO DE LEIRIA | CDRSP CENTRE FOR RAPID AND SUSTAINABLE PRODUCT DEVELOPMENT | SPM | FCT | ANI | COMPETE 2020 | PORTUGAL 2020 | MATERIAIS 2022

Materiais 2023 – XXI Congresso da Sociedade Portuguesa de Materiais and XII International Symposium on Materials

Mechanically recycled thermoplastics: thermal and mechanical analysis

A. A. Costa [1,2,*], P. G. Martinho [1,2], F. M. Barreiros [1,2]

[1] *Centre for Rapid and Sustainable Product Development, Polytechnic of Leiria, 2430-028 Marinha Grande, Portugal;*

[2] *School of Technology and Management, Polytechnic of Leiria, 2411-901 Leiria, Portugal;*

*andre.a.costa@ipleiria.pt

Keywords : injection moulding; mechanical recycling; polycarbonate (PC); polystyrene (PS); glass fibre-reinforced polyamide 6 (PA6-GF30); polyethylene terephthalate (PET)

Abstract

Due to the growth of plastic waste, the ever-increasing necessity of controlling the materials used in this industry has led to research new recycling processes as well as an understanding of the behaviour of plastics when recycled [1–3]. To help further increase the knowledge about this subject, some tests were performed to evaluate the dynamic mechanical analysis and thermal behaviour of commonly used thermoplastics after being mechanically recycled. The materials studied in this study were polycarbonate, polystyrene, polystyrene terephthalate, and glass-fibre-reinforced polyamide 6. In this analysis, the virgin materials were injected into a mould with a cavity geometry of a tensile and flexural test specimen. After injecting the virgin materials, these were ground and re-injected twice, as described in a previous study [4]. In this work, the analysis of these four materials was done by Fourier-Transform Infrared Spectroscopy (FTIR), Dynamic Mechanical Analysis (DMA) and Differential Scanning Calorimetry (DSC). The FTIR analysis shows changes in some functional groups, namely polyethylene terephthalate (PET) at the wavenumbers 3700-2800 cm^{-1}. DMA tests show no variation for polycarbonate (PC), polystyrene (PS), and glass fibre-reinforced polyamide 6 (PA6-GF30), nevertheless, PET shows an increase in tan-δ after recycling. Through DSC analysis, there are no significant changes in PC and PS glass-transition temperature (Tg), while PA6-GF30 shows almost no change in Tg and an increase in its melting temperature (Tm), meanwhile, PET shows a slight variation in Tg and Tm, but after recycling a new peak defined as "cold crystallization" temperature (Tc) appears. This peak may explain some changes observed in the optical characteristics.

References

1. Al-Salem, S.M.; Lettieri, P.; Baeyens, J. The Valorization of Plastic Solid Waste (PSW) by Primary to Quaternary Routes: From Re-Use to Energy and Chemicals. *Progress in Energy and Combustion Science* **2010**, *36*, 103–129, doi:10.1016/J.PECS.2009.09.001.
2. Goodship, V. Plastic Recycling. *https://doi.org/10.3184/003685007X228748* **2019**, *90*, 245–268, doi:10.3184/003685007X228748.
3. Briassoulis, D.; Pikasi, A.; Hiskakis, M. Recirculation Potential of Post-Consumer /Industrial Bio-Based Plastics through Mechanical Recycling - Techno-Economic Sustainability Criteria and Indicators. *Polymer Degradation and Stability* **2021**, *183*, 109217, doi:10.1016/J.POLYMDEGRADSTAB.2020.109217.
4. Costa, A.A.; Martinho, P.G.; Barreiros, F.M. Comparison between the Mechanical Recycling Behaviour of Amorphous and Semicrystalline Polymers: A Case Study. *Recycling 2023, Vol. 8, Page 12* **2023**, *8*, 12, doi:10.3390/RECYCLING8010012.

Materiais 2023 – XXI Congresso da Sociedade Portuguesa de Materiais and XII International Symposium on Materials

Evaluation of high wall thickness variation on the properties of injected components through CIM and RHCM processes: A case study

A. A. Costa[1,*], A. Mateus[1], T. Ruivo[2]

[1] *Centre for Rapid and Sustainable Product Development, Polytechnic of Leiria, 2430-028 Marinha Grande, Portugal;*
[2] *Erofio Atlantico, 2440-373 Batalha, Portugal*

*andre.a.costa@ipleiria.pt

Keywords : injection moulding; styrene-acrylonitrile resin (SAN); property variation; wall thickness; shrinkage; variotherm.

Abstract

One of the parameters that can affect the properties and characteristics of injected moulded parts is the wall thickness [1,2]. Since injection moulding is highly dependent on pressure to obtain a good quality part, due to the significant effect that it has on both shrinkage and final dimensions of the part. These pressures should be high enough to compensate shrinkage, but not so high that the cavity overpacks which lead to high values of residual stress on the component [1].
If the injected component has a thicker cross-section, it will take longer to cool and may require additional packing. This will lead to the appearance of shrinkage voids due to cavitation effect, sink marks because of non-uniform cooling, higher internal stresses that can lead to short- or long-term warpage and reduction in mechanical performance [1,3]. A variable wall thickness throughout the part, leads to a more difficult filling and in turn shrinkage-related internal stresses will appear in the transition regions [1].
This work uses a styrene-acrylonitrile resin (SAN) to evaluate the variation of wall thickness on injected parts while comparing the results when using conventional injection moulding (CIM) to Rapid Heat Cycle Molding (RHCM) or variotherm. This material allows for easily inspect internal stresses due to its transparency. The component possesses multiple wall thickness variation to clearly create problems during the injection process. Using a polarized light, it is possible to understand the regions where internal stresses are higher, and where eventually will lead to a decrease in mechanical performance. Figure 1 shows the part injected through CIM and the results of using the polarized light.

Figure 1. Evaluation of internal stresses on a multiple wall thickness part: no evaluation (left); polarized light evaluation (right).

References

1. Malloy, R.A. Plastic Part Design for Injection Molding: An Introduction: Second Edition; Hanser, 2010; ISBN 9783446404687.
2. General Electric Plastics Engineering Thermoplastics Design Guide; Pittsfield, MA, 1998;
3. Lee, B.H.; Kim, B.H. Optimization of Part Wall Thicknesses to Reduce Warpage of Injection-Molded Parts Based on The Modified Complex Method. **2006**, 34, 793–811, doi:10.1080/03602559508009600.;